

# MODELING GROWTH AND PRODUCTION DYNAMICS OF *SPARTINA ALTERNIFLORA*

by

YEAJIN JUNG

(Under the Direction of Adrian Burd)

## ABSTRACT

The goal of this work is to investigate the growth and production dynamics of the dominant salt marsh grass in the southeastern United States, *Spartina alterniflora*, including documenting non-structural carbohydrate pools and investigating seasonal changes in translocated biomass between above- and below-ground tissues.

In Chapter 2, the dynamics of several non-structural carbohydrates (NSC) stored in *S. alterniflora* is investigated. Results show that sucrose is the dominant NSC in both above- and below-ground tissues and that the total NSC as a percentage of total biomass is highest in the summer through to early winter. The study suggests that sucrose is likely used for long-term storage whereas glucose is preferentially utilized for short-term storage.

In Chapter 3, the growth and production dynamics of short, medium, and tall height forms of *S. alterniflora* are investigated using a phenology-based growth model (PG model), which includes the effects of light, temperature, and salinity on plant production. The model is used in combination with field observations of biomass to estimate values of physiological parameters such as mass-specific rates of carbon translocation. Once parameterized, the model is used in forward mode to predict whole-plant production, growth, respiration, mortality, and

translocation. Model results indicate that the short height form of *S. alterniflora* translocates a higher proportion of photosynthates or remobilization of assimilates to below-ground tissues during periods of growth and senescence periods than medium or tall *S. alterniflora*, although the absolute amount of carbon translocation to below-ground tissues is greatest in the tall form of *S. alterniflora* because of its larger above-ground biomass.

In Chapter 4, the model is used to compare the production and translocation dynamics of *S. alterniflora* along a latitudinal gradient using sites in Delaware, South Carolina, and Louisiana. Model results indicate that photosynthates make up the main source of carbon translocated to below-ground tissues at low latitudes, whereas at high latitudes, both photosynthates and remobilization of assimilates in senescing shoots are preferentially used. This shows the importance of taking into account the different translocation dynamics of the plants when comparing growth and production across sites at different latitudes.

INDEX WORDS: *Spartina alterniflora*, Growth and production model, Latitudinal changes, Non-structural carbohydrates, Salinity

MODELING GROWTH AND PRODUCTION DYNAMICS OF *SPARTINA ALTERNIFLORA*

by

YEAJIN JUNG

B.S., Pukyong National University, South Korea, 2008

A Dissertation Submitted to the Graduate Faculty of The University of Georgia in Partial  
Fulfillment of the Requirements for the Degree

DOCTOR OF PHILOSOPHY

ATHENS, GEORGIA

2018

© 2018

Yeajin Jung

All Rights Reserved

MODELING GROWTH AND PRODUCTION DYNAMICS OF *SPARTINA ALTERNIFLORA*

by

YEAJIN JUNG

Major Professor:	Adrian Burd
Committee:	Merryl Alber
	Lisa Donovan
	James Morris
	Steven Pennings

Electronic Version Approved:

Suzanne Barbour  
Dean of the Graduate School  
The University of Georgia  
May 2018

## DEDICATION

To my Lord, Jesus Christ, and my mom, Myougsuk Kim--they are the reasons why I did not give  
up.

## ACKNOWLEDGEMENTS

I would first like to thank my Lord, Jesus Christ, who used this long graduate school experience to train me and my family to be humble and to be more like Him. Although it was not easy, He provided us with all our needs during our studies in the United States.

I want to thank my advisor, Adrian Burd, for his diligent advisement and critical comments. Even though I have a long way to go in terms of growth in my field, it is definite that I acquired more experience and wisdom in many areas through his guidance. I would also like to thank my committee members for their valuable discussions and guidance when we set up this dissertation's outline.

In addition, I would like to thank the Arthur Roberts' lab and Charles Hopkinson's lab for providing me with the facilities and lab areas while I ran my research experiment. Thanks to Cody Luedtke, Jessica O'Connell, and David Miklesh for their valuable discussions and comments regarding the research topics.

I am thankful to our graduate coordinator, Christof Meile, for his support and care for students including me. He even created accommodations for a breastfeeding room when I had my first baby. I would like to thank our department head, Daniela Di Iorio, for her invaluable counseling. Without her support, I would not have been able to finish this graduate school life. I am thankful Catherine Teare Ketter for her mentoring and thoughtful consideration during teaching at Marine Sciences.

I want to give special acknowledgement to my husband, Hyoungjin Park, my life companion and my love. We went through this long journey together as foreigners, as a student couple, and as parents of two children by God's grace. The fruit that I reaped from this experience studying abroad at UGA was meeting him, my next door neighbor during my first year of graduate school. I would also like to thank my oldest daughter, Onyu Park, for cheering me on and for loving me. I would like to extend a special blessing to my second daughter, Sarang Park, who was with me in my womb the whole time I was working on this dissertation. She was born four days after I submitted my final draft to committee members.

I am greatly thankful to my mom, Myoungsuk Kim, and my father, Soonyeol Jung, for their steadfast prayer, support, and encouragement for my family. I would not have been able to complete this task without the faith in God that I learned from their lives and examples. I thank my brother, Kyung-kwon Jung, and his wife, Boram Im, for their love and prayers. Finally, I am thankful to my pastor, Daniel Park, and friends at the Athens Korean Baptist Church for their longstanding prayers and fellowship in Him.

## TABLE OF CONTENTS

	Page
ACKNOWLEDGEMENTS .....	v
LIST OF TABLES .....	viii
LIST OF FIGURES .....	x
CHAPTER	
1 INTRODUCTOIN AND LITERATURE EVIEW .....	1
2 SEASONAL CHANGES IN ABOVE- AND BELOW-GROUND NON- STRUCTURAL CARBOHYDRATES (NSC) IN <i>SPARTINA ALTERNIFLORA</i> IN A MARSH IN GEORGIA, USA.....	13
3 MODELING THE PHENOLOGY-BASED GROWTH DYNAMICS OF SHORT, MEDIUM, AND TALL <i>SPARTINA ALTERNIFLORA</i> IN A GEORGIA MARSH, USA.....	47
4 MODELING THE VARIABILITY IN PHENOLOGY-BASED GROWTH DYNAMICS <i>SPARTINA ALTERNIFLORA</i> WITH LATITUDE.....	97
5 SUMMARY.....	145

## LIST OF TABLES

	Page
Table 2.1: Definitions of symbols and parameter values. ....	33
Table 2.2: Distribution of the total NSC as a percentage of dry weight within different tissues of <i>Spartina alterniflora</i> .....	34
Table 2.3: <i>Spartina alterniflora</i> : contribution of each NSC in eight different tissues .....	35
Table 3.1: The monthly average above- and below-ground biomass and the root to shoot ratio from two destructive cores.....	74
Table 3.2: Definitions of symbols and parameter values.....	75
Table 3.3: Definitions of symbols of parameters estimated in the inverse model.....	75
Table 3.4: Phenological date applied on three height forms of <i>S. alterniflora</i> on Sapelo Island, Georgia, U.S.A.in the PG model.....	76
Table 3.5: Three phenological events and dates on Sapelo Island, Georgia, USA.....	76
Table 3.6: Parameter values from the inverse model .....	77
Table 3.7: Total translocation and the daily mean translocation of the three types of <i>S. alterniflora</i> during each phenology period.....	78
Table 3.8: The modeled mean root: shoot ratio of three height forms of <i>S. alterniflora</i> .....	79
Table 3.9: Daily mean gross and net production calculated in the PG model.....	79
Table 3.10: Daily mean above- and below-ground mortality rates estimated in the PG model...80	80
Table 3.11: Daily mean above- and below-ground respiration rates estimated in the PG model.80	80
Table 3.12: Sensitivity analysis of phenological dates.....	81

Table 4.1: Characteristic of three regions (Delaware, South Carolina, and Louisiana) in latitudinal study using the PG model.....	123
Table 4.2: Definitions of symbols and parameter values.....	124
Table 4.3: Least-square estimates of parameters used for temperature simulations in PG model.....	125
Table 4.4: Site-specific phenological input data implied on the latitudinal study in the PG model.....	125
Table 4.5: Parameter values from the inverse model .....	126
Table 4.6: The modeled mean root: shoot ratio at three latitudes.....	126
Table 4.7: Daily mean gross and net production calculated in the PG model.....	127
Table 4.8: Total carbon translocation at each phenological cycle at the three latitudes.....	127
Table 4.9: Daily mean above- and below-ground respiration rates estimated in the PG model in the latitudinal study.....	128

## LIST OF FIGURES

	Page
Figure 2.1: Measured dry weight and non-structural carbohydrates in each core. ....	38
Figure 2.2: Above- and below-ground glucose, fructose, sucrose, and starch concentrations as percentages of above- and below-ground dry weight.....	39
Figure 2.3: Within-core measurements of glucose, fructose, sucrose and starch as a percentage of dry weight in green stems, green leaves.....	40
Figure 2.4: Within-core measurements of glucose, fructose, sucrose and starch as a percentage of dry weight in yellow stems and yellow leaves .....	41
Figure 2.5: Within-core measurements of glucose, fructose, sucrose and starch concentrations as percentages of dry weight in below-ground tissue, divided in to shallow (0–10 cm) and deep (10–30 cm) zones .....	42
Figure 2.6: Estimated daily net production using the Morris model and local environmental variables (Figure 2.9).....	43
Figure 2.7: Comparison of monthly net primary production with observed monthly changes in green biomass, below-ground non-structural carbohydrate and above-ground non-structural carbohydrate.....	44
Figure 2.8: Site map showing the location and boundary of the Georgia Coastal Ecosystems Long Term Ecological Research (GCE-LTER) site on Sapelo Island (Georgia, USA), the location of the flux tower, and the location of the 6 sampling sites used in this study.....	45

Figure 2.9: Environmental data measured at the GCE-LTER flux tower .....	46
Figure 3.1: Site map .....	82
Figure 3.2: Structure of the <i>S. alterniflora</i> phenology-based growth dynamic model.....	83
Figure 3.3: Monthly above-ground (AG) and below-ground (BG) biomass .....	84
Figure 3.4: The effect of salinity on the gross production rate in the PG model.....	85
Figure 3.5: $\Delta D_i$ values quantifying the differences between observed and modeled biomass in above- and below-ground biomass .....	86
Figure 3.6: The PG model result of tall form <i>S. alterniflora</i> on Sapelo Island, Georgia.....	87
Figure 3.7: The PG model result of medium form <i>S. alterniflora</i> on Sapelo Island, Georgia.....	88
Figure 3.8: The PG model result of short form <i>S. alterniflora</i> on Sapelo Island, Georgia.....	89
Figure 3.9: Observed irradiance and temperature on Sapelo Island, Georgia.....	90
Figure 3.10: Gross production and net production of the three types of <i>S. alterniflora</i> on Sapelo Island, Georgia.....	91
Figure 3.11: Translocated photosynthate and assimilate of the tall form <i>S. alterniflora</i> on Sapelo Island, Georgia.....	92
Figure 3.12: Translocated photosynthate and assimilate of the form <i>S. alterniflora</i> on Sapelo Island, Georgia.....	93
Figure 3.13: Translocated photosynthate and assimilate of the short form <i>S. alterniflora</i> on Sapelo Island, Georgia.....	94
Figure 3.14: Modeled mortality rates of the three types of <i>S. alterniflora</i> on Sapelo Island, Georgia.....	95
Figure 3.15: Modeled respiration rates of the three types of <i>S. alterniflora</i> on Sapelo Island, Georgia.....	96

Figure 4.1:  $\Delta D_i$  values quantifying the differences between observed and modeled biomass in above- and below-ground biomass at three latitudinal regions.....129

Figure 4.2: Observed and modeled above- and below-ground biomass of *S. alterniflora* in Delaware.....130

Figure 4.3: Observed and modeled above- and below-ground biomass of *S. alterniflora* in South Carolina.....131

Figure 4.4: Observed and modeled above- and below-ground biomass of *S. alterniflora* in Louisiana.....132

Figure 4.5: Root to shoot ratio of modeled biomass of *S. alterniflora* at three different latitudes a) Delaware, b) South Carolina, c) Louisiana.....133

Figure 4.6: Calculated a) irradiance and b) temperature and the estimated c) gross production and net production of *S. alterniflora* in Delaware in the PG model.....134

Figure 4.7: Calculated a) irradiance and b) temperature and the estimated c) gross production and net production of *S. alterniflora* in South Carolina in the PG model.....135

Figure 4.8: Calculated a) irradiance and b) temperature and the estimated c) gross production and net production of *S. alterniflora* in Louisiana in the PG model.....136

Figure 4.9: Translocated photosynthate and assimilate of *S. alterniflora* in Delaware during three different phenological events.....137

Figure 4.10: Translocated photosynthate and assimilate of *S. alterniflora* in South Carolina during three different phenological events.....138

Figure 4.11: Translocated photosynthate and assimilate of *S. alterniflora* in Louisiana during three different phenological events.....139

Figure 4.12: Mortality rates of above- and below-ground biomass calculated in the PG model in

the latitudinal study on a) Delaware, b) South Carolina, and c) Louisiana.....	140
Figure 4.13: Respiration rates of above- and below-ground biomass calculated by the PG model in the latitudinal study on a) Delaware, b) South Carolina, and c) Louisiana.....	141
Figure 4.14: Observed above- and below-ground biomass of Louisiana <i>S. alterniflora</i> in Louisiana and modeled above- and below-ground biomass of Louisiana <i>S. alterniflora</i> transplanted in Delaware.....	142
Figure 4.15 Observed above- and below-ground biomass of South Carolina <i>S. alterniflora</i> in South Carolina and modeled above- and below-ground biomass of South Carolina <i>S.</i> <i>alterniflora</i> transplanted in Delaware.....	143
Figure 4.16 Observed above- and below-ground biomass of Delaware <i>S. alterniflora</i> in Delaware and modeled above- and below-ground biomass of Delaware <i>S. alterniflora</i> transplanted in Louisiana.....	144

CHAPTER 1  
INTRODUCTION AND LITERATURE REVIEW

**The role of *Spartina alterniflora* in salt marsh ecosystem**

Salt marshes play important roles in the global carbon cycle and ecological functioning of coastal ecosystems. Carbon burial rates per square meter in salt marshes are high (mean of 218 g C m<sup>-2</sup> y<sup>-1</sup>) compared to other ecosystems such as tropical, temperate, and boreal forests that have burial rates between 0.7 – 13.1 g C m<sup>-2</sup> y<sup>-1</sup> (McLeod et al., 2011). Salt marshes are the main drivers of secondary production in near-shore coastal waters through the production and export of detrital material (Odum, 1967). This view of a detritus-driven coastal ecosystem was echoed Wiegert et al. (1981), who asserted that "...the preservation of fisheries depends as much upon the protection of the tidal creeks as upon protection of the marsh and its *Spartina alterniflora* production." The dominant macrophyte found in salt marshes in the southeastern United States is *Spartina alterniflora*. For example, *S. alterniflora* covers more than 80% of the total salt marsh area on Sapelo Island, Georgia (Hladik et al., 2013). This plant also forms a major component of salt marsh ecosystems. The above-ground parts of the plant are important sources of food and shelter to various marine organisms and the below-ground parts stabilize marsh edges (Knutson, 1988) and serve as a source of organic matter for microbial biomass (Boschker et al., 1999).

Production and growth of *S. alterniflora* are closely related to environmental factors such as salinity, nutrient level, and soil redox potential, and these factors affect the typical heights of the plants and their zonation within the marsh (Mendelssohn 1979; Mendelssohn & Morris, 2002). Although plant height is a continuum, the tall height form of *S. alterniflora* (> 1.0m) has the highest productivity and dominates regularly-flooded creek bank areas with relatively low porewater salinity (20 – 28 ppt). In contrast, the shortest height form of *S. alterniflora* (< 0.5m) is found in the irregularly flooded high marsh where typical porewater salinities are higher (27.5 – 30.2 ppt). The medium height form of *S. alterniflora* dominates mid-marsh areas characterized by an intermediate porewater salinity range.

Below-ground biomass of *S. alterniflora* is typically larger than above-ground biomass (Good et al., 1982; Schubauer & Hopkinson, 1984). Areal production rates of above- and below-ground biomass on Sapelo Island in Georgia lie between 643 – 1,098 g m<sup>-2</sup> y<sup>-1</sup> (Smalley, 1958) and 4,780 g m<sup>-2</sup> y<sup>-1</sup> respectively (Schubauer & Hopkinson, 1984). Greater annual below-ground production rates (6,500 g m<sup>-2</sup> y<sup>-1</sup>) compared to above-ground production rates (1,487 g m<sup>-2</sup> y<sup>-1</sup>) have also been measured at the Canary Creek salt marsh in Delaware (Roman & Daiber, 1984). This suggests that understanding the dynamics of both above- and below-ground biomass components is necessary for understanding growth and production dynamics of *S. alterniflora*.

### **Non-structural carbohydrates in *Spartina alterniflora***

Plants use most of the carbon acquired through photosynthesis for respiration and to build structural biomass (Robson, 1973; Danckwerts & Gordon, 1987). A smaller portion is stored in the form of non-structural carbohydrates (NSC) which include glucose, fructose, sucrose, and starch (Gorham et al., 1980; Smith, 1973). Different components of NSC play different roles in

plant metabolism. For example, sucrose serves as an ideal sugar for transport and long-term storage because it is non-reducing and not readily metabolized (Arnold, 1968; Lemoine, 2000). On the other hand, glucose and fructose present in smaller amounts, and mainly function as metabolic intermediates or breakdown products for respiration (Pollock et al., 1999). The stored NSC in plant tissues are later used to support metabolism at night, provide energy for regrowth in the spring (Lytle & Hull, 1980) and sustain plant functions under stressful environmental conditions such as drought, high salinity, and low nutrient concentrations (Watts, 2009; Dietze et al., 2014). Accordingly, plants use stored NSC or remobilization of reserves stored in the biomass (Morvan-Bertrand et al., 1999; Skinner et al., 1999) when carbon supply via photosynthesis does not meet overall demands.

Despite its critical role in the plant carbon balance, our understanding of the dynamics and role of NSC storage in *S. alterniflora* remains limited, and there have been few studies of NSC and its dynamics in *S. alterniflora*. Lytle and Hull (1980) used radiolabeled carbon to demonstrate that photosynthate generated at the end of the growing season was translocated to below-ground tissues and utilized for the early re-growth in the following spring; however the types of stored carbon were not specified in that study. The majority of studies on NSC in *S. alterniflora* report only total NSC concentrations in total below-ground biomass or above-ground biomass, and for only part of the year, though some studies have specified which forms of NSC were measured, and others have measured NSC in various tissue parts (Garza et al., 1994; Livingstone & Patriquin, 1981; Gallagher et al., 1984; Colmer et al., 1996). To gain a greater understanding of the variability and dynamics of NSC stored in different plant tissues and how this is affected by the environmental factors, the assessment on the seasonal changes of the amount and the types of NSC stored in different tissues of *S. alterniflora* is required.

## **Modeling production dynamics**

Harvesting plant material is a direct measure of the plant. However, it is a destructive and labor intensive method and is also affected by when the harvesting takes place (e.g. Smalley vs. Peak live standing crop method). For example, the Peak live standing crop method assumes that the highest value of standing live biomass harvested during the year indicates net primary production whereas the Smalley (1958) method is developed specifically for estimating production in salt marshes using changes in dead and live biomass between sampling period. Roman and Daiber demonstrated that the net annual above-ground production estimated by the peak live standing crop was about  $450 \text{ g m}^{-2} \text{ y}^{-1}$  less than one calculated by Smalley method in the tall form *S. alterniflora*.

Alternatively, using a computational model to analyze production dynamics has several advantages. First, models can aid in developing a quantitative understanding of the mechanisms of plant growth without destructive sampling. For example, models can be used to estimate gross and net production and rates of carbon loss through respiration and mortality and these can help us to understand carbon pathways within the plants. Second, models can be used to promote an integrative understanding of the interplay between environmental drivers, physiological process, and carbon allocation in different plant tissues. And lastly, computational models can be used to predict biomass under varying scenarios of environmental conditions, identify areas where improved measurements can provide the biggest improvement to our understanding, and guide future areas of research.

## **Formulating a model of phenology-based growth dynamics**

Phenology is recognized as an important factor in determining the growth of *S. alterniflora*, but it is rarely included in *S. alterniflora* growth models. The timing and duration of periods of resource translocation between above- and below-ground tissues appears to be linked to the timing of events such as bud-burst, flowering, and seedling. Crosby et al. (2015) demonstrated that *S. alterniflora* in Massachusetts starts to allocate biomass to below-ground tissues when flowering begins in August and suggested that the dominant below-ground biomass accumulation occurs during the time between flowering and senescence in September. Elsey-Quirk et al. (2011) showed that rhizome biomass increases as leaf senescence starts. These studies indicate that phenology may control the timing and amount of carbon a plant allocate to below-ground, thereby affecting the carbon availability for growth in the following spring.

There have been only a handful of published models of the growth and production of *S. alterniflora*, and few of those include both above- and below-ground dynamics. Morris et al. (1984) estimated maximum annual below-ground production rates using an above-ground production model and mass balance for below-ground production. Dai and Wiegert (1996) later developed a canopy model that estimated the below-ground net production by subtracting actual above-ground growth from calculated net aboveground production. This latter model showed that it is essential to include the carbon translocation between above- and below-ground tissues in order to avoid considerable overestimates of total net production, though the model only included translocation from above- to below-ground tissue. A recently published model does incorporate phenology and resource translocation into a *S. alterniflora* model (Zheng et al., 2016). While Zheng et al.'s model (2016) was developed based on observational data that was assembled from the literature with a wide geographic distribution along the East Coast of the

USA and the coastline of China, it used the same phenology dates and allocation rates between the above- and below-ground tissues as it applies to *S. alterniflora* in a particular region. The model used the same physiological parameter values for *S. alterniflora* in all regions but varied the timing and duration of life history events. It also did not include the effects of salinity on growth and production and so could not distinguish plant zonation within marshes.

The importance of *S. alterniflora* in terms of its high productivity and ecological role in the wetland ecosystem has led to the development of different mathematical models, ranging from descriptions of growth dynamic under different nutrient levels (Morris et al., 1982), to a canopy profile approach (Dai & Wiegert, 1996) and implication of phenology (Zheng et al., 2016). Integration of such models of environmentally important plants in carbon dynamic simulations would clearly benefit forecasting biological responses to changing macroscopic conditions in wetland ecosystems.

### **Structure and purpose of dissertation**

The purpose of this study is to investigate growth and production dynamics in *S. alterniflora*, including the seasonal variability of non-structural carbon in different tissues and analyzing the production dynamics of three height forms of *S. alterniflora* on Sapelo Island, Georgia using the Phenology-based Growth model (PG model). The model includes the effect of salinity on growth, and we use the model to study *S. alterniflora* growth dynamics at three different latitudes. One application of the PG model is to simulate translocated photosynthates or assimilate within *S. alterniflora* at several phenological events such as growth, senescence, and dormancy periods. With the high carbon burial rates of salt marshes (Mcleod et al., 2011) and large carbon sequestration (44.6 Tg C y<sup>-1</sup>) in wetland ecosystems (Chmura et al., 2003)

compared to their small areas on the world's land (6%), understanding the carbon allocation dynamics of the dominant plant in salt marshes is of great importance from a global carbon cycle perspective. Therefore, in Chapter 2, seasonal changes in above- and below-ground non-structural carbohydrates (NSC) in different tissue parts of *S. alterniflora* are measured along with an analysis of both above- and below-ground biomass in a Georgia marsh. In addition, the Morris et al. (1984) model is applied to estimate the net above- and below-ground productions and its strengths and limitations are assessed through comparisons with measured NSC and biomass data. In Chapter 3, to better elucidate the growth and production dynamics of *S. alterniflora*, the PG model is developed to include the salinity effect on the production of *S. alterniflora*. The model is used in an inverse mode to estimate the physiological parameters. The calculated parameter values are applied to compute the growth dynamics of three different height forms of *S. alterniflora* on Sapelo Island, Georgia. Chapter 4 presents the implication of PG model to the latitudinal study focusing on analyzing the translocated photosynthates or assimilate between above- and below-ground biomass at various phenological events including growing, senescing, and dormancy periods at three sites. Finally, in chapter 5, a summary of the results of these chapters is provided.

## References

- Arnold, W. N. (1968). The selection of sucrose as the translocate of higher plants. *Journal of Theoretical Biology*, 21(1), 13-20.
- Asaeda, T., & Karunaratne S. (2000). Dynamic modeling of the growth of *Phragmites australis*: model description. *Aquatic Botany*, 67(4), 301–318.

- Asaeda, T., Hai, D. N., Manatunge, J., Williams, D., & Roberts, J. (2005). Latitudinal characteristics of below-and above-ground biomass of *Typha*: a modelling approach. *Annals of Botany*, *96*(2), 299-312.
- Boschker, H. T. S., De Brouwer, J. F. C., & Cappenberg, T. E. (1999). The contribution of macrophyte-derived organic matter to microbial biomass in salt-marsh sediments: Stable carbon isotope analysis of microbial biomarkers. *Limnology and Oceanography*, *44*(2), 309-319.
- Chmura, G. L., Anisfeld, S. C., Cahoon, D. R., & Lynch, J. C. (2003). Global carbon sequestration in tidal, saline wetland soils. *Global biogeochemical cycles*, *17*(4).
- Colmer, T. D., Teresa WM, F., Läuchli, A., & Higashi, R. M. (1996). Interactive effects of salinity, nitrogen and sulphur on the organic solutes in *Spartina alterniflora* leaf blades. *Journal of Experimental Botany*, *47*(3), 369-375.
- Crosby, S. C., Ivens-Duran, M., Bertness, M. D., Davey, E., Deegan, L. A., & Leslie, H. M. (2015). Flowering and biomass allocation in U.S. Atlantic coast *Spartina alterniflora*. *American journal of botany*, *102*(5), 669-676. doi: 10.3732/ajb.1400534
- Dai, T., & Wiegert, R. G. (1996). Estimation of the primary productivity of *Spartina alterniflora* using a canopy model. *Ecography*, *19*(4), 410-423.
- Danckwerts, J. E., & Gordon, A. J. (1987). Long-term partitioning, storage and re-mobilization of <sup>14</sup>C assimilated by *Lolium perenne* (cv. Melle). *Annals of Botany*, *59*(1), 55-66.
- Dietze, M. C., Sala, A., Carbone, M. S., Czimczik, C. I., Mantooh, J. A., Richardson, A. D., & Vargas, R. (2014). Nonstructural carbon in woody plants. *Annual review of plant biology*, *65*, 667-687.
- Elsley-Quirk, T., Seliskar, D. M., & Gallagher, J. L. (2011). Differential population response of

- allocation, phenology, and tissue chemistry in *Spartina alterniflora*. *Plant Ecology*, 212, 1873-1885.
- Gallagher, J. L., Wolf, P. L., & Pfeiffer, W. J. (1984). Rhizome and root growth rates and cycles in protein and carbohydrate concentrations in Georgia *Spartina alterniflora* Loisel. plants. *American Journal of Botany*, 71(2), 165-169.
- Garza Jr, A., McLendon, T., & Drawe, D. L. (1994). Herbage yield, protein content, and carbohydrate reserves in gulf cordgrass (*Spartina spartinae*). *Journal of Range Management*, 47(1), 16-21.
- Good, R. E., Good, N. F., & Frasco, B. R. (1982). A review of primary production and decomposition dynamics of the belowground marsh component. In V. S. Kennedy (Eds.), *Estuarine comparisons* (pp. 139-157). Elsevier.
- Gorham, J., Hughes, L. L., & Wyn Jones, R. G. (1980). Chemical composition of salt-marsh plants from Ynys Môn (Anglesey): the concept of physiotypes. *Plant, Cell & Environment*, 3(5), 309-318.
- Hladik, C., Schalles, J., & Alber, M. (2013). Salt marsh elevation and habitat mapping using hyperspectral and LIDAR data. *Remote Sensing of Environment*, 139, 318-330.
- Knutson, P. L. (1988). Role of coastal marshes in energy dissipation and shore protection. In H. Décamps & R. J. Naiman (Eds.), *The ecology and management of wetlands* (pp. 161-175). Boston, MA: Springer.
- Lemoine, R. (2000). Sucrose transporters in plants: update on function and structure. *Biochimica et Biophysica Acta (BBA)-Biomembranes*, 1465(1), 246-262.
- Livingstone, D. C., & Patriquin, D. G. (1981). Belowground growth of *Spartina alterniflora* Loisel.: habit, functional biomass and non-structural carbohydrates. *Estuarine, Coastal and*

- Shelf Science*, 12(5), 579-587.
- Lytle, R. W., & Hull, R. J. (1980). Photoassimilate distribution in *Spartina alterniflora* Loisel. II. autumn and winter storage and spring regrowth. *Agronomy Journal*, 72(6), 938-942. doi: 10.2134/agronj1980.00021962007200060018x
- McLeod, E., Chmura, G. L., Bouillon, S., Salm, R., Björk, M., Duarte, C. M., Lovelock, C. E., Schlesinger, W. H., & Silliman, B. R. (2011). A blueprint for blue carbon: toward an improved understanding of the role of vegetated coastal habitats in sequestering CO<sub>2</sub>. *Frontiers in Ecology and the Environment*, 9(10), 552-560.
- Mendelssohn, I. A. (1979). Nitrogen Metabolism in the Height Forms of *Spartina Alterniflora* in North Carolina. *Ecology*, 60(3), 574-584. doi: 10.2307/1936078
- Mendelssohn, I. A., & Morris, J. T. (2002). Eco-physiological controls on the productivity of *Spartina alterniflora* Loisel. In M. P. Weinstein & D. A. Kreeger (Eds.), *Concepts and controversies in tidal marsh ecology* (pp. 59-80). Dordrecht, Netherlands: Springer.
- Morris, J. T. (1982). A Model of growth responses by *Spartina Alterniflora* to nitrogen limitation. *Journal of Ecology*, 70(1), 25-42. doi: 10.2307/2259862
- Morris, J. T., Houghton, R. A., & Botkin, D. B. (1984). Theoretical limits of belowground production by *Spartina alterniflora*: An analysis through modelling. *Ecological Modelling*, 26(3), 155-175. doi: [https://doi.org/10.1016/0304-3800\(84\)90068-1](https://doi.org/10.1016/0304-3800(84)90068-1)
- Morvan-Bertrand, A., Pavis, N., Boucaud, J., & Prud'Homme, M. P. (1999). Partitioning of reserve and newly assimilated carbon in roots and leaf tissues of *Lolium perenne* during regrowth after defoliation: assessment by <sup>13</sup>C steady-state labelling and carbohydrate analysis. *Plant, Cell & Environment*, 22(9), 1097-1108.
- Odum, E. P. (1967). Particulate organic detritus in a Georgia salt marsh-estuarine ecosystem.

- Estuaries*, 83, 333-388.
- Pollock, C. J., Cairns, A. J., Gallagher, J., & Harrison, J. (1999). The integration of sucrose and fructan metabolism in temperate grasses and cereals. In N. J. Kruger, S. A. Hill & R. G. Ratcliffe (Eds.), *Regulation of primary metabolic pathways in plants* (pp. 195-226). Dordrecht, Netherlands: Springer
- Robson, M. J. (1973). The growth and development of simulated swards of perennial ryegrass: I. Leaf growth and dry weight change as related to the ceiling yield of a seedling sward. *Annals of Botany*, 37(3), 487-500.
- Roman, C. T., & Daiber, F. C. (1984). Aboveground and belowground primary production dynamics of two Delaware bay tidal marshes. *Bulletin of the Torrey Botanical Club*, 111(1), 34-41. doi: 10.2307/2996208
- Schubauer, J. P., & Hopkinson, C. S. (1984). Above-and belowground emergent macrophyte production and turnover in a coastal marsh ecosystem, Georgia. *Limnology and Oceanography*, 29(5), 1052-1065.
- Skinner, R. H., Morgan, J. A., & Hanson, J. D. (1999). Carbon and nitrogen reserve remobilization following defoliation: nitrogen and elevated CO<sub>2</sub> effects. *Crop Science*, 39(6), 1749-1756.
- Smalley, A. E. 1958. *The role of two invertebrate populations, Littorina irrorata and Orchelimum fiducinum in the energy flow of a salt marsh eco- system* (Doctoral dissertaion). University of Georgia, Athens, GA.
- Smith, D. (1973). Influence of drying and storage conditions on nonstructural carbohydrate analysis of herbage tissue—a review. *Grass and Forage Science*, 28(3), 129-134.
- Watts, K. A. (2009). Carbohydrates in forage: What is a safe grass?. In J. D. Pagan (Eds.), *Advances in equine nutrition IV* (pp. 29-42). Nottigham University Press

Wiegert, R. G., Pomeroy, L. R., & Wiebe, W. J. (1981). Ecology of salt marshes: an introduction.

In, L. R. Pomeroy & R. G. Wiegert (Eds.), *The ecology of a salt marsh* (pp. 3-19). New York, NY: Springer.

Zheng, S., Shao, D., Asaeda, T., Sun, T., Luo, S., & Cheng, M. (2016). Modeling the growth dynamics of *Spartina alterniflora* and the effects of its control measures. *Ecological Engineering*, 97, 144-156.

## CHAPTER 2

# SEASONAL CHANGES IN ABOVE- AND BELOW-GROUND NON-STRUCTURAL CARBOHYDRATES (NSC) IN *SPARTINA ALTERNIFLORA* IN A MARSH IN GEORGIA, USA<sup>1</sup>

---

<sup>1</sup>Jung, Y., & Burd, A. (2017). *Aquatic Botany*, 140, 13-22. Reprinted here with permission of the publisher

## **Abstract**

*Spartina alterniflora* is the dominant grass appearing in salt marshes along the east coast of the USA. The development of predictive, mechanistic models of *S. alterniflora* has been hindered by the lack of information on below-ground biomass and its dynamics, and in particular the storage of resources that can be used for spring regrowth. We studied the dynamics of non-structural carbohydrates (glucose, fructose, sucrose, and starch) and biomass in 8 different above- and below-ground tissues in *S. alterniflora* over the course of a year in a salt marsh on Sapelo Island, Georgia, USA. We found greater seasonal variability in non-structural carbohydrates in *S. alterniflora* than had been previously reported, with concentrations varying between 3.3% through 17.3% of the total biomass and between 0% and 19.5% of dry weight depending on the type of tissue, with statistical differences between the different tissues. We found that sucrose was the dominant non-structural carbohydrate in above- and below-ground tissue, and that this sugar was likely used for long-term storage during winter months and as a resource for early spring growth. Glucose, fructose, and starch showed less variability, with glucose following changes in above-ground biomass more closely indicating their use as short-term storage. We were unable to develop a coherent carbon budget for the plants largely because of uncertainties in modeled net primary production and heterogeneity in below-ground biomass.

## **1. Introduction**

Salt marshes are highly productive, transitional wetland ecosystems lying at the interface between terrestrial and marine systems. Carbon burial rates in salt marshes are typically high, with global estimates varying up to  $1,713 \text{ g C m}^{-2} \text{ y}^{-1}$  (mean of  $218 \pm 24 \text{ g C m}^{-2} \text{ y}^{-1}$ ) compared to carbon burial rates in temperate, tropical, and boreal forests between  $0.7$  and  $13.1 \text{ g C m}^{-2} \text{ y}^{-1}$

(McLeod et al., 2011). Along the eastern coast of the United States, salt marshes are dominated by the halophyte C<sub>4</sub> plant, *Spartina alterniflora* (Pennings et al., 2012). The extensive below-ground components of *S. alterniflora* protect the salt marsh from erosion by sea level rise and storms (Knutson, 1988) and also serve as a source of organic matter for microbial biomass (Boschker et al., 1999).

Biomass and height forms of *S. alterniflora* differ along the marsh. The tall height form (> 1 m) grows adjacent to tidal creeks and has a higher productivity than the more inland short form (< 50 cm); the medium height form (50 – 100 cm) is both intermediate in location and productivity (Mendelssohn, 1979). Although the tall-form *S. alterniflora* inhabits only about 10% of a marsh surface area, it accounts for 30–50% of total marsh production (Gallagher et al., 1980; Giurgevich & Dunn, 1979).

Developing carbon budgets for *S. alterniflora* is complicated by the fact that organic carbon produced through photosynthesis can be respired, used for growth and reproduction, or stored as non-structural carbohydrates (NSC) (Morris et al., 1984). In general, non-structural carbohydrates are among the first products of photosynthesis in plants (Danckwerts & Gordon, 1987; Fulkerson and Donaghy, 2001) and about half of NSC produced from photosynthesis is utilized in respiration (Robson, 1973; Lambers, 1985; Danckwerts & Gordon, 1987). The remaining NSC is either metabolized for growth within a few days (Gordon et al., 1977) or stored for long-term use (Danckwerts & Gordon, 1987; Volenec, 1986; Alberda, 1957; Smith, 1974; Slack et al., 2000) providing energy for regrowth. The main components of NSC in most salt marsh grasses are glucose, sucrose, and fructose (Gorham et al., 1980) and C<sub>4</sub> plants are also known to predominantly accumulate starch (Smith, 1973). Different sugars play different roles in plant metabolism. For example, sucrose is known from studies of other plants to be ideal for

transport and long-term storage because it is nonreducing and relatively insensitive to metabolism (Arnold, 1968; Lemoine, 2000).

There have been only a handful of studies of NSC and its dynamics in *S. alterniflora*. Lytle and Hull (1980) used radiolabeled carbon to show that photosynthate produced late in the growing season was translocated to the rhizomes and used during growth in the following spring, but the form of that photosynthate was not specified. Many studies of NSC in *S. alterniflora* give only total NSC concentrations and examine only total above- and total below-ground biomass, though some studies have measured starch, and others have divided below-ground biomass into roots and rhizomes (Garza et al., 1994; Livingstone & Patriquin, 1981; Gallagher et al., 1984; Colmer et al., 1996).

Without data on the amount and type of carbon being stored for growth in the following season, it is hard to develop a predictive model for above- and below-ground production that can be used over multiple years. Models that do not incorporate below-ground storage will begin to diverge from observations as this material is used to promote growth during the spring months. Our study was aimed at getting a better understanding of how NSC and its different components are distributed within *S. alterniflora* and how this changes over time. Based on literature from other plants, we hypothesize that NSC concentrations will be greatest in the below-ground tissues during winter in the tall phenotype of *S. alterniflora*, with sucrose being the main NSC component used for long-term storage, and this will be reflected in different temporal changes in different NSC components. Our ultimate scientific goal is the creation of a data set to be used in developing a mechanistic model of *S. alterniflora* above- and below-ground production that can be run for multiple years and used to help understand marsh biogeochemical processes.

## **2. Materials and methods**

### **2.1. Site location**

Samples of above- and below-ground biomass were collected from among 6 sites within the domain of the Georgia Coastal Ecosystem Long Term Ecological Research (GCE-LTER) program on Sapelo Island, Georgia, on the southeastern coast of the USA (Figure 2.8). The chosen sites were located within a monotypic area of tall form *S. alterniflora*, close to the Duplin River, and adjacent to the GCE-LTER flux tower (31°26'38.2" N, 81°17'1.0" W) which provided meteorological data. Samples were collected monthly between September 2013 and August 2014.

### **2.2 Sampling and experimental methods**

Two cores were collected from locations randomly selected from within 6 long-term sampling sites (Figure 2.8). Above-ground samples were clipped at the ground level and the below-ground samples were collected using a 7.5 cm diameter PVC pipe. Cores were taken to a depth of 30 cm, taking care to preserve above-ground shoots; cores were collected such that there were 1 or 2 above-ground shoots per core. Samples were kept at 4 °C for one night. On the next day, the cores were gently washed with flowing fresh water over an 800 µm sieve to remove mud, then dried in an oven at 60 °C for 3 days. Above-ground tissues were separated into 6 distinct categories; green leaves, green stems, senescing yellow leaves, senescing yellow stems, flowers, and brown leaves and stems representing dead material. Only live roots and rhizomes were used and these were distinguished using the method described by Valiela et al. (1976). Below-ground cores were divided into 2 categories; shallow (0–10 cm) and deep (10–30 cm) parts. Each component of the plant biomass was weighed, and approximately 4 g of each tissue part was ground to a fine powder using a ball mill (model 8000-D Mixer/Mill, Spex Sample

Prep, Metuchen, NJ) until the material passed through a 1 mm screen. Ground samples were stored in airtight scintillation vials. NSC content in samples was analyzed using a method modified from Zhao et al. (2010). Approximately 16 mg of each dried powder sample were placed in a 1.5 mL micro-centrifuge tube. Sugars in samples were solubilized using 80% ethanol in an 80 °C water bath and the extraction process repeated three times to ensure all solubilized sugars from the samples were collected. The final extract volume was centrifuged for 15 min at  $13,500 \times g$ . Three replicates of supernatant were incubated with a sequence of enzymes in 96-well plates to quantify glucose, fructose, and sucrose content in each sample. Between extraction of each soluble NSC process, the tube containing supernatant was placed in boiling water to halt any digestion of sugars. Starch, the water-insoluble sugar remaining in the pellet after removal of the supernatant, was solubilized following the procedure specified in Zhao et al. (2010) and then reduced to glucose. The absorbance of each sample was determined photometrically at 340 nm using a 96-Well plate reader (Flexstation3 Benchtop Multi-mode Multiplate Reader, Molecular Devices, Sunnyvale, CA). NSC concentrations were quantified according to standard curves using D-(+)-glucose standards that were run with each plate.

### **2.3 Statistical analysis**

Differences in the amount of NSC as a percentage of dry weight between different tissues in the same core (e.g. differences between green leaves and green stems) were determined by calculating the Z-scores using the within-measurement means and standard deviations.

Differences were deemed significant at the 99% confidence level ( $p < 0.01$ ). In addition, we calculated the cross correlations using the sample cross correlation function (CCF) between the time series of NSC in the different above- and below-ground plant tissue compartments (using R) to look for potential relationships and lags.

## 2.4 Net primary production estimation

Net production was estimated using a model that depends on biomass, total irradiance at the top of the canopy, the angle of the sun above the horizon, temperature, ratio of green to total aboveground biomass, and percent nitrogen in dry leaves (Morris et al., 1984):

$$P = \frac{\psi TNF \sin(\vartheta) \left\{ \ln \left( L e^{\frac{\alpha B_c}{\sin(\vartheta)} + \lambda} \right) - \ln(L + \lambda) \right\}}{(\alpha(N + \eta))} - \rho T (F B_c + B_b) \quad (1)$$

where the symbols and values for constants are given in Table 2.1. Total irradiance was estimated from PAR measured at the flux tower (Figure 2.9) assuming that PAR was 50% of total irradiance and that there were  $2.77 \times 10^{18}$  quanta  $s^{-1} W^{-1}$  (Kirk, 1994); measured PAR was available as 5-minute data-logged values. The angle of the sun above the horizon was calculated using standard equations (Kirk, 1994) and air temperature was measured at the GCE Flux Tower, a level 3 weather station, adjacent to the sampling site.

Above- and below-ground areal biomasses were calculated on a per meter square basis by making use of stem density measurements made in adjacent plots along a transect near the flux tower at the same time as the cores were taken; above- and below-ground biomasses measured in the sample cores were scaled up assuming an average of two stems per core. Daily values of biomass were obtained by fitting a piecewise cubic Hermite interpolating polynomial to the monthly data. The ratio of green to total above-ground biomass was calculated from the core data as well—daily values were calculated using the same technique as for biomass. Nitrogen concentrations in above-ground components of *S. alterniflora*, including the brown, yellow and green tissues, were measured next to our plots by colleagues (unpubl. results). This nitrogen data showed a slightly lower concentration ( $\sim 0.3\%$ ) than the data from Morris et al. (1984) which measured nitrogen in only green leaves; both data sets show the same seasonal pattern. We have

compared model results using the new nitrogen data with those using Morris' data and found no significant change (mean = 0.03, variance = 0.007) in the difference of the two results in the model. Consequently, the percent nitrogen in leaves was assumed to be same as that given in Morris et al. (1984). All computer code was written and run using Matlab 2016b.

### **3. Results**

#### **3.1 Environmental conditions**

Solar irradiance and air temperature showed the expected seasonal cycles (Figure 2.9). The minimum daily average temperature was generally above 0 °C except for a brief period during January 2014. Daily precipitation was less than about 10.5 mm d<sup>-1</sup> and over the year was typical for the location (Figure 2.9).

#### **3.2 Biomass**

The total above-ground biomass showed a typical, strong annual cycle with maximum biomass occurring in late summer through early fall and a minimum in February (Figure 2.1a). Spring growth started to occur in early spring, with the initial greening of above-ground biomass occurring in March. On the whole, the total below-ground biomass was approximately constant within measurement uncertainty with the highest values occurring in December ( $20.9 \pm 6.2$  g core<sup>-1</sup>) and July ( $20.8 \pm 9.0$  g core<sup>-1</sup>) and the lowest in March ( $9.4 \pm 3.7$  g core<sup>-1</sup>). The total above-ground biomass leads the below-ground biomass with a 1-month lag ( $\rho = 0.91$ ).

#### **3.3 Non-structural carbohydrates**

Total non-structural carbohydrates show distinct above- and belowground patterns. Unsurprisingly, above-ground NSC follows a similar seasonal pattern to above-ground biomass (Figure 2.1). Below-ground total NSC shows distinct patterns suggestive of carbon net primary

production and translocation (Figure 2.1b). Below-ground total NSC peaks in midwinter ( $4.4 \pm 1.5 \text{ g core}^{-1}$  in December) as above-ground biomass and NSC are declining—there is a suggestion of an increase in belowground biomass, but this is well within the measurement uncertainties (Figure 2.1a). Below-ground total NSC drops approximately an order of magnitude to a minimum of  $0.44 \pm 0.12 \text{ g core}^{-1}$  in late February, remaining approximately constant at these low levels until April and then increasing to  $2.9 \pm 1.7 \text{ g core}^{-1}$  in July.

The dynamics of the four measured NSC differ between above- and below-ground tissues. Glucose and fructose were generally larger, as a percentage of dry mass, in above-ground tissues (Figure 2.2). Sucrose concentrations were generally similar between above- and belowground tissues, whereas starch concentrations were greater in belowground tissues during the winter (Figure 2.2). Glucose concentrations showed broadly similar temporal patterns to above-ground biomass, with peaks in above-ground biomass occurring in October and late May (Figures 2.1 & 2.2). Sucrose was generally the dominant form of NSC in both above- and below-ground tissues, with concentrations in above-ground tissue varying between approximately 5% and 14% of dry weight and between approximately 1% and 17% of dry weight in below-ground tissue. Starch concentrations showed distinctive temporal patterns (Figure 2.2). Above-ground starch concentrations were high in late autumn, dropping to almost zero in December before increasing again in early summer. Below-ground concentrations were between approximately 2% and 5% of dry weight until March when they dropped to zero before increasing again in June.

The dynamics of the different NSC components also varied between different tissue types. Changes in glucose and fructose showed similar patterns in green leaves and stems (Table 2.3, Figure 2.3), with two peaks in October and early summer. Both sugars were a generally higher proportion of dry weight and showed greater temporal variability in green stems. Similarly,

sucrose concentrations in green leaves and green stems showed very similar temporal patterns, with concentrations in green stems being generally higher than in green leaves. Interestingly, the peak in sucrose concentrations occurs a month later than the peak in glucose and fructose concentrations. Starch was almost absent from green leaves except during the summer. However, starch in green stems showed a distinctive pattern with peaks in October and July and being zero or less than 1% between December and May. Although there is a lot of scatter in the data and differences between cores, NSC in green leaves and stems were for the most part statistically different within individual cores throughout the year.

Glucose and fructose in yellow leaves and stems were generally lower than in green leaves and stems (Figure 2.4). Glucose concentrations were generally higher in the fall and winter, with values typically < 0.5% dry weight throughout the spring—a similar pattern was seen in sucrose concentrations, though concentrations in the fall and winter were higher than those for glucose. Fructose concentrations tended to remain slightly higher throughout the early spring, decreasing in April to < 1% dry weight. Within-core concentrations of both fructose and sucrose were generally statistically different between yellow stems and yellow leaves; some differences were seen for glucose when concentrations were relatively high in the fall and winter, but within-core yellow leaf and yellow stem concentrations were statistically similar for the lower concentrations found in the spring and summer. The seasonal pattern for starch in yellow leaves and stems was similar to that for green leaves and stems (Figures 2.3 & 2.4). Non-structural carbohydrates were extremely low or below the detection level in brown leaves and stems and flowers (not shown).

Concentrations of glucose, sucrose, and starch in below-ground tissue tended to show minimum values in late spring or early summer, whereas fructose concentrations were approximately constant (Figure 2.5). Sucrose was the dominant with maximum concentrations of

approximately 20% dry weight, similar to those seen in green leaves and stems. In general, within core NSC concentrations in 0 – 10 cm below-ground tissues were statistically different from those in the 10 – 30 cm depth range. However, there was considerable below-ground heterogeneity as depicted by the increase in non-overlapping patches in Figure 2.5. What is more, within-core measurements sometimes showed greater NSC concentrations in the 0 – 10 cm than the 10 – 30 cm depth range, while this was reversed at other times; such reversals did not appear in green or yellow tissues (Figure 2.3 and 2.4).

Maximum concentrations of NSC were found in above- and belowground tissues at different times of the year. Green stems had the highest concentration (measured as a percent of dry weight) of NSC at the start of the sampling in September 2013, and again between March through June of 2014. Maximum NSC concentrations showed a progression from green stems, through yellow stems, to below-ground biomass (Table 2.2) suggestive of a time progression of storage.

### **3.4. Net primary production**

Estimates of net primary production show an expected seasonal cycle, with values in late February and early March being consistently negative (Figure 2.6), corresponding the times of lowest above-ground biomass (Figure 2.1) and lowest sucrose and starch concentrations in above- and below-ground tissue (Figure 2.2). Estimates of net primary production reached maximum values of 88 g dry wt (dry weight) m<sup>-2</sup> d<sup>-1</sup> during the summer months. Annual estimates of below-ground gross and net production and below-ground respiration were made using the same calculations as found in Morris et al. (1984). Below-ground gross production was estimated to be 4.2 × 10<sup>3</sup> g C m<sup>-2</sup> y<sup>-1</sup> and belowground respiration was 1.3 × 10<sup>3</sup> g C m<sup>-2</sup> y<sup>-1</sup>.

## 4. Discussion

### 4.1. Differences in NSC Dynamics

The dynamics of above- and below-ground NSC components were quite different, indicating that different components are used for different purposes. Total NSC in below-ground tissue showed an expected seasonal pattern consistent with a significant component of NSC being translocated to the below-ground tissue where it was stored and used for metabolism during the winter and to help with regrowth in the spring. Most of this change appeared to be a result of changes in below-ground sucrose concentrations, which made up ~50 – 90% of the below-ground NSC. Starch also showed significant changes in belowground tissue, but these were far more variable and harder to interpret (Figure 2.5). Below-ground glucose concentrations also declined during fall and winter, but results were very variable and accounted for, at most, 2% of dry weight. Previous results by Lytle and Hull (1980) suggest that photosynthate is translocated below-ground and used for growth in the following spring. Our results are consistent with this finding and suggest that sucrose is mainly used for this purpose. Non-structural carbohydrate content in above-ground tissue peaked in fall and summer, with a distinct minimum in early spring. Glucose tends to be used in plants for short term energy storage and use, so we would expect it to show seasonal changes.

Our results are in general agreement with previous measurements but shed additional light on the distribution of the different sugars within the plant over time. Live above- and below-ground biomass showed similar annual variation to that found for *S. alterniflora* at Sapelo by Schubauer and Hopkinson (1984). Previous measurements of NSC in *S. alterniflora* from Georgia salt marshes showed NSC accounting for 4 – 10% of biomass (McIntire & Dunstan, 1976), whereas values between 9 and 31% were found for *S. alterniflora* growing in Nova

Scotia, Canada (Livingstone & Patriquin, 1981). In our samples, total NSC concentration varied between 3 and 17% of dry weight, a slightly larger range than that seen by McIntire and Dunstan (1976) but still lower than values seen in Nova Scotia. Studies transplanting short form *S. alterniflora* from different regions suggest that such a variation may be genetically determined and a result of *S. alterniflora* from higher latitudes storing more NSC in order to survive under harsher winter conditions (Seliskar et al., 2002). In addition, the distribution of the total NSC as a percentage of dry weights within different tissues of *S. alterniflora* showed an interesting pattern where by the total NSC is stored most in above-ground parts (Table 2.2) during the fall but its main distribution moves toward the below-ground in winter and returns back to the above-ground as the spring seasons approach.

#### **4.2. Consequences for modeling of *S. alterniflora***

Our main scientific objective for this study was to develop a data set that would inform the development of a model of above- and belowground production of *S. alterniflora*. Predictive models of *S. alterniflora* production rely on accurately determining the net balance between the production of new biomass and the loss of old biomass. Current models for *S. alterniflora* do not account for the storage and subsequent use of non-structural carbohydrates. Such models may under-predict year-to-year biomass if, as has been suggested, this material is used to maintain biomass during conditions of low primary production and to provide energy for initial production of photosynthetic biomass in the spring.

Morris et al. (1984) used a model to predict annual total NPP for tall *S. alterniflora* on Sapelo Island of  $2,200 \text{ g C m}^{-2} \text{ y}^{-1}$ , split between  $800 \text{ g C m}^{-2} \text{ y}^{-1}$  above-ground and  $1,400 \text{ g C m}^{-2} \text{ y}^{-1}$  below-ground. Total NPP over our sampling period, September 2013 to August 2014, estimated using the model given in Morris et al. (1984) was  $2,608 \text{ g C m}^{-2} \text{ y}^{-1}$ . A carbon

concentration of 42.9% g dry wt (Morris et al., 1984) was used to convert from dry weight biomass to carbon since our observed carbon concentration data (unpublished) showed a similar value ( $41 \pm 0.6\%$ ) throughout the seasons. The comparison of monthly net primary production estimated from the Morris et al. model with observed monthly changes in green biomass, non-structural carbohydrates of above- and below-ground tissues (Figure 2.7). The green above-ground biomass was calculated from the sum of measured green stem and green leaf biomass. The Morris et al. model does not allow for loss of above-ground tissue through grazing, the assumption being that loss of above-ground tissue occurs when respiration exceeds gross production. However, Figure 2.7 shows months (e.g. October – November) when there was a decrease in above-ground green tissue and a simultaneous positive total NPP. This period corresponded to a period of decrease in total above-ground biomass (Figure 2.1). This may also be a result of the equation for NPP not including yellow tissue in calculating the respiration. The high NPP from July to August (Figure 2.7) may be partially due to the fact that the equation for NPP does not include increased transpiration, energy consumed for osmotic adjustment (Hessini et al., 2009) or increased dark respiration (Giurgevich & Dunn, 1979).

We were unable to develop a consistent carbon budget for the whole plant. For some months the plants appear to be in a state of approximately balanced growth (e.g. September to October), but in others, there is an excess of estimated net primary production (e.g. December to January). There are several possible causes for this. One is that there are processes missing from the model we used to estimate NPP. For example, loss of above-ground biomass due to herbivory is not included in the model. Another possibility is that sampling was not representative of the actual biomass. As discussed below, this is always a problem in dealing with strongly heterogeneous environments such as salt marshes.

*Spartina alterniflora* is a clonal plant with significant below-ground biomass. Above-ground annual primary production ranges between  $150 \text{ g m}^{-2} \text{ y}^{-1}$  and  $900 \text{ g m}^{-2} \text{ y}^{-1}$  (Kirwan et al., 2009) and belowground net production between 600 and  $1,400 \text{ g C m}^{-2} \text{ y}^{-1}$  with an estimated translocation between 1,200 and  $6,800 \text{ g C m}^{-2} \text{ y}^{-1}$  of aboveground production to below-ground tissues (Morris et al., 1984). The heterogeneity of the below-ground biomass makes a precise and accurate sampling of this material something of a problem. NSC measurements from replicate cores differed sometimes by a factor of 2. We can estimate the number of cores that would have had to be taken to achieve an accuracy of  $1 \text{ mg g dry wt}^{-1}$  in determining NSC. If we assume that the parent distribution is a normal distribution with a range of approximately 4 times the population standard deviation (Thomson & Emery, 2014), then we estimate that typically we would need of the order of 20 cores per time point to achieve this kind of precision. This not only constitutes a considerable investment of labor but would also significantly alter the salt marsh and suggests that nondestructive methods (e.g. O'Connell et al., 2015) using the relationship between the leaf nitrogen concentration and root:shoot ratio may provide better approaches for at least assessing below-ground biomass. There was significant between-core variability in NSC concentrations, especially for below-ground material. Differences between the 0 – 10 cm and 10 – 30 cm depth ranges were generally significant ( $p < 0.01$ ). However, the maximum concentration of NSC could occur in either depth range. Patterns of above-ground NSC concentrations were more clearly delineated; for example, green stems generally had greater NSC concentrations than green leaves. We suggest that this heterogeneity in below-ground properties, along with the relatively constant below-ground biomass, argues for considering below-ground biomass as a single component in models, rather than subdividing it.

## Acknowledgements

This work was funded by a National Science Foundation grant (OCE-1237140) and with support from the UGA Graduate School. We would like to thank the editor and two anonymous reviewers for their comments which greatly improved the manuscript. We would like to thank M. Alber, S. Pennings, J. Morris, L. Donovan, and C. Luedtke for helpful discussions, A. Roberts and C. Hopkinson for the use of laboratory space and assistance in experimental procedures, and C. Reddy for sample collection.

## References

- Alberda, T. (1957). The effects of cutting, light intensity and night temperature on growth and soluble carbohydrate content of *Lolium perenne* L. *Plant and Soil*, 8(3), 199-230. doi: 10.1007/bf01666158
- Arnold, W. N. (1968). The selection of sucrose as the translocate of higher plants. *Journal of Theoretical Biology*, 21(1), 13-20. doi: [https://doi.org/10.1016/0022-5193\(68\)90056-8](https://doi.org/10.1016/0022-5193(68)90056-8)
- Boschker, H. T. S., de Brouwer, J. F. C., & Cappenberg, T. E. (1999). The contribution of macrophyte-derived organic matter to microbial biomass in salt-marsh sediments: Stable carbon isotope analysis of microbial biomarkers. *Limnology and Oceanography*, 44(2), 309-319. doi: 10.4319/lo.1999.44.2.0309
- Colmer, T. D., Teresa W-M, F., Läuchli, A., & Higashi, R. M. (1996). Interactive effects of salinity, nitrogen and sulphur on the organic solutes in *Spartina alterniflora* leaf blades. *Journal of Experimental Botany*, 47(3), 369-375. doi: 10.1093/jxb/47.3.369
- Danckwerts, J. E., & Gordon, A. J. (1987). Long-term partitioning, storage and re-mobilization of <sup>14</sup>C assimilated by *Lolium perenne* (cv. Melle). *Annals of Botany*, 59(1), 55-66. doi:

10.1093/oxfordjournals.aob.a087285

- Fulkerson, W. J., & Donaghy, D. J. (2001). Plant-soluble carbohydrate reserves and senescence - key criteria for developing an effective grazing management system for ryegrass-based pastures: a review. *Australian Journal of Experimental Agriculture*, 41(2), 261-275. doi: <https://doi.org/10.1071/EA00062>
- Gallagher, J. L., Wolf, P. L., & Pfeiffer, W. J. (1984). Rhizome and root growth rates and cycles in protein and carbohydrate concentrations in Georgia *Spartina alterniflora* Loisel. plants. *American Journal of Botany*, 71(2), 165-169.
- Gallagher, J. L., Reimold, R. J., Linthurst, R. A., & Pfeiffer, W. J. (1980). Aerial production, mortality, and mineral accumulation-export dynamics in *Spartina alterniflora* and *Juncus roemerianus* plant stands in a Georgia salt marsh. *Ecology*, 61(2), 303-312. doi: 10.2307/1935189
- Garza Jr, A., McLendon, T., & Drawe, D. L. (1994). Herbage yield, protein content, and carbohydrate reserves in gulf cordgrass (*Spartina spartinae*). *Journal of Range Management*, 47(1), 16-21.
- Giurgevich, J. R., & Dunn, E. L. (1979). Seasonal patterns of CO<sub>2</sub> and water vapor exchange of the tall and short height forms of *Spartina alterniflora* Loisel in a Georgia salt marsh. *Oecologia*, 43(2), 139-156. doi: 10.1007/bf00344767
- Gordon, A. J., Ryle, G. J. A., & Powell, C. E. (1977). The strategy of carbon utilization in unculm barley I. The chemical fate of photosynthetically assimilated <sup>14</sup>C. *Journal of Experimental Botany*, 28(6), 1258-1269. doi: 10.1093/jxb/28.6.1258
- Gorham, J., Hughes, L. L., & Wyn Jones, R. G. (1980). Chemical composition of salt-marsh plants from Ynys Môn (Anglesey): the concept of physiotypes. *Plant, Cell & Environment*, 3(5),

309-318. doi: 10.1111/1365-3040.ep11581858

Hessini, K., Martínez, J. P., Gandour, M., Albouchi, A., Soltani, A., & Abdelly, C. (2009). Effect of water stress on growth, osmotic adjustment, cell wall elasticity and water-use efficiency in *Spartina alterniflora*. *Environmental and Experimental Botany*, 67(2), 312-319.

Kirk, J. T. O. (1994). *Light and photosynthesis in aquatic ecosystems*. Cambridge University Press

Kirwan, M. L., Guntenspergen, G. R., & Morris, J. T. (2009). Latitudinal trends in *Spartina alterniflora* productivity and the response of coastal marshes to global change. *Global Change Biology*, 15(8), 1982-1989. doi: 10.1111/j.1365-2486.2008.01834.x

Knutson, P. L. (1988). Role of coastal marshes in energy dissipation and shore protection. In D.D. Hook, W. H. McKee Jr, L. Gregory, V. G. Burrell Jr, M. R. DeVoe,...& T. H. Shear (Eds.), *The ecology and management of wetlands* (pp. 161-175). Boston, MA: Springer.

Lambers, H. (1985). Respiration in intact plants and tissues: Its regulation and dependence on environmental factors, metabolism and invaded organisms. In R. Douce & D. A. Day (Eds.), *Higher Plant Cell Respiration* (pp. 418-473). Berlin, Heidelberg: Springer

Lemoine, R. (2000). Sucrose transporters in plants: update on function and structure. *Biochimica et Biophysica Acta (BBA)-Biomembranes*, 1465(1), 246-262.

Livingstone, D. C., & Patriquin, D. G. (1981). Belowground growth of *Spartina alterniflora* Loisel.: habit, functional biomass and non-structural carbohydrates. *Estuarine, Coastal and Shelf Science*, 12(5), 579-587. doi: [https://doi.org/10.1016/S0302-3524\(81\)80084-9](https://doi.org/10.1016/S0302-3524(81)80084-9)

Lytle, R. W., & Hull, R. J. (1980). Photoassimilate distribution in *Spartina alterniflora* Loisel. II. autumn and winter storage and spring regrowth1. *Agronomy Journal*, 72(6), 938-942. doi: 10.2134/agronj1980.00021962007200060018x

McIntire, G. L., & Dunstan, W. M. (1976). Non-structural carbohydrates in *Spartina alterniflora*

- Loisel. *Botanica marina*, 19(2), 93-96.
- McLeod, E., Chmura, G. L., Bouillon, S., Salm, R., Björk, M., Duarte, C. M., . . . & Silliman, B. R. (2011). A blueprint for blue carbon: toward an improved understanding of the role of vegetated coastal habitats in sequestering CO<sub>2</sub>. *Frontiers in Ecology and the Environment*, 9(10), 552-560. doi: 10.1890/110004
- Mendelssohn, I. A. (1979). Nitrogen metabolism in the height forms of *Spartina alterniflora* in North Carolina. *Ecology*, 60(3), 574-584. doi: 10.2307/1936078
- Morris, J. T., Houghton, R. A., & Botkin, D. B. (1984). Theoretical limits of belowground production by *Spartina alterniflora*: An analysis through modelling. *Ecological Modelling*, 26(3), 155-175. doi: [https://doi.org/10.1016/0304-3800\(84\)90068-1](https://doi.org/10.1016/0304-3800(84)90068-1)
- O'Connell, J., Byrd, K., & Kelly, M. (2015). A hybrid model for mapping relative differences in belowground biomass and root: shoot ratios using spectral reflectance, foliar N and plant biophysical data within coastal marsh. *Remote Sensing*, 7(12), 15837.
- Pennings, S. C., Merrily, A., Clark, R. A., Booth, M., Burd, A. B., Wei-Jun, C., ... & Joye, S. B. (2012). South Atlantic tidal wetlands. In D. P. Batzer & A. H. Baldwin (Eds.), *Wetland Habitats of North America: Ecology and Conservation Concerns* (pp. 45-61). University of California Press
- Robson, M. J. (1973). The growth and development of simulated swards of perennial ryegrass II. carbon assimilation and respiration in a seedling sward. *Annals of Botany*, 37(3), 501-518. doi: 10.1093/oxfordjournals.aob.a084717
- Schubauer, J. P., & Hopkinson, C. S. (1984). Above- and belowground emergent macrophyte production and turnover in a coastal marsh ecosystem, Georgia. *Limnology and Oceanography*, 29(5), 1052-1065. doi: 10.4319/lo.1984.29.5.1052

- Seliskar, D. M., Gallagher, J. L., Burdick, D. M., & Mutz, L. A. (2002). The regulation of ecosystem functions by ecotypic variation in the dominant plant: a *Spartina alterniflora* salt-marsh case study. *Journal of Ecology*, *90*(1), 1-11.
- Slack, K., Fulkerson, W. J., & Scott, J. M. (2000). Regrowth of prairie grass (*Bromus willdenowii* Kunth) and perennial ryegrass (*Lolium perenne* L.) in response to temperature and defoliation. *Australian Journal of Agricultural Research*, *51*(5), 555-561.
- Smith, D. (1973). Influence of drying and storage conditions on nonstructural carbohydrate analysis of herbage tissue—a review. *Grass and Forage Science*, *28*(3), 129-134.
- Smith, D. (1974). Growth and development of timothy tillers as influenced by level of carbohydrate reserves and leaf area. *Annals of Botany*, *38*(3), 595-606.
- Thomson, R. E., & Emery, W. J. (2014). *Data analysis methods in physical oceanography*. Newnes.
- Valiela, I., Teal, J. M., & Persson, N. Y. (1976). Production and dynamics of experimentally enriched salt marsh vegetation: Belowground biomass<sup>1</sup>. *Limnology and Oceanography*, *21*(2), 245-252. doi: 10.4319/lo.1976.21.2.0245
- Volenc, J. J. (1986). Nonstructural carbohydrates in stem base components of tall fescue during regrowth 1. *Crop Science*, *26*(1), 122-127.
- Zhao, D., MacKown, C. T., Starks, P. J., & Kindiger, B. K. (2010). Rapid analysis of nonstructural carbohydrate components in grass forage using microplate enzymatic assays. *Crop Science*, *50*(4), 1537-1545.

**Table 2.1** Definitions of symbols and parameter values. Parameter values were taken from Morris et al., (1984).

Symbol	Name	Units & Value
$P$	Total net production	$\text{g dry wt m}^{-2} \text{ h}^{-1}$
$B_c$	Above ground biomass	$\text{g dry wt m}^{-2}$
$B_b$	Below ground biomass	$\text{g dry wt m}^{-2}$
$T$	Air temperature	$^{\circ}\text{C}$
$\vartheta$	Solar elevation	radians
$L$	Solar irradiance at the top of canopy	$\text{W m}^{-2}$
$\lambda$	Half saturation constant for irradiance	$300 \pm 100 \text{ W m}^{-2}$
$\alpha$	Irradiance extinction rate within canopy	$(3.4 \pm 1.0) \times 10^{-4} \text{ m}^2 \text{ g dry wt}^{-1}$
$N$	Percent nitrogen in dry leaves	%
$F$	Ratio of green tissue to total canopy biomass	dimensionless
$\psi$	Temperature coefficient for gross production	$(7.1 \pm 1.7) \times 10^{-4} \text{ }^{\circ}\text{C}^{-1} \text{ h}^{-1}$
$\eta$	Half saturation constant for nitrogen	$0.36 \pm 0.29 \text{ \% dry wt}$
$\rho$	Temperature coefficient for dark respiration	$(2.3 \pm 0.6) \times 10^{-5} \text{ }^{\circ}\text{C}^{-1} \text{ h}^{-1}$

**Table 2.2** Distribution of the total NSC as a percentage of dry weight within different tissues of *Spartina alterniflora*. Values obtained by combining measurements from the two cores.

	Green leaves (%)	Green stems (%)	Yellow leaves (%)	Yellow stems (%)	Belowground 0-10 cm (%)	Belowground 10-30 cm (%)	Brown leaves and stems (%)	Flowers (%)	Total biomass (%)
Sep. 2013	2.70	57.16	0.03	0.24	28.37	11.51	0.00	0.00	13.04
Oct. 2013	8.67	37.94	1.03	29.08	14.37	8.64	0.07	0.20	15.82
Nov. 2013	2.64	20.53	0.65	19.52	42.09	14.33	0.17	0.06	11.98
Dec. 2013	3.31	13.05	0.74	12.57	38.49	31.85	0.00	0.00	15.33
Jan. 2014	3.16	12.68	0.61	5.35	50.93	26.65	0.63	n.p	10.09
Feb. 2014	9.87	7.91	2.40	n.p	39.36	40.45	n.p	n.p	3.28
Mar. 2014	20.54	39.05	0.67	0.10	18.34	21.30	n.p	n.p	6.20
Apr. 2014	20.28	59.79	0.06	0.10	11.23	8.55	n.p	n.p	6.74
May. 2014	17.95	41.18	0.13	0.17	27.43	13.14	n.p	n.p	13.00
June. 2014	17.80	50.42	0.57	0.45	14.96	15.80	n.p	n.p	17.28
July. 2014	9.24	31.98	0.28	0.33	43.82	14.35	n.p	n.p	13.85
Aug. 2014	9.65	47.80	0.95	0.20	21.54	19.64	0.23	n.p	14.84

n.p. : not present

**Table 2.3** *Spartina alterniflora*: contribution of each NSC in eight different tissues (n=3,  $\pm$ SDM, N.D=Not detected)

Tissue	Time	dry weight (g core <sup>-1</sup> )		Glucose (g dw <sup>-1</sup> core <sup>-1</sup> ) x 10 <sup>-2</sup>		Fructose (g dw <sup>-1</sup> core <sup>-1</sup> ) x 10 <sup>-2</sup>		Sucrose (g dw <sup>-1</sup> core <sup>-1</sup> ) x 10 <sup>-2</sup>		Starch (g dw <sup>-1</sup> core <sup>-1</sup> ) x 10 <sup>-2</sup>	
		core 1	core 2	core 1	core 2	core 1	core 2	core 1	core 2	core 1	core 2
Green Leaves	Sep. 13	4.95	6.18	0.50±0.00	1.11±0.66	0.24±0.00	1.30±1.64	5.85±2.91	18.78±2.60	1.05±0.42	0.50±0.00
	Oct. 13	8.43	7.65	9.18±8.58	9.20±0.89	12.42±5.99	7.89±0.81	55.66±4.56	48.89±1.28	0.64±0.00	0.54±0.00
	Nov. 13	2.31	1.49	3.37±1.01	1.00±0.50	2.53±2.18	0.57±0.46	13.95±4.43	6.00±0.40	1.54±0.23	N.D
	Dec. 13	1.24	5.20	N.D	N.D	1.20±0.28	3.62±0.50	5.68±0.59	34.08±0.90	0.00±0.00	N.D
	Jan. 14	1.91	2.19	N.D	0.04±0.00	0.89±0.97	0.16±0.23	10.79±2.72	6.15±0.61	0.82±0.12	N.D
	Feb. 14	1.20	0.79	0.79±0.37	0.19±0.12	1.42±0.59	0.61±0.28	5.73±0.90	2.12±0.16	0.57±0.10	0.03±0.04
	Mar. 14	2.37	3.09	N.D	N.D	4.70±0.49	5.08±0.05	13.02±1.90	14.77±0.38	0.15±0.11	N.D
	Apr. 14	6.40	3.04	8.21±0.55	1.53±0.83	11.25±0.55	0.12±0.00	26.78±1.11	15.73±2.15	0.00±0.00	0.43±0.19
	May 14	6.43	4.30	1.45±1.18	1.84±1.68	8.33±1.97	6.72±2.24	52.54±3.12	34.87±8.11	0.72±0.13	2.51±0.09
	Jun. 14	13.18	8.70	3.93±4.53	13.03±1.23	3.81±3.30	8.34±1.69	40.86±22.70	161.51±9.94	0.00±0.00	10.88±0.28
Jul. 14	4.44	8.34	1.09±1.34	2.17±3.10	2.08±2.08	6.22±5.84	17.75±10.27	36.36±14.22	9.42±3.43	16.69±6.01	
Aug. 14	5.40	3.72	6.01±5.69	1.01±0.75	4.97±5.28	2.40±0.85	45.99±7.88	17.52±1.24	15.25±0.87	N.D	
Green Stems	Sep. 13	16.10	14.05	35.45±0.67	18.38±6.32	18.80±0.83	8.30±7.02	207.56±2.67	169.17±8.23	40.64±0.85	97.99±0.75
	Oct. 13	10.70	9.69	83.12±1.18	47.74±1.70	47.51±2.97	4.76±5.20	180.50±4.67	158.98±4.36	89.21±0.18	22.32±2.97
	Nov. 13	9.78	7.77	12.46±2.14	10.46±1.47	6.08±3.57	5.67±1.15	60.77±18.89	60.06±6.83	3.67±0.90	45.13±0.94
	Dec. 13	5.58	7.04	2.84±1.11	0.00±0.00	2.39±1.30	35.25±1.12	25.96±1.42	105.98±6.44	0.00±0.00	N.D
	Jan. 14	2.40	3.20	3.10±0.24	5.77±0.47	2.93±0.42	2.71±0.65	33.06±3.86	29.41±2.72	0.67±0.12	N.D
	Feb. 14	0.56	0.29	0.73±0.15	0.16±0.08	1.28±0.28	0.99±0.11	3.30±0.64	2.39±0.09	0.00±0.00	N.D
	Mar. 14	1.63	3.24	0.88±0.23	3.50±0.23	5.19±0.40	19.24±0.50	11.37±1.43	39.37±0.62	0.00±0.00	N.D
	Apr. 14	7.68	6.45	6.25±0.47	11.96±0.88	5.52±0.55	26.96±1.97	45.22±1.08	77.93±2.66	0.00±0.00	N.D
	May 14	3.70	6.77	14.83±0.77	26.82±1.68	13.05±0.88	23.15±1.48	66.02±0.59	108.71±6.83	0.00±0.00	N.D
	Jun. 14	25.65	12.25	50.20±21.34	17.36±5.12	29.36±27.02	11.94±6.28	417.99±53.31	244.88±7.57	0.00±0.00	4.93±0.75
Jul. 14	6.71	7.97	11.14±1.64	31.58±2.85	7.63±2.18	20.74±4.03	86.06±10.57	101.21±9.99	35.78±7.25	22.76±8.07	
Aug. 14	8.71	11.30	22.68±3.24	22.17±2.30	20.99±5.57	13.90±3.58	128.68±2.30	188.53±6.28	31.40±2.07	N.D	
Yellow Leaves	Sep. 13	N.D	0.25		0.12±0.08		0.09±0.08		0.56±0.14		0.02±0.00
	Oct. 13	1.54	0.45	3.05±0.45	0.25±0.14	0.99±0.54	0.06±0.07	19.46±2.20	0.48±0.21	0.11±0.00	N.D
	Nov. 13	1.21	0.78	0.94±0.16	0.88±0.20	0.46±0.31	0.08±0.09	2.74±0.80	1.64±0.21	N.D	N.D
	Dec. 13	0.75	4.42	0.00±0.00	N.D	0.05±0.05	0.00±0.00	2.18±0.25	2.35±0.82	N.D	N.D
	Jan. 14	1.20	1.38	0.02±0.00	0.02±0.00	0.09±0.13	0.55±0.51	1.46±0.30	1.66±0.48	N.D	N.D
	Feb. 14	0.39	0.30	0.09±0.07	0.01±0.00	0.10±0.10	0.45±0.11	0.35±0.15	1.11±0.09	N.D	N.D
	Mar. 14	0.21	0.15	0.00±0.00	N.D	0.16±0.04	0.44±0.03	0.07±0.03	0.32±0.01	N.D	N.D
	Apr. 14	0.32	0.27	0.00±0.00	0.04±0.01	0.01±0.00	0.01±0.00	0.01±0.00	0.08±0.01	N.D	N.D
	May 14	0.74	0.14	0.15±0.07	0.02±0.02	0.17±0.04	0.03±0.01	0.60±0.19	0.05±0.02	0.02±0.02	0.01±0.01
	Jun. 14	1.83	1.13	0.59±0.46	N.D	0.93±0.54	0.00±0.00	5.26±0.84	0.93±0.24	0.13±0.11	1.59±0.09
Jul. 14	0.35	0.57	0.01±0.00	0.01±0.00	0.03±0.02	0.01±0.00	0.42±0.04	0.67±0.00	0.59±0.13	0.73±0.00	
Aug. 14	0.31	1.89	0.31±0.52	0.92±1.29	0.01±0.00	0.75±1.30	0.60±0.07	4.18±1.82	0.54±0.18	N.D	
Yellow Stems	Sep. 13	1.44	2.18	0.17±0.00	0.65±0.35	0.17±0.09	0.20±0.06	0.27±0.10	0.90±0.50	0.11±0.00	0.17±0.00
	Oct. 13	15.61	14.40	30.96±4.56	16.83±3.56	10.02±5.43	10.19±6.36	197.27±22.28	103.16±19.82	1.08±0.00	110.90±1.51
	Nov. 13	9.45	12.14	18.33±0.87	12.70±2.23	15.76±1.29	5.21±3.58	40.85±1.28	84.79±15.85	12.23±0.65	11.97±0.28
	Dec. 13	5.75	3.07	4.84±0.95	7.36±0.97	2.55±1.38	5.92±1.57	91.95±5.60	41.84±3.07	N.D	0.46±0.07
	Jan. 14	2.70	2.54	1.81±0.60	1.57±0.18	1.02±0.51	1.11±0.52	13.91±2.06	14.36±1.48	N.D	N.D

Feb. 14	N.D	N.D									
Mar. 14	N.D	0.09		N.D		0.08±0.00		0.08±0.01			N.D
Apr. 14	0.45	0.26	0.02±0.02	0.03±0.03	0.04±0.02	0.01±0.00	0.08±0.06	0.07±0.02		N.D	N.D
May 14	0.92	0.27	0.22±0.09	0.07±0.06	0.10±0.06	0.03±0.06	0.58±0.05	0.10±0.03		N.D	N.D
Jun. 14	2.08	1.60	0.04±0.06	0.01±0.01	0.06±0.11	0.15±0.13	3.61±2.32	0.87±0.12		N.D	2.43±0.09
Jul. 14	0.21	0.70	0.01±0.01	0.02±0.01	0.01±0.01	0.05±0.03	0.28±0.03	0.92±0.12	0.41±0.11		1.11±0.04
Aug. 14	0.31	0.22	0.04±0.05	0.04±0.03	0.08±0.12	0.01±0.02	1.06±0.08	0.03±0.04	0.58±0.19		N.D

Tissue	Time	dry weight (g core <sup>-1</sup> )		Glucose (g dw <sup>-1</sup> core <sup>-1</sup> ) x 10 <sup>-2</sup>		Fructose (g dw <sup>-1</sup> core <sup>-1</sup> ) x 10 <sup>-2</sup>		Sucrose (g dw <sup>-1</sup> core <sup>-1</sup> ) x 10 <sup>-2</sup>		Starch (g dw <sup>-1</sup> core <sup>-1</sup> ) x 10 <sup>-2</sup>	
		core 1	core 2	core 1	core 2	core 1	core 2	core 1	core 2	core 1	core 2
Brown leaves & stems	Sep. 13	0.98	0.12	N.D	N.D	N.D	N.D	N.D	N.D	N.D	N.D
	Oct. 13	0.03	1.65	N.D	0.99±0.24	N.D	0.06±0.01	N.D	1.18±0.31	N.D	N.D
	Nov. 13	0.90	1.72	N.D	0.76±0.58	N.D	0.24±0.31	N.D	1.26±0.44	N.D	N.D
	Dec. 13	4.67	0.88	N.D	N.D	N.D	N.D	N.D	N.D	N.D	N.D
	Jan. 14	0.43	N.D	0.08±0.08		0.03±0.04		0.12±0.08		N.D	
	Feb. 14	N.D	N.D								
	Mar. 14	N.D	N.D								
	Apr. 14	N.D	N.D								
	May 14	N.D	N.D								
	Jun. 14	N.D	N.D								
Flowers	Jul. 14	N.D	N.D								
	Aug. 14	N.D	2.87		0.51±0.66		0.30±0.43		1.25±1.58		N.D
	Sep. 13	N.D	0.69		N.D		N.D		N.D		N.D
	Oct. 13	1.54	N.D	1.18±0.35		0.34±0.23		4.64±0.47		0.11±0.00	
	Nov. 13	0.21	0.55	0.15±0.07	N.D	0.02±0.02	N.D	0.15±0.04	N.D	N.D	N.D
	Dec. 13	0.18	N.D	N.D		N.D		N.D		N.D	
	Jan. 14	N.D	N.D								
	Feb. 14	N.D	N.D								
	Mar. 14	N.D	N.D								
	Apr. 14	N.D	N.D								
Below-ground 0-10cm	May 14	N.D	N.D								
	Jun. 14	N.D	N.D								
	Jul. 14	N.D	N.D								
	Aug. 14	N.D	N.D								
	Sep. 13	9.39	15.67	3.13±1.24	13.35±1.94	5.23±1.76	3.46±1.73	91.74±3.34	116.23±4.11	27.47±1.12	27.08±0.56
	Oct. 13	7.23	14.17	14.41±1.64	8.01±3.37	5.97±2.31	6.20±5.17	60.35±3.16	88.90±25.67	6.57±0.36	40.74±1.67
	Nov. 13	10.69	14.82	8.17±0.63	14.35±3.16	1.43±1.03	8.29±3.34	71.30±6.33	261.90±22.74	40.96±1.43	49.85±1.62
	Dec. 13	12.34	8.68	6.57±1.75	5.15±0.56	1.50±1.55	0.50±0.73	223.57±3.08	155.54±2.14	47.49±3.79	36.55±2.64
Jan. 14	10.47	9.76	6.41±0.55	3.61±0.31	2.46±0.33	2.53±0.19	107.08±7.19	76.49±10.26	65.92±1.52	56.72±0.24	
Feb. 14	6.36	8.87	7.12±1.49	N.D	0.08±0.00	7.48±1.13	4.33±0.42	26.84±1.72	0.00±0.00	0.00±0.00	
Mar. 14	7.94	3.67	N.D	N.D	5.74±1.02	3.05±0.22	13.25±0.78	9.47±0.37	0.00±0.00	0.00±0.00	
Apr. 14	4.44	2.79	0.47±0.27	1.29±0.54	0.65±0.45	0.73±0.57	24.86±1.36	7.20±0.83	1.35±0.68	0.00±0.00	
May 14	4.07	8.47	4.26±0.16	7.29±1.51	3.58±0.25	4.27±1.92	55.14±0.74	70.47±3.96	3.26±0.07	7.46±0.03	
Jun. 14	6.94	5.92	8.59±1.78	4.24±0.97	6.69±2.21	2.08±1.14	135.57±7.46	72.68±5.48	14.37±0.71	0.00±0.00	

	Jul. 14	3.69	21.57	1.65±0.45	11.64±2.37	0.96±0.41	8.10±3.18	45.70±6.10	287.85±9.56	13.19±3.91	70.63±3.81
	Aug. 14	6.96	2.87	4.56±0.72	1.72±0.33	9.43±0.41	N.D	112.11±0.70	44.17±3.01	24.85±5.16	6.07±0.98
Below-ground 10-30cm	Sep. 13	5.77	2.47	3.73±0.17	1.19±0.11	2.46±0.43	0.13±0.00	91.12±2.79	18.05±0.26	26.31±0.59	0.44±0.22
	Oct. 13	6.34	5.27	8.05±1.04	4.97±0.89	0.35±0.00	4.70±1.47	49.12±1.43	40.45±9.68	0.49±0.00	31.50±0.60
	Nov. 13	1.62	10.55	0.33±0.06	14.04±1.04	0.25±0.35	5.41±1.71	4.06±1.00	175.82±5.29	N.D	30.48±1.88
	Dec. 13	4.45	16.36	0.80±0.88	4.98±0.93	2.79±0.97	4.18±2.77	81.74±5.96	233.03±16.98	7.93±1.24	35.38±3.54
	Jan. 14	10.33	4.39	9.20±2.80	1.20±0.58	9.44±2.91	0.80±0.49	90.44±14.38	25.93±2.26	58.16±1.77	0.20±0.30
	Feb. 14	9.04	5.57	1.98±1.56	N.D	0.13±0.00	5.00±0.60	10.56±2.45	21.05±0.39	N.D	N.D
	Mar. 14	5.13	2.03	N.D	N.D	2.90±1.00	2.07±0.24	14.16±1.23	13.22±0.24	N.D	N.D
	Apr. 14	6.58	6.18	3.72±2.09	0.09±0.00	0.25±0.00	0.40±0.30	13.00±1.26	8.59±1.09	N.D	N.D
	May 14	7.42	4.09	2.38±0.97	2.73±0.67	1.75±0.84	1.23±0.85	72.52±4.24	5.04±0.83	10.61±0.55	N.D
	Jun. 14	9.23	3.54	8.38±3.69	3.74±0.56	3.47±5.05	1.25±0.70	169.62±7.85	62.40±2.69	5.13±0.75	N.D
	Jul. 14	9.33	7.08	0.44±0.41	1.80±0.54	0.64±0.54	1.04±0.63	11.69±2.46	73.57±2.14	11.03±0.00	27.40±1.41
Aug. 14	3.13	13.28	1.02±0.98	5.68±6.19	2.12±1.28	3.53±5.90	38.35±3.14	84.14±24.54	4.36±0.00	N.D	

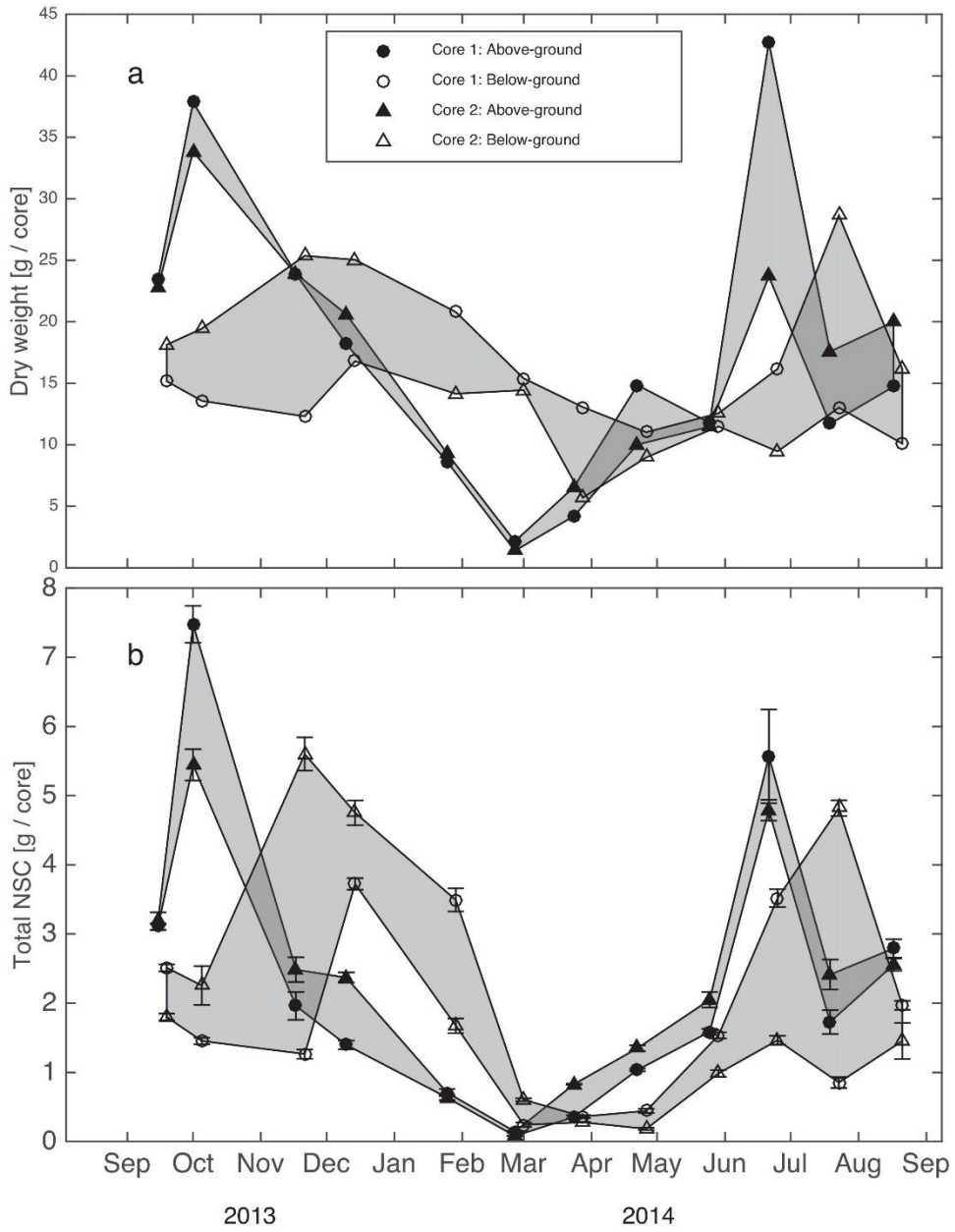


**Figure 2.1** Measured dry weight and non-structural carbohydrates in each core. (a) Above- and below-ground dry mass. (b) Amount of non-structural carbohydrate from triplicate measurements of the same core ( $n = 3$ ), error bars represent standard deviation. Shaded areas are guides to indicate when measurements between the cores overlap. Values for core 1 and core 2 are offset by 2 days from the actual day of measurement for clarity (both cores were taken on the same day).

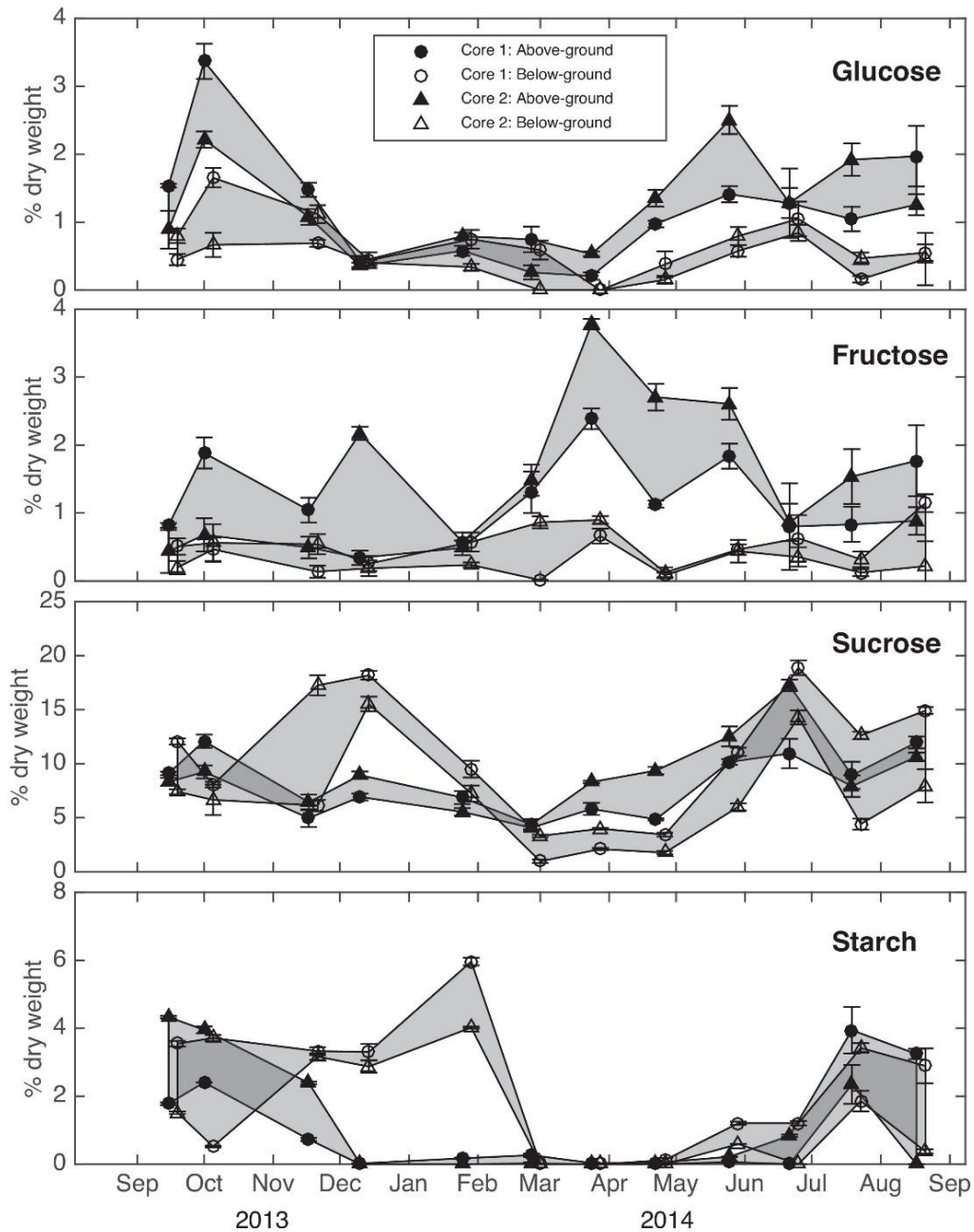


**Figure 2.2** Above- and below-ground glucose, fructose, sucrose, and starch concentrations as percentages of above- and below-ground dry weight combined from triplicate measurements of the same core ( $n = 3$ ); error bars represent standard deviation. Shaded areas are guides to indicate when measurements between the cores overlap. Values for core 1 and core 2 are offset by 2 days from the actual day of measurement for clarity (both cores were taken on the same day)

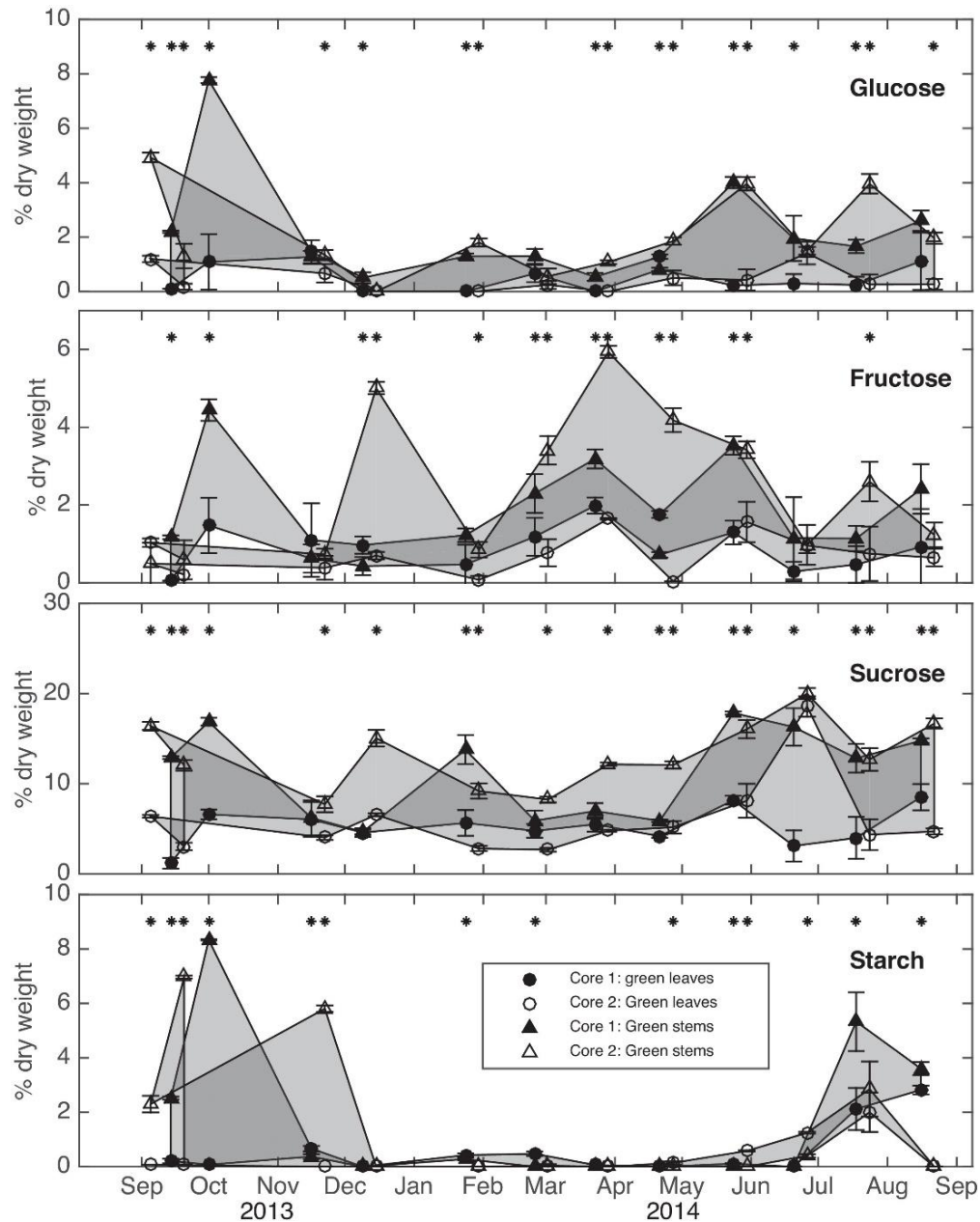


**Figure 2.3** Within-core measurements of glucose, fructose, sucrose and starch as a percentage of dry weight in green stems, green leaves ( $n = 3$ ). Error bars represent standard deviation. Asterisks indicate significant differences ( $p = 0.01$ ,  $n = 3$ ) between green leaves and green stems for each individual core. Shaded areas are guides to indicate when measurements between the cores overlap. Values for core 1 and core 2 are offset by 2 days from the actual day of measurement for clarity (both cores were taken on the same day).

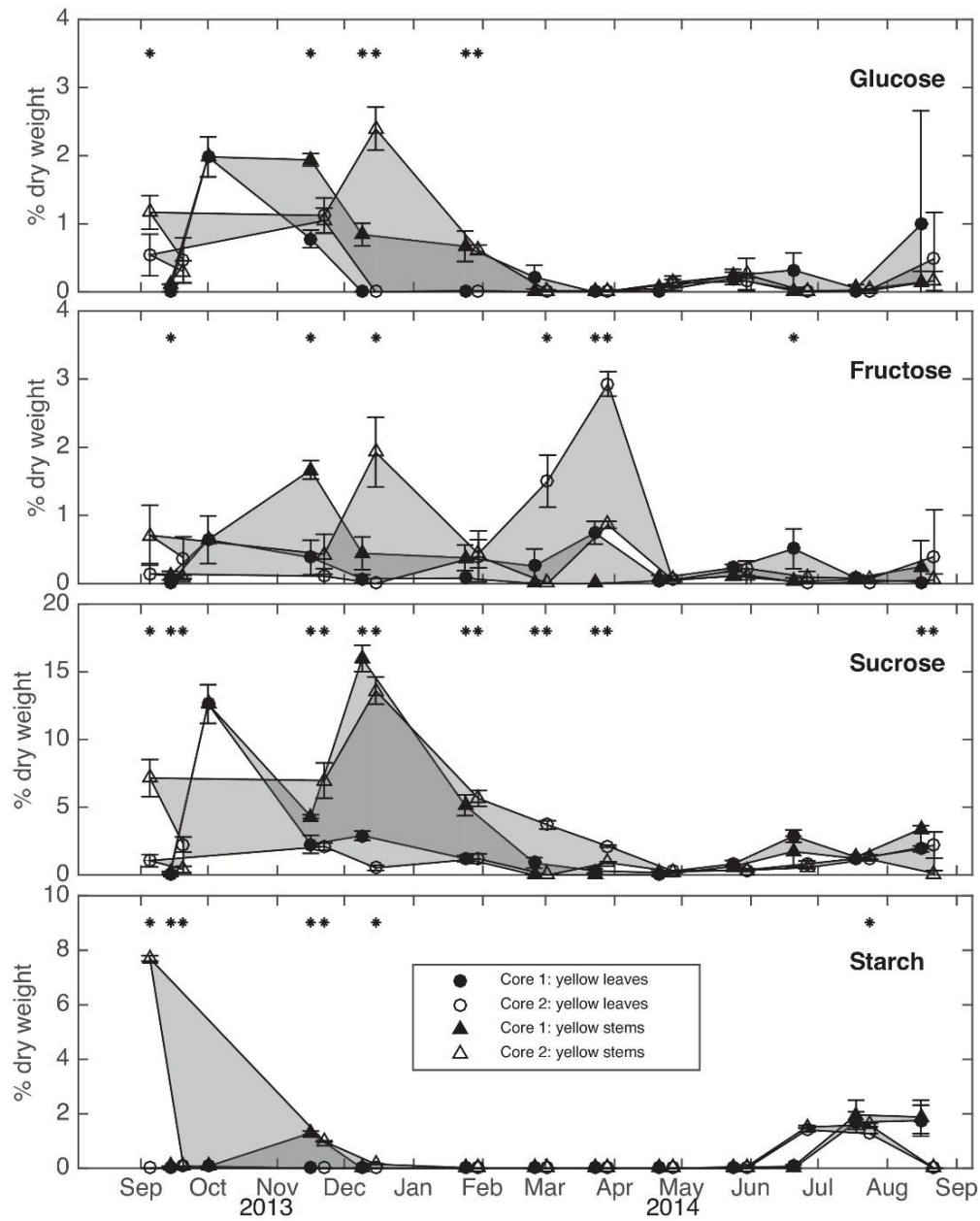


**Figure 2.4** Within-core measurements of glucose, fructose, sucrose and starch as a percentage of dry weight in yellow stems and yellow leaves ( $n = 3$ ). Error bars represent standard deviation. Asterisks indicate significant differences ( $p = 0.01$ ,  $n = 3$ ) between green leaves and green stems for each individual core. Shaded areas are guides to indicate when measurements between the cores overlap. Values for core 1 and core 2 are offset by 2 days from the actual day of measurement for clarity (both cores were taken on the same day).

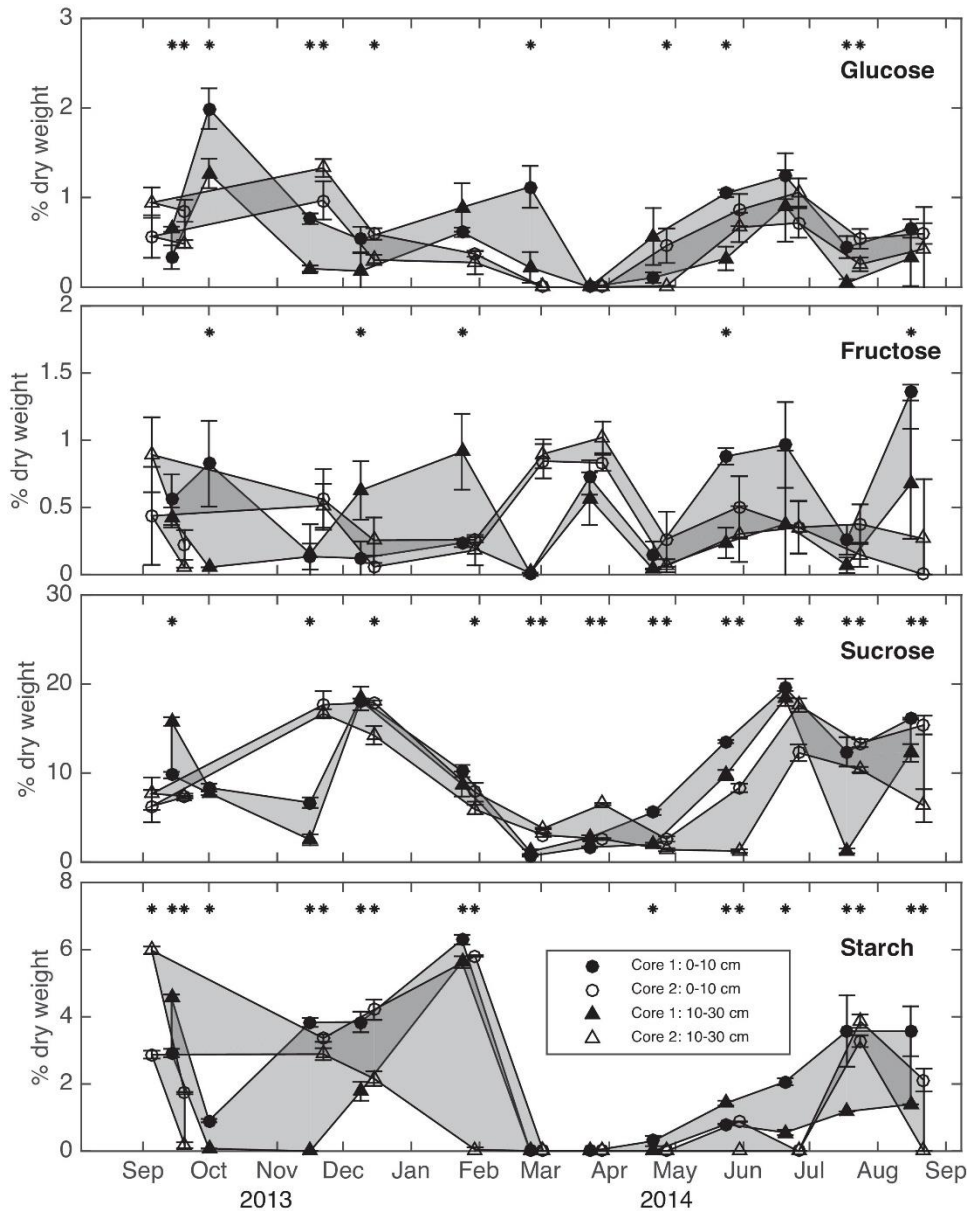


**Figure 2.5** Within-core measurements of glucose, fructose, sucrose and starch concentrations as percentages of dry weight in below-ground tissue, divided in to shallow (0–10 cm) and deep (10–30 cm) zones (n = 3). Error bars represent standard deviation. Asterisks indicate significant differences (p = 0.01, n = 3) between green leaves and green stems for each individual core. Shaded areas are guides to indicate when measurements between the cores overlap. Values for core 1 and core 2 are offset by 2 days from the actual day of measurement for clarity (both cores were taken on the same day).

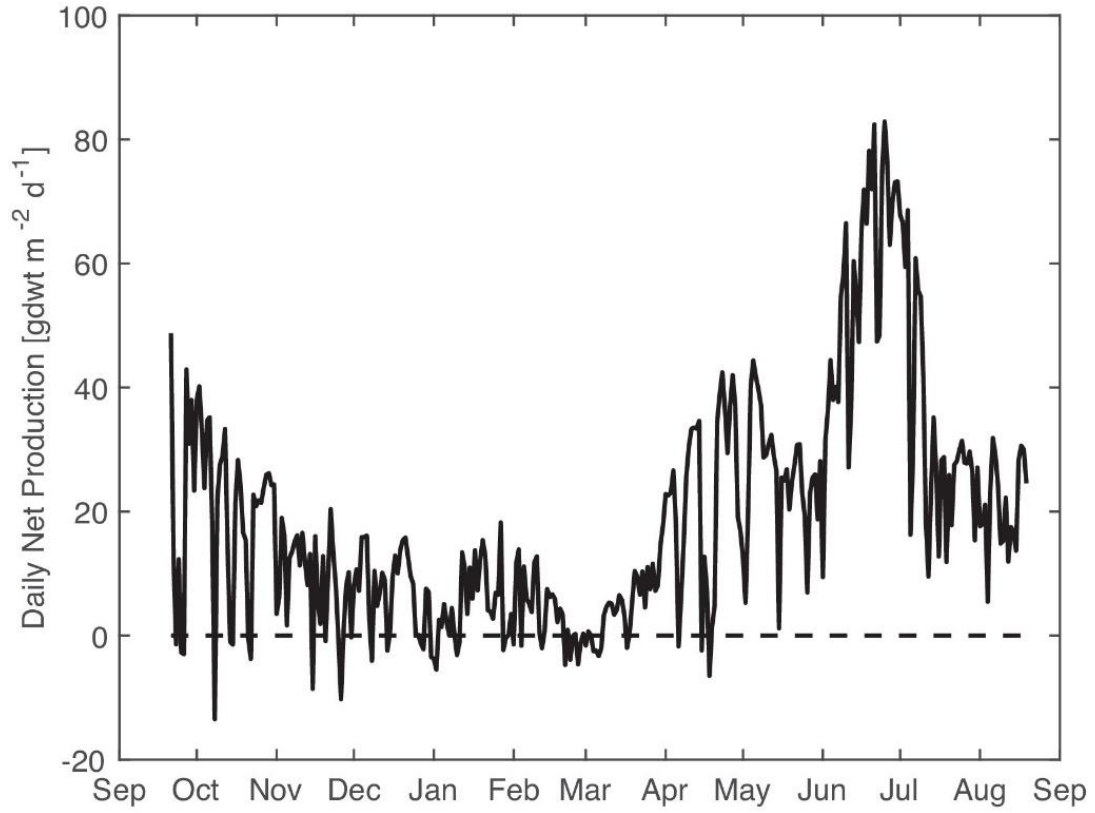


**Figure 2.6** Estimated daily net production using the Morris model (Equation (1)) and local environmental variables (Figure 2.9).

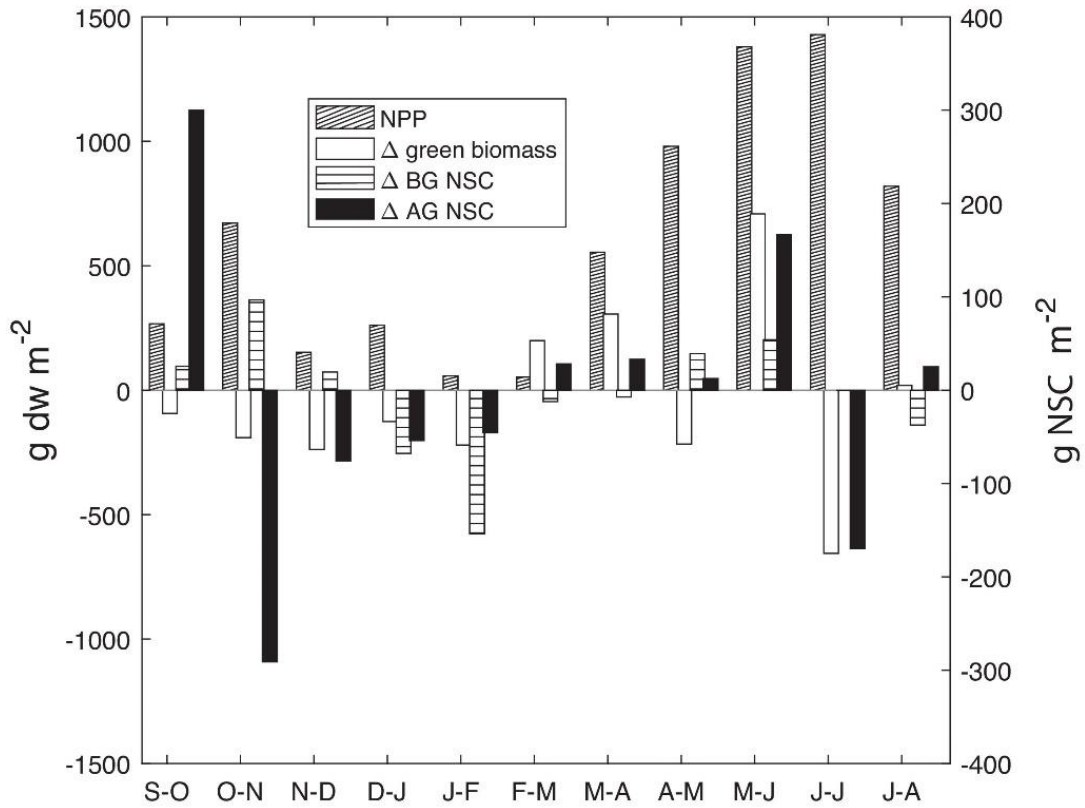


**Figure 2.7** Comparison of monthly net primary production (estimated from the model, Equation (1)) with observed monthly changes in green biomass, below-ground non-structural carbohydrate and above-ground non-structural carbohydrate.

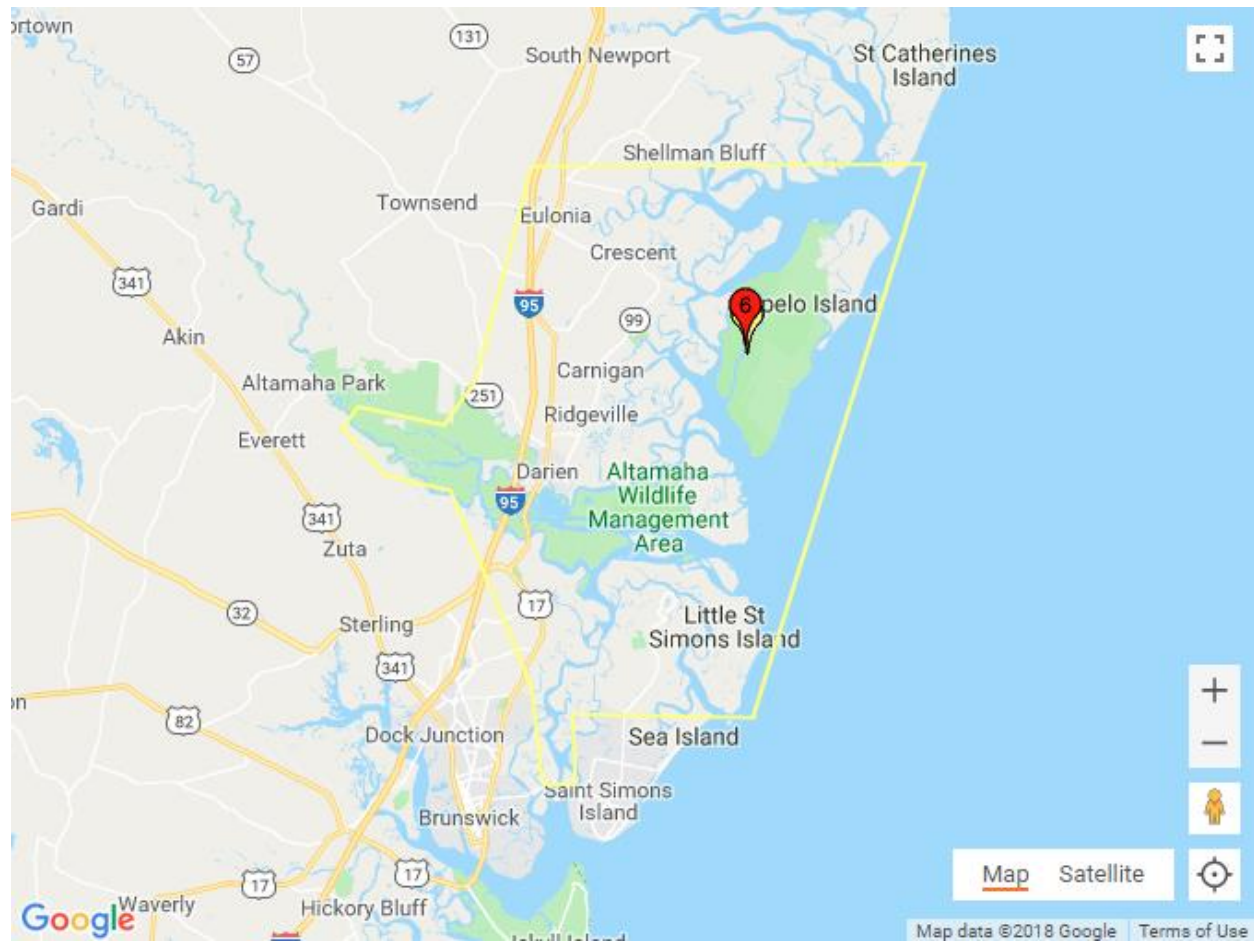


**Figure 2.8** Site map (as a KMZ file view) showing the location and boundary of the Georgia Coastal Ecosystems Long Term Ecological Research (GCE-LTER) site on Sapelo Island (Georgia, USA), the location of the flux tower, and the location of the 6 sampling sites used in this study.

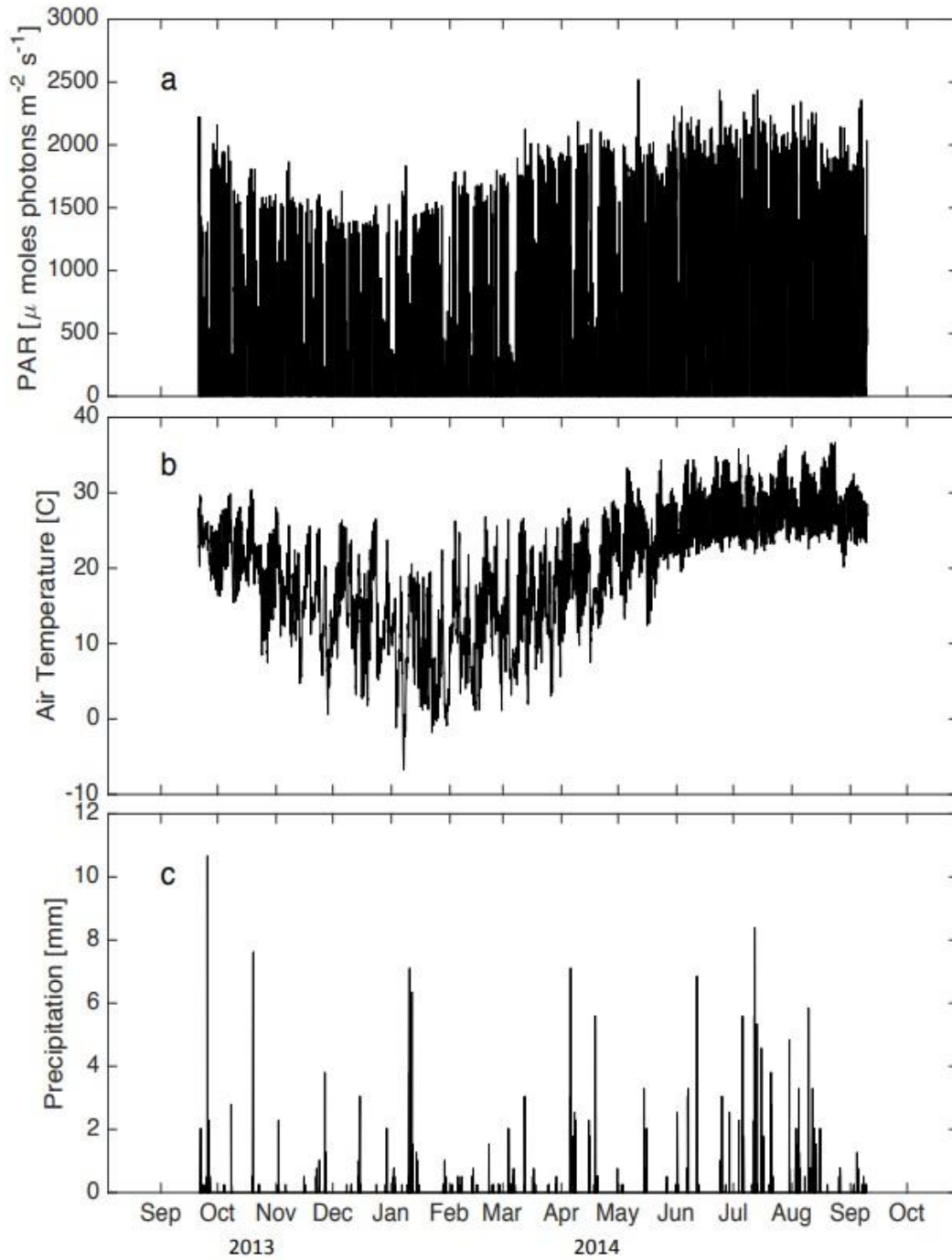


**Figure 2.9** Environmental data measured at the GCE-LTER flux tower (located near the sampling site) during the sampling period. (a) Photosynthetically active radiation, (b) air temperature, (c) precipitation

## CHAPTER 3

# MODELING THE PHENOLOGY-BASED GROWTH DYNAMICS OF SHORT, MEDIUM, AND TALL *SPARTINA ALTERNIFLORA* IN A GEORGIA MARSH, USA<sup>1</sup>

---

<sup>1</sup> Jung, Y., & Burd, A. To be submitted to *Ecological Modeling*

## Abstract

The growth and production dynamics of short, medium, and tall types of *Spartina alterniflora* on Sapelo Island in a Georgia marsh, USA were examined using a phenology-based growth model (PG model). The model included the salinity effect on the growth and computed the carbon translocation between above- and below-ground tissues during three periods (growth, senescence, and dormancy periods). Model results indicate that short form *S. alterniflora* allocates 82% of its photosynthate to the below-ground biomass during the growing season compared to tall (0.52%) and medium (0.22%) type *S. alterniflora*. The proportion of the carbon translocation from the above-ground senescing tissues to the below-ground biomass was also highest in short form *S. alterniflora*. However, the absolute amount of carbon translocated from above- to below-ground tissues during growing and senescing periods were highest in tall form *S. alterniflora* due to its greatest live and senescing above-ground biomass. Model results reveal that the carbon translocation from below- to above-ground tissues may not be required for survival during winter on Sapelo Island, Georgia.

## 1. Introduction

*Spartina alterniflora* is a C4 deciduous halophyte and is the dominant and most productive salt marsh grass along the east coast of the United States (Dawes, 1998; O'Donnell & Schalles, 2016). Above-ground production varies between  $0.4 \text{ kg m}^{-2} \text{ y}^{-1}$  –  $2.2 \text{ kg m}^{-2} \text{ y}^{-1}$ , but below-ground production is typically larger, varying between  $3.5 \text{ kg m}^{-2} \text{ y}^{-1}$  –  $3.9 \text{ kg m}^{-2} \text{ y}^{-1}$  (Valiela et al., 1976; Tripathee & Schäfer, 2015), but can reach as high as  $7.4 \text{ kg m}^{-2} \text{ y}^{-1}$  in marshes along the northern Gulf of Mexico (Stagg et al., 2017). In spite of this, most production studies have

been limited to above-ground dynamics, missing the important components of below-ground production, storage, and timing of resource translocation (Jung & Burd, 2017).

Growth and production of *S. alterniflora* are affected by environmental factors such as salinity, oxygen, nutrient availability, and soil redox potential, and these factors determine the typical heights of the plants and their zonation within the marsh (Mendelssohn, 1979; Mendelssohn & Seneca, 1980; Howes et al., 1981). The tallest height form (> 1 m) has the highest production and grows near creek banks in soils that have relatively low porewater salinity. In contrast, the shortest height form (< 50 cm) is found in the marsh interior where porewater salinities are higher — the medium height form grows in regions with an intermediate salinity range.

The productivity of *S. alterniflora* varies on both spatial and temporal scales. Spatial differences in productivity on a local scale are largely determined by abiotic factors, particularly porewater salinity (Adam, 1963; O'Donnell & Schalles, 2016). The infrequently-flooded high marsh environment accumulates salinity in soils. The increased salinity reduces stomatal conductance which in turn, decreases CO<sub>2</sub> assimilation (Giurgevich & Dunn, 1979) and increases leaf respiration (Levering & Thomson, 1971). Consequently, salinity inversely affects the growth of *S. alterniflora* with greatest growth rates at salinities less than 20 ppt (Phleger, 1971; Parrondo et al., 1978, Ge et al., 2014). Differences in below-ground biomass change with salinity, with root-shoot biomass ratios of 1.4, 11.2, and 48.9 for tall, medium and short forms of *S. alterniflora* (Gallagher, 1974). Field experiments indicate that *S. alterniflora* biomass is negatively correlated with salinity (Drake & Gallagher, 1984; Nestler, 1977) and *S. alterniflora* does not exist at salinities greater than 75 ppt. Richards et al. (2005) demonstrated that the number of leaves of salt marsh grasses increases and their leaf sizes decreases as salinity

increase, which in turn affect their above-ground biomass. These reasons suggest that it is essential to include salinity when modeling production of *S. alterniflora*.

Productivity differences on regional scales are largely dependent on geographical differences in climate, tidal amplitude, wetland types and phenology (Seneca & Broome, 1972; Seneca & Blum, 1984). In spite of its important role in determining the growth of *S. alterniflora*, phenology is rarely included in models of production. In *S. alterniflora*, longer photoperiods are associated with increased net primary production (NPP) (O'Donnell & Schalles, 2016). In addition, the timing and duration of resource translocation between above- and below-ground tissues appear to be linked to other events in the life history of the plant. For example, *S. alterniflora* starts to allocate carbon to below-ground tissues when flowering begins (Crosby et al., 2015) and rhizome biomass increases as foliage senescence starts (Elsley-Quirk et al., 2011). The timing and duration of these events may control the amount of material a plant can store below-ground during the winter, thereby affecting the resources available for growth in early spring of the following year. This suggests that including both above- and below-ground processes, and the phenological connections between them, is important for long term modeling of *S. alterniflora* growth.

There are only a few published models of the growth and production of *S. alterniflora*, and few of those include both above- and below-ground processes. Estimates of the maximum annual below-ground production rates using an above-ground production model and mass balance indicate that the maximum net below-ground production for *S. alterniflora* on Sapelo Island is  $15.5 \times 10^3$  g dry wt  $m^{-2} y^{-1}$  with the maximum sustainable biomass of  $4 \times 10^3$  g dry wt  $m^{-2}$  (Morris et al. 1984). A canopy model was used to estimate below-ground annual net production for tall *S. alterniflora* growing on Sapelo Island of  $2.03 \times 10^3$  g dry wt  $m^{-2} y^{-1}$  (converted from a

value of  $872 \text{ g C m}^{-2} \text{ y}^{-1}$  using a carbon conversion factor of 42.9% of dry mass (Morris et al., 1984)) and  $0.925 \times 10^3 \text{ g dry wt m}^{-2} \text{ y}^{-1}$  ( $397 \text{ g C m}^{-2} \text{ y}^{-1}$ ) for short *S. alterniflora*, respectively (Dai & Wiegert, 1996). This latter model demonstrated that failure to include carbon translocation between above- and below-ground tissues can lead to considerable overestimates of total net production, though the model only included translocation from above- to below-ground tissues.

A recent model of *S. alterniflora* by Zheng et al. (2016) includes both phenology and translocation of material in both directions. The model is based on one developed for two species of *Typha* and *Phragmites australis* (Asaeda & Karunaratne, 2000; Asaeda et al., 2005). The *S. alterniflora* version of the model was parameterized using data available in the literature and covered a broad geographic distribution from the east coast of the USA to China. Also, model results showed considerable geographic differences in the root to shoot ratio. However, the model required the use of data that are hard to obtain such as the mortality and respiration rate of 1-year-old and older rhizomes.

In this study, we combined Morris et al.'s production model (1984) with components of the Zheng et al. model (2016) and added the effects of salinity on plant production. We call this combined model the Phenology-based Growth dynamics model (PG model). Our goal is to be able to accurately model above- and below-ground production and biomass in short, medium, and tall form *S. alterniflora* and estimate the amount of carbon translocation between above- and below-ground tissues during three periods; growth, senescence, and dormancy periods. In our model, we define the dormancy period as the period during which the below-ground tissues remobilize assimilates and translocates soluble carbon to the above-ground biomass to support above-ground survival during the winter and growth in early spring. This period is also the time

when plants are not actively growing even though there may be sufficient irradiance to support photosynthesis. We use the model as an inverse model, to determine the values of unknown parameters that produce the best fits with observed biomass, and as a forward model to predict biomass, translocation, and daily production throughout the year.

Our research questions are: (1) Does the PG model accurately predict above- and below-ground biomass of the short, medium and tall forms of *S. alterniflora*? (2) How do translocation rates and the amount of translocated material differ for the three types of *S. alterniflora* during growth, senescence, and dormancy? (3) How do seasonal mortality and respiration rates differ between the different forms of *S. alterniflora*?

We hypothesize that for *S. alterniflora* in Georgia: (1) short form *S. alterniflora* translocates a greater proportion of its above-ground photosynthate and remobilization of assimilates to below-ground tissues compared to medium and tall form *S. alterniflora* in order to support to the higher root:shoot ratio. (2) the below-ground assimilate translocation to above-ground tissue occurs in all three forms of *S. alterniflora* during the dormancy period which includes winter and early spring.

## **2. Methods and Materials**

### **2.1 Site location**

Plants were collected close to 18 permanent plots, 6 for each height form of *S. alterniflora*, located in monotypic areas of tall, medium and short form *S. alterniflora*. The plots are located within the domain of the Georgia Coastal Ecosystem Long Term Ecological Research (GCE-LTER) program on Sapelo Island, Georgia on the southeastern coast of the USA (Figure 3.1), and close to the Duplin River and adjacent to the GCE-LTER flux tower (31°26'37.6" N, -

81°17'1.9" W). Irradiance data was taken from the climate monitoring station at Marsh Landing (31°25'4.2" N, -81°17'43.5" W).

## 2.2. Sampling and biomass estimating methods

The GCE-LTER field crew performed destructive core sampling exclusively close to 6 tall, 6 medium, and 6 short *S. alterniflora* permanent plots located near the GCE flux tower monthly between October 2013 and December 2015. Above-ground tissues were harvested at ground level, and below-ground tissues were obtained using a 7.5 cm diameter PVC pipe pushed into the sediments to a depth of 30 cm. Samples were stored at 4 °C for one night and washed over an 800 µm sieve to separate the living roots and rhizomes from the soil particles on the next day. Samples were then oven-dried at 60 °C for 3 days and weighed. The data for each core is available at the following link on GCE-LTER web site ([https://gce-lter.marsci.uga.edu/private/flux\\_tower\\_veg/data/](https://gce-lter.marsci.uga.edu/private/flux_tower_veg/data/)). In addition, plant height data was collected non-destructively by recording the heights of all shoots taller than 10 cm in same plots as an input data of the allometric equation for estimating the above-ground biomass. The height data was collected from 0.25m x 0.25m quadrat placed in the center of each plot for short and medium *S. alterniflora*. The 0.5 m x 0.5 m quadrat was used for collecting the tall *S. alterniflora* heights.

Allometric equations were developed for a similar site (GCE site 10) using data collected in 2002. The allometric equation for *S. alterniflora* growing on the creek bank (i.e. tall form *S. alterniflora*) is

$$\text{Aboveground biomass (g)} = \exp(-6.11 + 1.75 \log(\text{plant height(cm)})) \quad (1)$$

The allometry equation applied for *S. alterniflora* growing in the mid-marsh is

$$\text{Aboveground biomass (g)} = \exp(-7.31 + 1.99 \log(\text{plant height(cm)})) \quad (2)$$

and was used for medium and short *S. alterniflora*. Below-ground biomass per unit area was obtained from the above-ground estimates by multiplication by the root:shoot ratio determined from the destructive cores (Table 3.1). Because only live below-ground biomass was measured in the cores, the model calculates live below-ground biomass.

### **2.3 Biotic variables**

The fraction of a *S. alterniflora* canopy that is green and is able to actively photosynthesize changes seasonally. To account for this, the production model uses time series of two biotic variables: the fraction ( $F$ ) of the plant canopy that is green (i.e. the sum of green leaf and green stem biomass divided by the total canopy biomass) and the percent nitrogen content of green leaves (Morris et al., 1984). The canopy data was only measured in tall *S. alterniflora* collected between 2013 – 2014 (Jung & Burd, 2017) to calculate  $F$  on an approximately monthly basis and was used for all plants. Monthly estimates of percent nitrogen in green leaves for the tall form of *S. alterniflora* on Sapelo Island were obtained from Morris et al. (1984).

### **2.4 Abiotic variables**

Air temperature and irradiance data are also used to drive the model. Hourly temperature data were obtained from GCE Flux Tower, a level 3 weather station measuring the environmental data at 3 elevations (e.g. temperature) located near the sampling site. Hourly downwelling irradiance data were obtained from the weather station at Marsh Landing.

### **2.5 Model formulation**

#### **2.5.1 Net primary production**

The basic structure of the model is shown schematically in Figure 3.2. Gross production ( $G$ ) and respiration rates were estimated using the model described in Morris et al. (1984). Gross production is a function of total canopy biomass, irradiance at the top of the

canopy, solar elevation, air temperature, green-leaf ratio, and leaf nitrogen content (Equation 3).

Above- and below-ground respiration rates were calculated as functions of temperature, green-leaf ratio and biomass (Equation 3). Total net production was then given by

$$P = \frac{\psi TNF \sin(\vartheta) \left\{ \ln \left( L e^{\frac{\alpha B_c}{\sin(\vartheta)}} + \lambda \right) - \ln(L + \lambda) \right\}}{(\alpha(N + \eta))} - \rho T (FB_{above} + B_{below}) \quad (3)$$

$\leftarrow$                      $G$                      $\rightarrow$      $\leftarrow$                      $R$                      $\rightarrow$

where the symbols and values for constants are given in Table 3.2.

Equation (3) does not include any explicit representation of translocation between above- and below-ground tissue, or mortality. To incorporate these flows, we included formulations for mortality and translocation between above- and below-ground tissues from the model developed by Zheng et al. (2016). Equations for the rates of above- and below-ground biomass were then written as a balance between production, respiration, mortality losses, and translocation

$$dB_{above}/dt = G - R_{above} - M_{above} - TB_{above\_to\_below} + TB_{below\_to\_above} - TP_{above\_to\_below} \quad (4)$$

$$dB_{below}/dt = TB_{above\_to\_below} + TP_{above\_to\_below} - TB_{below\_to\_above} - R_{below} - M_{below} \quad (5)$$

where B, G, and R represent biomass, gross production rate, and respiration rate, while M, TB, and TP denote mortality rates, carbon translocation rates between above- and below-ground biomass and photosynthate translocation rates between above- and below-ground biomass.

The hourly mortality rate was described as a function of temperature and biomass (Zheng et al., 2016)

$$M_{above} = m_a \theta^{(T-20)} B_{above} \quad (6)$$

$$M_{below} = m_b \theta^{(T-20)} B_{below} \quad (7)$$

The parameter values of  $m_a$  and  $m_b$  for different height forms of *S. alterniflora* on Sapelo Island were estimated using the PG model in inverse mode (see below).

## 2.5.2 Carbon translocation between the above- and below-ground tissues and phenological dates

The carbon translocation rates between above- and below-ground tissues were calculated using the following equations (Zhang et al., 2016):

$$TP_{\text{above\_to\_below}} = \alpha_{AB} G \quad (8)$$

$$TB_{\text{above\_to\_below}} = \gamma B_{\text{above}} \quad (9)$$

$$TB_{\text{below\_to\_above}} = \alpha_{BA} \theta^{(T-20)} B_{\text{below}} \quad (10)$$

where  $TP_{\text{above\_to\_below}}$  is the translocation rate of photosynthate from above- to below-ground tissues during the growing season,  $TB_{\text{above\_to\_below}}$  is the assimilate translocation rate from above- to below-ground tissues during plant senescence, and  $TB_{\text{below\_to\_above}}$  is the assimilate translocation rate from below- to above-ground tissues during the dormancy period. The definitions of symbols of parameters in Equations 8 – 10 are given in Table 3.3.

We used the local phenological dates of our study site in the PG model. (Table 3.4 & 3.5). All dates are represented as numerical day-of-year with January 1<sup>st</sup> being day 1. The major phenological dates (Table 3.4) and the corresponding phenological events in the present model are summarized as follows:

- 1)  $SB_{\text{below\_to\_above}}$ : the start date of the translocation of remobilization of below-ground assimilates to above-ground tissues during the dormancy period;
- 2)  $EB_{\text{below\_to\_above}}$ : the end date when below-ground remobilized assimilate is translocated to above-ground tissues during the dormancy period;
- 3)  $SP_{\text{above\_to\_below}}$ : the start date when the photosynthates from the above-ground tissues is translocated to below-ground tissues during the growing season;

4)  $EP_{\text{above\_to\_below}}$ : the end date for translocation of photosynthates from the above-ground tissues to below-ground tissues during the growing period, and the start date for the remobilization and translocation of assimilate from the above-ground senescing tissues to the below-ground tissues during the senescence period.

The phenological dates for the tall form of *S. alterniflora* were estimated based on the timing of the first observation of senescing tissues in collected above-ground biomass, and by observing the seasonal above- and below-ground biomass patterns. To do this, the average monthly above- and below-ground biomass and their standard deviations were calculated from Oct. 2013 - Dec. 2015 (Figure 3.3). A cubic spline was used to interpolate between the data points. Previous studies have shown that the biomass of yellow leaves and stems rapidly increased in October (Jung & Burd, 2016). We chose the sampling date of 2nd October when we first observed yellow senescing shoot biomass of more than  $10 \text{ g core}^{-1}$  as the date of onset of senescence ( $EP_{\text{above\_to\_below}}$ ). From the date of the start of senescence, we assume that *S. alterniflora* starts to remobilize assimilate from senescing tissues and translocate soluble carbon to the below-ground biomass in order to store the energy in the root and rhizome. From the middle of December to the end of February, we observed a continuous decrease in below-ground biomass (Figure 3.3), and we defined this period as the dormancy period. Once the dormancy period ends, environmental conditions become favorable for active growth, and the plants start to increase above-ground biomass. We denote this phenological point as  $SP_{\text{above\_to\_below}}$ , and the period between  $SP_{\text{above\_to\_below}}$  to the start of senescence ( $EP_{\text{above\_to\_below}}$ ) as the growing period. Since our tall, medium and short *S. alterniflora* sites are all located within a  $5,000 \text{ m}^2$  area and the Phenocam, a high-resolution digital camera, takes a picture of salt marshes remotely near our

study site every 30 minutes was not able to distinguish the zonation of different forms of *S. alterniflora*, we applied same phenological dates to three different forms of *S. alterniflora*.

### 2.5.3. Effect of porewater salinity on the production of *S. alterniflora*

To account for the effects of salinity on production, and therefore plant height of *S. alterniflora*, we developed a salinity dependent factor that multiplied gross production. Average porewater salinity in the tall, medium, and short form *S. alterniflora* zones at our site were 24.4 ppt, 26.7 ppt and 28.1 ppt, respectively (Miklesh, pers. comm.). Equation (3) and its associated parameter values were derived from the *S. alterniflora* cultures under different shading and nitrogen levels (Morris *et al.*, 1982); the average salinity of the water in these cultures was approximately 17.5 ppt. To incorporate the effects of variable salinity on production, we developed a parameterization of the effects of salinity on the gross production rate for *S. alterniflora* (Figure 3.4) based on data from studies of the relationship between salinity and production (Linthurst & Seneca, 1981; Ge *et al.*, 2014). This relationship provided a factor that multiplied the gross production and was designed such that it has a value of 1 for a salinity of 17.5 ppt environment. In developing this parameterization, we assumed that gross production was zero at salinities of 60 ppt and above based on reference data (Bertness & Ewanchuk, 2002).

### 2.5.4. The inverse model.

To determine the values of the parameters used in the PG model (Table 3.3), we used the model in inverse mode allowing us to find the values of the parameters that best fit the observed biomasses between October 2013 and December 2014. To do this, we minimized the cost function

$$\chi^2 = \sum_{i=t_s}^{t_e} \frac{((observed\ AG_i - modeled\ AG_i)^2 + (modeled\ AG_i - modeled\ BG_i)^2)}{\sigma_i^2} \quad (11)$$

where,  $t_s$  is the date of the first observation,  $t_e$  is the time of the last observation, *observed AG* and *observed BG* are the field above- and below-ground biomass at  $i$ -th time point. The *observed AG* biomass was obtained through the allometry equation which calculates the above-ground biomass using the relationship of plant height (cm). The plant heights of all shoots taller than 10 cm were measured at the center of each plot within the quadrat. The *observed BG* is acquired by multiplying the root: shoot ratio obtained from the monthly destructive core samples to the *observed AG* biomass. *Modeled AG* and *modeled BG* are the calculated above- and below-ground biomass in the PG model at  $i$ -th time point. The cost function was minimized using a constrained nonlinear minimization routine (the Matlab function `fmincon`) employing an interior point algorithm. The *S. alterniflora* model was used in inverse mode for each of the three types of *S. alterniflora* individually.

#### 2.5.5. Forward Model and Numerical Methods.

The forward model simulations were run by solving equations (4) and (5) using the translocation and mortality parameter values for salinity ranges corresponding to regions where short, medium, and tall form *S. alterniflora* were found. Equations (4) and (5) for above- and below-ground biomass we solved using a 4<sup>th</sup> order Runge-Kutta method (e.g. Press et al. 2002) with a constant time step of 1 hour. All computer codes were written and run using Matlab 2016b. Forward simulations were run for the period October 2013 – December 2015 (i.e. extending beyond the period used to parameterize the model) and the model results were compared with corresponding observed above- and below-ground biomass.

The differences between observed and modeled biomass,  $\Delta D_i$ , were quantified based on the following equations

$$\Delta D a_i = \frac{(\text{observed } AG_i - \text{modeled } AG_i)}{\sigma_i} \quad (12)$$

$$\Delta Db_i = \frac{(\text{observed } BG_i - \text{modeled } BG_i)}{\sigma_i} \quad (13)$$

where,  $\Delta Da_i$  and  $\Delta Db_i$  are the differences in above-ground biomass and below-ground biomass normalized to the standard deviation of the field estimates.

### 3. Results

#### 3.1. Parameter values of three types of *S. alterniflora* on Sapelo Island from inverse model

The fractions of the photosynthate translocated from above- to below-ground ( $\alpha_{ab}$ ) tissues in tall, medium, and short form *S. alterniflora* were 0.52, 0.22, and 0.82, respectively (Table 3.6). However, the amount of photosynthate ( $\text{g m}^{-2}$ ) translocated from above- to below-ground tissues throughout the whole growth period was highest in tall form *S. alterniflora* (Table 3.7 & Figure 3.11) and was approximately 3 – 6 times that of the other height forms.

The fraction of above-ground carbon translocated from above- to below-ground tissues per hour during senescence ( $\gamma$ ) was higher in short form *S. alterniflora* (0.0013) compared to tall and medium form *S. alterniflora*, 0.0008,  $2.6 \times 10^{-12}$ , respectively (Table 3.6). However, the absolute biomass translocated from above- to below-ground during the whole senescence period was greater in tall form *S. alterniflora* (Table 3.7).

The fraction of below-ground assimilate translocation to above-ground tissues ( $\alpha_{ba}$ ) per hour during the dormancy period is, to all intents and purposes, zero in all types of *S. alterniflora*. The low value of  $\alpha_{ba}$  suggest that *S. alterniflora* on Sapelo Island do not translocate stored resources during the winter.

The specific rate of above-ground mortality at 20°C (parameter  $m_a$ ) of above-ground tissues were 0.0006 and 0.0012  $\text{gg}^{-1} \text{d}^{-1}$  in tall and medium form *S. alterniflora*, respectively but

essentially zero in short form *S. alterniflora* (Table 3.6). The specific rate of below-ground mortality at 20°C of below-ground tissues was similar for tall and short height forms but almost zero in medium form *S. alterniflora* (Table 3.6).

### **3.2. Above- and below-ground biomass in the PG model**

The model was fitted to the observed biomass from Oct. 2013 to Dec. 2014 for estimating parameters. In the following year 2015, both above- and below-ground biomass was predicted by the model using the calculated parameters. The PG model underestimated above-ground biomass (AG) of tall *S. alterniflora* during the last year (2015) of the study (Figure 3.6). A similar pattern was observed in the model results for medium *S. alterniflora* (Figure 3.7), and from the fall seasons for the short form (Figure 3.8). The model predicted the general pattern of below-ground biomass of tall *S. alterniflora* whereas it underestimated the below-ground biomass in other two height forms (Figures 3.6 – 3.8). Overall, the model predicted the above- and below-ground biomass of short form *S. alterniflora* best based on its lowest total  $\Delta D_i$  values (Table 3.6 & Figure 3.5).

### **3.3. Gross production and net production**

The general patterns of the gross and net production (Figure 3.10) of the three height forms of *S. alterniflora* closely followed seasonal irradiance and temperature cycles (Figure 3.9). Both gross and net production were highest in the tall form *S. alterniflora*, followed by the medium and short *S. alterniflora* (Figure 3.10). The gross production was approximately five times higher in tall *S. alterniflora* than in short *S. alterniflora* during the active growing season between late spring (April) and late summer (August) (Figure 3.10). The net productions of medium and short *S. alterniflora* had negative values in the first winter of the study period, which indicates that there was more consumption from respiration than production from

photosynthesis. During this period, the gross production dropped rapidly and stayed near zero. The negative net production may be mainly driven by the decreased above-ground biomass compared to the respiration of below-ground tissues during winter season.

### **3.4. Translocated biomass**

We estimated total carbon translocation during growth, senescence, and dormancy periods using the PG model. The assimilate translocation from below- to above-ground tissues during the dormancy period was very low (close to zero) in all types of *S. alterniflora* (Figure 3.11 – 3.13). Translocation of the remobilization of assimilate from above-ground tissues during senescence in tall *S. alterniflora* was 1.5 fold that in short height forms in 2014 and similar in 2015 (Table 3.7 & Figure 3.11). During the growing season, tall *S. alterniflora* translocated approximately 24 g d<sup>-1</sup> during summer 2014 compared to 4 g d<sup>-1</sup> for medium and 9 g d<sup>-1</sup> for short *S. alterniflora* (Figures 3.11 - 3.13) with lower values during 2015.

### **3.5. Mortality rates of above- and below-ground tissues**

The mortality rates in all three types of *S. alterniflora* followed a seasonal pattern with the highest rate occurring in tall *S. alterniflora*, followed by medium and short *S. alterniflora*. The mortality rates are similar for both above- and below-ground tissues of tall and medium form *S. alterniflora*. In short form *S. alterniflora*, the above-ground mortality was almost zero and the average daily below-ground mortality was about 2 g dwt d<sup>-1</sup>, the least among three types of *S. alterniflora* (Table 3.10 & Figure 3.14).

### **3.6. Respiration rates of above- and below-ground tissues**

The below-ground respiration rate was generally higher than the above-ground biomass in all three types of *S. alterniflora*. The tall form respire the most throughout the seasons followed by short and medium *S. alterniflora*. The below-ground respiration rate in short form *S.*

*alterniflora* was about 4 times higher than in above-ground biomass. All types of *S. alterniflora* respire most during the summer season when the temperature is high and the above-ground respiration rate drops down to less than 8 g dry wt d<sup>-1</sup> in early spring (Figure 3.15).

#### **4. Discussion**

The PG model prediction for the above- and below-ground biomass of tall and short forms of *S. alterniflora* was compared with field estimates of biomass (Figures 3.6 – 3.8). The model significantly underestimates the above-ground biomass of tall and medium *S. alterniflora* during the last year of the study period. This may be because parameter values estimated for the first 15 months (Oct. 2013 - Dec. 2014) are not applicable to the following year (Jan. 2015 - Dec. 2015). This could be due to the fact that the cycle of biomass pattern used for the inverse model was not enough to describe the actual biomass pattern, so setting a different time period for fitting the model may be required.

The modeled below-ground biomasses in 2015 were also generally less than the field estimates of below-ground biomass (Figures 3.6 – 3.8). However, field estimates of below-ground biomass depend on measured root:shoot ratios that are determined using sediment cores and are strongly affected by heterogeneity in below-ground biomass and by not necessarily capturing the below-ground biomass of a whole ramet. This is reflected in the large uncertainties in some of the field estimates of below-ground biomass (Figures 3.6 – 3.8). Gross et al. (1991) assessed the effect of coring tube size on the variability of the below-ground biomass estimates in a homogeneous area of short form *S. alterniflora* using 3.7cm, 10.2 cm, 16.5 cm and 21.5 cm stainless steel coring tubes. They found that the lowest below-ground biomass and largest coefficient of variation (CV) occurred with the smallest diameter cores; the coefficient of

variation varied from 0.59 for a core with a diameter of 3.7 cm to approximately 0.1 for a core with a diameter larger than 16.5 cm. The study showed that using a core larger than 16.5 cm in diameter is required to largely overcome the effects of below-ground heterogeneity. Our below-ground biomass was measured using a 7.5 cm tube resulting in a less representative estimate of the true below-ground biomass.

Accurate field estimates of above- and below-ground biomass are important when using the inverse model to determine parameter values. This is because the generally higher below-ground biomass dominates the cost function (Equation 11) leading to less accurate estimates of important above-ground parameters such as translocation and mortality rates. This can be seen particularly in the case of the short form *S. alterniflora* (Figure 3.8) where, even in the time period when the model was being fitted to the data (October 2013 – December 2014), the agreement between the model and field estimates of below-ground biomass was better than that for the above-ground biomass.

We initially hypothesized that the short form *S. alterniflora* would translocate a greater proportion of its above-ground assimilates and photosynthates to below-ground tissues. However, while the translocation parameters  $\alpha_{ab}$  and  $\gamma$  (Equations 8 – 10) were larger in the short height form (Table 3.6), the total amount of material translocated was largest in the tall form (Table 3.7). This is not surprising given the larger above-ground biomass of the tall form. However, because the short form has proportionally more below-ground biomass, it is reasonable that a greater proportion of above-ground resources are translocated to the below-ground tissue. The main differences in the below-ground biomass dynamics between tall and short *S. alterniflora* may be partially a response to physical disturbances, generic differences or different properties of the edaphic environment. In this study, tall form *S. alterniflora* was sampled from

creebank locations, whereas short form samples were collected from the high marsh.

Differences in inundation and nutrient supply to the soils may explain the model results. Marsh interior sites are generally inundated less frequently than creebank sites, leading to greater peat accumulation and lower nutrient concentrations in the soils (Redfield, 1972; Smart, 1986; Gross et al., 1991). The concept of balanced growth (Thornley, 1972) suggests that lower nutrient concentrations result in higher root:shoot ratios as the plants place more resources in the below-ground tissues to increase their nutrient uptake. In addition, sulfide concentrations increase from creebank to marsh interior (King et al., 1982) and the higher sulfide may provide additional stresses such as a more negative redox potential due to the free sulfide electron availability and the sulfide toxicity causing the plants to preferentially allocate resources, such as photosynthates or non-structural carbohydrates, to the below-ground tissues.

Nutrient uptake was not explicitly incorporated into the model. Instead we used leaf nitrogen concentrations measured for green leaves in tall *S. alterniflora* (Morris et al., 1984) and applied them to all height forms. Recent measurements of monthly leaf nitrogen content from mixtures of green, senescing, and brown leaves collected between the months of June and October indicate little difference between the three height forms of *S. alterniflora* (O'Connell, pers. comm.), though the range of values (1.03% – 1.99%) differs from the range (1.25% – 4%) found by Morris et al (1984), though the latter covered the whole year. To examine the effects of different nitrogen concentrations on model results, we ran the PG model using double the nitrogen concentration found by Morris et al (1984). This resulted in an increase in above- and below-ground biomass by approximately a factor of 2.

The second hypothesis, that *S. alterniflora* in Georgia translocates biomass from below- to above-ground biomass during dormancy, is not supported by our results. Translocated

assimilates from below- to above-ground tissues are close to zero in all types of *S. alterniflora* (Table 3.7). Geiger (1969) demonstrated that C3 plants of *Cirsium arvense* from Montana have a higher translocation rate than those from California at a lower temperature. In Potvin et al.'s study (1984), C4 grass from Quebec showed more active sinks than those from Mississippi. The low translocation rates from below- to above-ground during plant dormancy could be because the photosynthesis in *S. alterniflora* on Sapelo Island is sufficient to support the above-ground biomass, even during the winter, so the above-ground components may not serve as active sinks, which in turn decreases translocation from below- to above-ground. Another possible reason for the low translocation rate is that the stored carbon in below-ground tissues might be used to support the survival of below-ground tissues, thereby limiting the availability of biomass to translocate from below to above-ground tissues. Translocating the carbon from above- to below-ground takes energy in terms of remobilization of assimilates and transporting the soluble carbon to root and rhizomes. Supplying carbon from photosynthesis to the above-ground tissues and using the remobilized carbon from root and rhizome materials for below-ground tissues themselves might be more energy efficient on minimizing energy consumption from allocating carbon during unfavorable seasons for the growth and development of a plant. However, the model results do suggest the possibility that the internal dynamics of resource allocation and translocation may differ with the location of plants in the marsh. This suggests that further research, combining field work, green house experiments, and model development, is required, especially given the potential importance of below-ground storage and biomass at the end of the growing season in one year for plant production in the following year.

We performed sensitivity analyses on the PG model of phenological dates to determine the relative importance of the variation of phenological dates to above- and below-ground biomass

estimations (Table 3.12). We compiled four sets of each baseline date by varying between  $\pm 10$  and  $\pm 20$  days and compared the dates in this study to the dates estimated from the Phenocam data (O'Connell, pers. comm.). The model results were most sensitive to changes in the start date of assimilate translocation from below- to above-ground tissues, particularly in the above-ground biomass. However, the difference between our date and O'Connell's date was 5 days, which changed the above-ground biomass by about 19% and the below-ground biomass by approximately 4% from our modeled biomass. O'Connell's start date for photosynthate translocation from the above- to below-ground tissues was 7 days later than our date, but using the revised date led to variations in both above- and below-ground biomass by less than 15%. The biggest differences between our dates and O'Connell's date was found in the start date of assimilate translocation from senescing above-ground tissues to below-ground. Since samples were collected on a monthly basis and the dominant senescing biomass was observed first in the October samples, we chose the sampling date when we first observed the senescing tissues more than 10g per core as the end date of the photosynthates translocation and the start date of senescence. The O'Connell study estimated their end date 21 days earlier than our end date marking the translocation of above-ground assimilates to below-ground and led to a variation of 26 % in the above-ground biomass and 19% in the below-ground biomass. Overall, the differences in estimated biomass between our dates and O'Connell's dates were less than 26%, which support that the way we estimated phenological dates by using dead and live biomass patterns was reasonable, so our phenological date estimation method could be applicable to other study sites where the frequent field observation or the Phenocam data are not available, and the measurement of senescing period can be greatly improved if the senescing tissue data is collected at shorter intervals.

## 5. Conclusion

We have developed a new phenology-based model of the growth and production of above- and below-ground biomass for *S. alterniflora*. The model was parameterized using data collected at the LTER-GCE site on Sapelo Island, Georgia, USA between October 2013 and December 2014, and validated using data from January 2015 through to December 2015. Model results indicate that translocation from below-ground to above-ground tissues may not be essential for survival during the winter months in this region. Parameterization of the model also highlights the need for more accurate and precise field estimates of below-ground biomass, especially if hard to measure translocation parameters are to be determined from combining the model with field data.

## References

- Adams, D. A. (1963). Factors influencing vascular plant zonation in North-Carolina salt marshes. *Ecology*, 44(3), 445-456. doi: Doi 10.2307/1932523
- Asaeda, T., & Karunaratne, S. (2000). Dynamic modeling of the growth of *Phragmites australis*: model description. *Aquatic Botany*, 67(4), 301–318.
- Asaede, T., Hai, D.N., Manatunge, J., Williams, D., Roberts, J., (2005). Latitudinal characteristics of below- and above-ground biomass of *Typha*: a modelling approach. *Annals of Botany*, 96(2), 299–312.
- Bertness, M. D., & Ewanchuk, P. J. (2002). Latitudinal and climate-driven variation in the strength and nature of biological interactions in New England salt marshes. *Oecologia*, 132(3), 392-401.
- Crosby, S. C., Ivens-Duran, M., Bertness, M. D., Davey, E., Deegan, L. A., & Leslie, H. M. (2015).

- Flowering and biomass allocation in U.S. Atlantic coast *Spartina alterniflora*. *American journal of botany*, 102(5), 669-676. doi: 10.3732/ajb.1400534
- Dai, T., & Wiegert, R. G. (1996). Estimation of the primary productivity of *Spartina alterniflora* using a canopy model. *Ecography*, 19(4), 410-423.
- Dawes, C. J. (1998). *Marine botany*, New York, NY: John Wiley
- Drake, B. G., & Gallagher, J. L. (1984). Osmotic potential and turgor maintenance in *Spartina alterniflora* Loisel. *Oecologia*, 62(3), 368-375.
- Elsey-Quirk, T., Seliskar, D. M., & Gallagher, J. L. (2011). Differential population response of allocation, phenology, and tissue chemistry in *Spartina alterniflora*. *Plant Ecology*, 212(11), 1873-1885.
- Gallagher, J. L. (1974). Sampling macro-organic matter profiles in salt marsh plant root zones 1. *Soil Science Society of America Journal*, 38(1), 154-155.
- Ge, Z. M., Zhang, L. Q., Yuan, L., & Zhang, C. (2014). Effects of salinity on temperature-dependent photosynthetic parameters of a native C3 and a non-native C4 marsh grass in the Yangtze Estuary, China. *Photosynthetica*, 52(4), 484-492. doi: 10.1007/s11099-014-0055-4
- Geiger, D. R. (1969). Chilling and translocation inhibition. *The Ohio Journal of Science*, 69(6), 356-366
- Giurgevich, J. R., & Dunn, E. L. (1979). Seasonal patterns of CO<sub>2</sub> and water vapor exchange of the tall and short height forms of *Spartina alterniflora* Loisel in a Georgia salt marsh. *Oecologia*, 43(2), 139-156.
- Gross, M. F., Hardisky, M. A., Wolf, P. L., & Klemas, V. (1991). Relationship between aboveground and belowground biomass of *Spartina alterniflora* (smooth cordgrass).

- Estuaries*, 14(2), 180-191.
- Howes, B. L., Howarth, R. W., Teal, J. M., & Valiela, I. (1981). Oxidation-reduction potentials in a salt marsh: Spatial patterns and interactions with primary production1. *Limnology and Oceanography*, 26(2), 350-360. doi: 10.4319/lo.1981.26.2.0350
- Jung, Y., & Burd, A. (2017). Seasonal changes in above- and below-ground non-structural carbohydrates (NSC) in *Spartina alterniflora* in a marsh in Georgia, USA. *Aquatic Botany*, 140, 13-22. doi: <https://doi.org/10.1016/j.aquabot.2017.04.003>
- King, G. M., Klug, M. J., Wiegert, R. G., & Chalmers, A. G. (1982). Relation of soil water movement and sulfide concentration to *Spartina alterniflora* production in a Georgia salt marsh. *Science*, 218(4567), 61-63. doi: 10.1126/science.218.4567.61
- Levering, C. A., & Thomson, W. W. (1971). The ultrastructure of the salt gland of *Spartina foliosa*. *Planta*, 97(3), 183-196.
- Linthurst, R. A., & Seneca, E. D. (1981). Aeration, nitrogen and salinity as determinants of *Spartina alterniflora* Loisel. growth response. *Estuaries*, 4(1), 53-63.
- Mendelssohn, I. A. (1979). Nitrogen metabolism in the height forms of *Spartina alterniflora* in North Carolina. *Ecology*, 60(3), 574-584. doi: 10.2307/1936078
- Mendelssohn, I. A., & Seneca, E. D. (1980). The influence of soil drainage on the growth of salt marsh cordgrass *Spartina alterniflora* in North Carolina. *Estuarine and Coastal Marine Science*, 11(1), 27-40. doi: [https://doi.org/10.1016/S0302-3524\(80\)80027-2](https://doi.org/10.1016/S0302-3524(80)80027-2)
- Morris, J. T. (1982). A model of growth responses by *Spartina alterniflora* to nitrogen limitation. *Journal of Ecology*, 70(1), 25-42. doi: 10.2307/2259862
- Morris, J. T., Houghton, R. A., & Botkin, D. B. (1984). Theoretical limits of belowground production by *Spartina alterniflora*: An analysis through modelling. *Ecological Modelling*,

- 26(3), 155-175. doi: [https://doi.org/10.1016/0304-3800\(84\)90068-1](https://doi.org/10.1016/0304-3800(84)90068-1)
- Nestler, J. (1977). Interstitial salinity as a cause of ecophenic variation in *Spartina alterniflora*. *Estuarine and Coastal Marine Science*, 5(6), 707-714. doi: [https://doi.org/10.1016/0302-3524\(77\)90043-3](https://doi.org/10.1016/0302-3524(77)90043-3)
- O'Donnell, J., & Schalles, J. (2016). Examination of abiotic drivers and their influence on *Spartina alterniflora* biomass over a twenty-eight year period using landsat 5 TM satellite imagery of the central Georgia coast. *Remote Sensing*, 8(6), 477.
- Parrondo, R. T., Gosselink, J. G., & Hopkinson, C. S. (1978). Effects of salinity and drainage on the growth of three salt marsh grasses. *Botanical Gazette*, 139(1), 102-107.
- Phleger, C. F. (1971). Effect of salinity on growth of a salt marsh grass. *Ecology*, 52(5), 908-911.
- Potvin, C., Goeschl, J. D., & Strain, B. R. (1984). Effects of temperature and CO<sub>2</sub> enrichment on carbon translocation of plants of the C4 grass species *Echinochloa crus-galli* (L.) Beauv. from cool and warm environments. *Plant physiology*, 75(4), 1054-1057.
- Press, W. H., Teukolsky, S. A., Vetterling, W. T., Flannery, B. P. (2002). *Numerical Recipes in C++: The Art of Scientific Computing* (2nd ed.). Cambridge, UK: Cambridge University Press.
- Redfield, A. C. (1972). Development of a New England salt marsh. *Ecological Monographs*, 42(2), 201-237. doi: 10.2307/1942263
- Richards, C. L., Pennings, S. C., & Donovan, L. A. (2005). Habitat range and phenotypic variation in salt marsh plants. *Plant Ecology*, 176(2), 263-273.
- Seneca, E. D., & Blum, U. (1984). Response to photoperiod and temperature by *Spartina alterniflora* (Poaceae) from North Carolina and *Spartina folisa* from California. *American Journal of Botany*, 71(1), 91-99. doi: 10.2307/2443628

- Seneca, E. D., & Broome, S. W. (1972). Seedling response to photoperiod and temperature by smooth cordgrass, *Spartina alterniflora*, from Oregon Inlet, North Carolina. *Chesapeake Science*, 13(3), 212-215. doi: 10.2307/1351066
- Smart, M. L. (1986). *Intraspecific competition and growth form differentiation of the salt marsh plant, Spartina alterniflora Loisel* (Doctoral dissertation), University of Delaware, Newark, DE.
- Stagg, C. L., Schoolmaster Jr, D. R., Piazza, S. C., Snedden, G., Steyer, G. D., Fischenich, C. J., & McComas, R. W. (2017). A landscape-scale assessment of above- and belowground primary production in coastal wetlands: Implications for climate change-induced community shifts. *Estuaries and Coasts*, 40(3), 856-879. doi: 10.1007/s12237-016-0177-y
- Thornley, J.H.M. (1972). A balanced quantitative model for root:shoot ratios in vegetative plants. *Annals of Botany*, 36, 431-441.
- Tripathee, R., & Schäfer, K. V. R. (2015). Above- and belowground biomass allocation in four dominant salt marsh species of the eastern United States. *Wetlands*, 35(1), 21-30. doi: 10.1007/s13157-014-0589-z
- Valiela, I., Teal, J. M., & Persson, N. Y. (1976). Production and dynamics of experimentally enriched salt marsh vegetation: Belowground biomass<sup>1</sup>. *Limnology and Oceanography*, 21(2), 245-252. doi: 10.4319/lo.1976.21.2.0245
- Zheng, S., Shao, D., Asaeda, T., Sun, T., Luo, S., & Cheng, M. (2016). Modeling the growth dynamics of *Spartina alterniflora* and the effects of its control measures. *Ecological Engineering*, 97, 144-156. doi: <https://doi.org/10.1016/j.ecoleng.2016.09.006>

**Table 3.1** The monthly average above- and below-ground biomass and the root to shoot ratio from two destructive cores

	<i>Tall form S. alterniflora</i>			<i>Medium form S. alterniflora</i>			<i>Short form S. alterniflora</i>		
	Above-ground biomass (g core <sup>-1</sup> )	Below-ground biomass (g core <sup>-1</sup> )	Root to shoot ratio	Above-ground biomass (g core <sup>-1</sup> )	Below-ground biomass (g core <sup>-1</sup> )	Root to shoot ratio	Above-ground biomass (g core <sup>-1</sup> )	Below-ground biomass (g core <sup>-1</sup> )	Root to shoot ratio
<b>Oct-13</b>	35.89	16.51	0.47	8.27	17.87	2.30	2.10	9.30	4.91
<b>Nov-13</b>	24.26	18.84	0.77	9.95	17.09	1.73	5.31	14.86	3.00
<b>Dec-13</b>	19.39	20.92	1.07	10.30	16.15	1.60	1.83	10.69	6.27
<b>Jan-14</b>	8.66	17.48	2.06	1.85	9.33	5.08	0.97	5.25	5.38
<b>Feb-14</b>	1.77	14.92	8.81	1.00	7.65	7.60	0.64	4.77	7.82
<b>Mar-14</b>	5.36	9.39	1.98	2.63	8.10	3.33	1.10	2.90	2.57
<b>Apr-14</b>	12.44	10.00	0.82	2.56	6.48	2.83	1.41	3.83	2.69
<b>May-14</b>	11.64	12.03	1.03	3.85	6.64	1.73	1.75	7.08	4.15
<b>Jun-14</b>	33.21	12.82	0.39	6.38	9.16	1.47	2.36	7.90	3.44
<b>Jul-14</b>	14.65	20.84	1.37	7.51	11.39	1.63	2.46	8.54	3.58
<b>Aug-14</b>	17.37	13.12	0.75	8.84	8.21	1.15	4.04	7.94	1.98
<b>Sep-14</b>	22.64	17.32	0.79	7.83	15.42	2.03	5.80	9.42	1.62
<b>Oct-14</b>	17.74	12.61	0.76	8.19	9.73	1.29	4.45	8.62	2.81
<b>Nov-14</b>	21.21	10.70	0.48	5.11	7.52	1.99	1.43	6.60	4.67
<b>Dec-14</b>	17.66	13.93	0.78	8.42	12.50	1.49	0.98	5.33	6.17
<b>Jan-15</b>	15.11	11.61	0.77	5.86	9.88	1.70	0.54	6.01	11.10
<b>Feb-15</b>	6.07	7.77	1.27	2.78	11.03	4.08	0.70	7.37	10.48
<b>Mar-15</b>	7.06	13.53	1.91	3.00	10.88	3.59	0.81	8.07	10.00
<b>Apr-15</b>	13.97	8.89	0.76	2.15	9.05	4.30	1.14	7.92	7.45
<b>May-15</b>	6.49	11.65	1.78	3.55	13.09	3.77	1.43	7.53	5.23
<b>Jun-15</b>	21.42	20.29	0.96	5.57	9.44	1.87	2.46	11.10	4.46
<b>Jul-15</b>	17.98	9.80	0.53	7.92	12.99	1.66	2.94	9.96	3.25
<b>Aug-15</b>	22.36	13.31	0.86	8.91	10.10	2.29	2.19	9.32	5.11
<b>Sep-15</b>	17.99	9.06	0.52	12.22	17.88	1.60	2.09	9.01	4.61
<b>Oct-15</b>	38.06	19.27	0.56	5.63	12.96	3.42	1.69	10.70	6.35
<b>Nov-15</b>	18.57	13.07	0.72	5.52	17.09	3.12	1.48	10.31	9.58
<b>Dec-15</b>	21.75	17.86	0.81	5.07	13.37	3.20	1.24	7.30	14.50

**Table 3.2** Definitions of symbols and parameter values

Symbol	Name	Units & Value
$P$	Total net production	g dry wt m <sup>-2</sup> h <sup>-1</sup>
$B_{above}$	Above ground biomass	g dry wt m <sup>-2</sup>
$B_{below}$	Below ground biomass	g dry wt m <sup>-2</sup>
$T$	Air temperature	°C
$\vartheta$	Solar elevation	Radians
$L$	Solar irradiance at the top of the canopy	W m <sup>-2</sup>
$\lambda$	Half saturation constant for irradiance	300 ± 100 W m <sup>-2</sup>
$\alpha$	Irradiance extinction rate within the canopy	(3.4 ± 1.0) × 10 <sup>-4</sup> m <sup>2</sup> gdw <sup>-1</sup>
$N$	Percent of nitrogen in the dry leaves	%
$F$	Ratio of green tissue to total canopy biomass	Dimensionless
$\psi$	Temperature coefficient for gross production	(7.1 ± 1.7) × 10 <sup>-4</sup> °C <sup>-1</sup> h <sup>-1</sup>
$\eta$	Half saturation constant for nitrogen	0.36 ± 0.29 % dwt
$\rho$	Temperature coefficient for dark respiration	(2.3 ± 0.6) × 10 <sup>-5</sup> °C <sup>-1</sup> h <sup>-1</sup>
$F$	Green leave ratio	Percentage
$m_a$	Specific rate of above-ground mortality at 20°C	gg <sup>-1</sup> d <sup>-1</sup>
$m_b$	Specific rate of below-ground mortality at 20°C	gg <sup>-1</sup> d <sup>-1</sup>
$\theta$	Temperature constant	1.09

**Table 3.3** Definitions of symbols of parameters estimated in the inverse model

Symbol	Name
$\alpha_{ab}$	Fraction per hour of photosynthate translocated from above- to below-ground during growing period
$\alpha_{ba}$	Fraction per hour of below-ground assimilate translocated from below- to above-ground during dormancy period
$\gamma$	Fraction per hour of above-ground assimilate translocated from above- to below-ground during senescence
$m_a$	Specific rate of above-ground mortality at 20 °C
$m_b$	Specific rate of below-ground mortality at 20 °C

**Table 3.4** Phenological date applied on three height forms of *S. alterniflora* on Sapelo Island, Georgia, U.S.A.in the PG model

Parameters	Values
SB <sub>below_to_above</sub>	349 (Dec.15)
EB <sub>below_to_above</sub>	59 (Feb. 29)
SP <sub>above_to_below</sub> :	60 (Mar. 1)
EP <sub>above_to_below</sub> :	275 (Oct. 2)

**Table 3.5** Three phenological events and dates on Sapelo Island, Georgia, USA

Month	10	11	12	1	2	3	4	5	6	7	8	9	10
Phenological events and dates	<b>Senescing period :</b> Translocating biomass solubilized from AG's senescing tissues to BG tissues (10/2 ~ 12/15)			<b>Dormancy period :</b> Translocation biomass solubilized from BG tissues to AG tissues (12/15 ~ 2/28)		<b>Growing period :</b> Translocation immediate photosynthates generated from photosynthesis from AG tissues to BG tissues (3/1 ~ 10/2)							

**Table 3.6** Parameter values from the inverse model running from Oct. 2013 – Dec. 2014 and the sum of  $\Delta D\alpha_i$  and  $\Delta D\beta_i$  (Total  $\Delta D_i$ ) after using parameters from the inverse model and running the PG model for the whole study period (Oct. 2013 – Dec. 2015)

	<b>Tall form</b> <i>S. alterniflora</i>	<b>Medium form</b> <i>S. alterniflora</i>	<b>Short form</b> <i>S. alterniflora</i>
$\alpha_{ab}$ (fraction)	0.52	0.22	0.82
$\alpha_{ba}$ (fraction)	$3.0 \times 10^{-15}$	$1.0 \times 10^{-15}$	$6.0 \times 10^{-15}$
$\gamma$ (fraction)	0.0008	$2.6 \times 10^{-12}$	0.0013
$m_a$ ( $gg^{-1} d^{-1}$ )	0.0006	0.0012	$1.7 \times 10^{-13}$
$m_b$ ( $gg^{-1} d^{-1}$ )	0.0005	$1.0 \times 10^{-13}$	0.0002
<b>Total <math>\Delta D_i</math></b>	72.69	77.07	57.64

**Table 3.7** Total translocation and the daily mean translocation of the three types of *S. alterniflora* during each phenology period

	Height form	Tall		Medium		Short		
		2014	2015	2014	2015	2014	2015	
Phenological events (Period)	Growing (3/1 ~ 10/2)	Total biomass (g dry weight/m <sup>2</sup> /period)	5168.34	2713.42	820.90	186.79	1859.10	1218.22
		Daily biomass (g dry weight/m <sup>2</sup> /day)	24.15	12.68	3.84	0.87	8.69	5.69
	Senescence (10/2 ~ 12/15)	Total biomass (g dry weight/m <sup>2</sup> /period)	363.48	165.8	2.93 x 10 <sup>-7</sup>	5.25 x 10 <sup>-8</sup>	236.25	131.76
		Daily biomass (g dry weight/m <sup>2</sup> /day)	4.98	2.27	4.01 x 10 <sup>-9</sup>	7.20 x 10 <sup>-10</sup>	3.24	1.8
	Dormancy (12/15 ~ 2/28)	Total biomass (g dry weight/m <sup>2</sup> /period)	4.32 x 10 <sup>-9</sup>	2.49 x 10 <sup>-9</sup>	2.07 x 10 <sup>-9</sup>	4.06 x 10 <sup>-10</sup>	1.12 x 10 <sup>-8</sup>	5.12 x 10 <sup>-9</sup>
		Daily biomass (g dry weight/m <sup>2</sup> /day)	5.84 x 10 <sup>-11</sup>	3.37 x 10 <sup>-11</sup>	2.80 x 10 <sup>-11</sup>	5.48 x 10 <sup>-12</sup>	1.51 x 10 <sup>-10</sup>	6.91 x 10 <sup>-11</sup>

**Table 3.8** The modeled mean root: shoot ratio of three height forms of *S. alterniflora*

	<b>Tall form</b> <i>S. alterniflora</i>	<b>Medium form</b> <i>S. alterniflora</i>	<b>Short form</b> <i>S. alterniflora</i>
<b>Average root:shoot ratio</b>	1.13	2.05	3.23

**Table 3.9** Daily mean gross and net production ( $\text{g m}^{-2} \text{d}^{-1}$ ) calculated in the PG model

	<b>Tall form</b> <i>S. alterniflora</i>	<b>Medium form</b> <i>S. alterniflora</i>	<b>Short form</b> <i>S. alterniflora</i>
<b>Daily mean gross production (<math>\text{g m}^{-2} \text{d}^{-1}</math>)</b>	21.51	6.60	5.39
<b>Daily mean net production (<math>\text{g m}^{-2} \text{d}^{-1}</math>)</b>	12.94	2.72	0.54

**Table 3.10** Daily mean above- and below-ground mortality rates ( $\text{g m}^{-2} \text{d}^{-1}$ ) estimated in the PG model

	<b>Tall form <i>S. alterniflora</i></b>	<b>Medium form <i>S. alterniflora</i></b>	<b>Short form <i>S. alterniflora</i></b>
<b>Daily mean above-ground mortality rate (<math>\text{g m}^{-2} \text{d}^{-1}</math>)</b>	7.83	4.85	$5.78 \times 10^{-10}$
<b>Daily mean below-ground mortality rate (<math>\text{g m}^{-2} \text{d}^{-1}</math>)</b>	6.82	6.95	2.02

**Table 3.11** Daily mean above- and below-ground respiration rates ( $\text{g m}^{-2} \text{d}^{-1}$ ) estimated in the PG model

	<b>Tall form <i>S. alterniflora</i></b>	<b>Medium form <i>S. alterniflora</i></b>	<b>Short form <i>S. alterniflora</i></b>
<b>Daily mean above-ground respiration rate (<math>\text{g m}^{-2} \text{d}^{-1}</math>)</b>	3.60	1.17	1.02
<b>Daily mean below-ground respiration rate (<math>\text{g m}^{-2} \text{d}^{-1}</math>)</b>	4.97	2.71	3.82

**Table 3.12 Sensitivity analysis of phenological dates**

(BG_to_AG_START =349) <b>12/15 (This study)</b>	Variation (day)	AGB(%)	BGB(%)
	-20	95.98	13.05
	-10	41.48	7.68
	+10	-30.77	-9.34
	+20	-46.17	-17.19
<b>12/10 (O'Connell)</b>	<b>- 5</b>	<b>19.26</b>	<b>4.06</b>

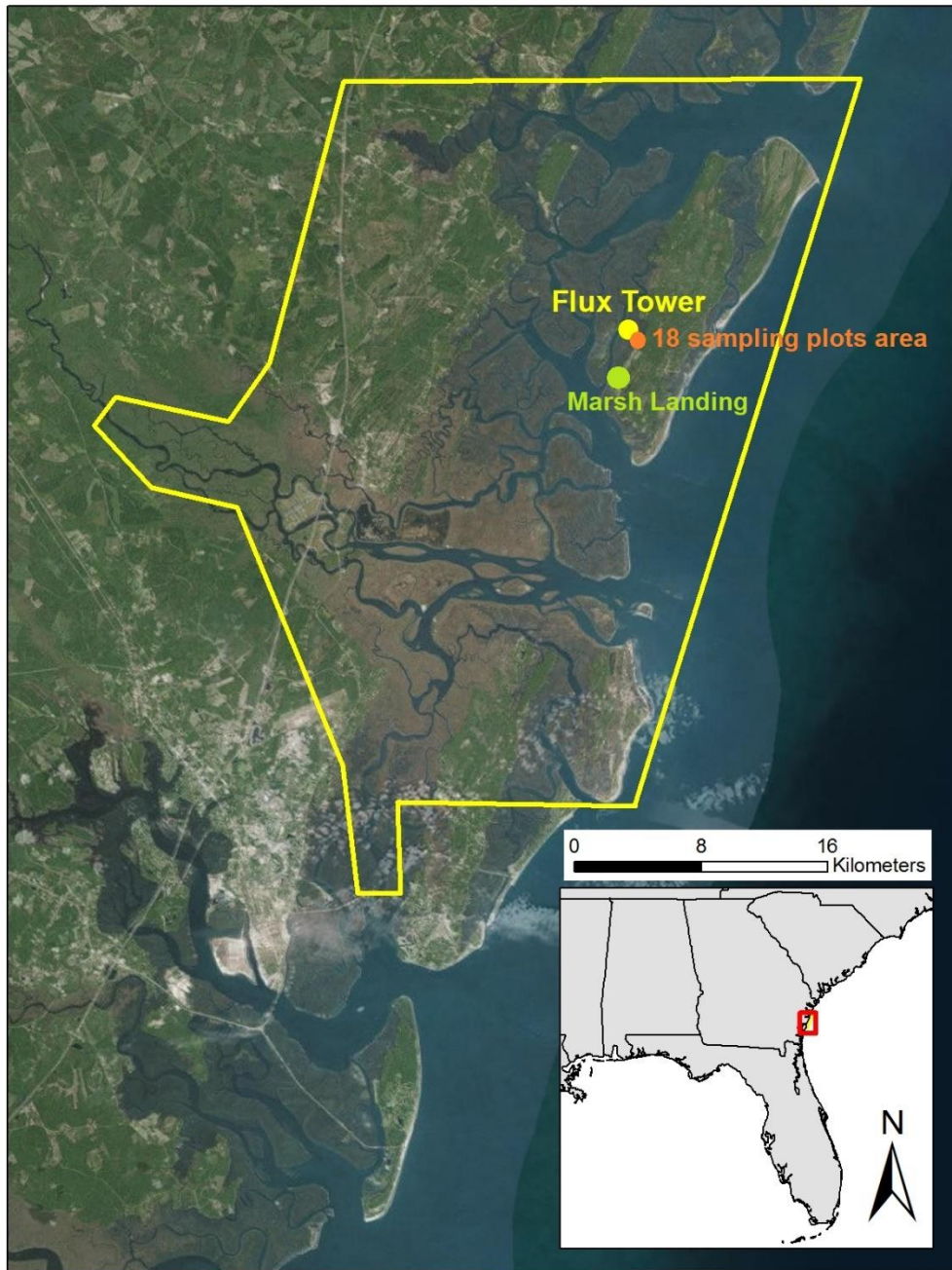
(BG_to_AG_end =59) <b>2/28 (This study)</b>	Variation (day)	AGB(%)	BGB(%)
	-20	0.00	0.00
	-10	0.00	0.00
	+10	0.00	0.00
	+20	0.00	0.00
<b>3/8 (O'Connell)</b>	<b>+ 8</b>	<b>0.00</b>	<b>0.00</b>

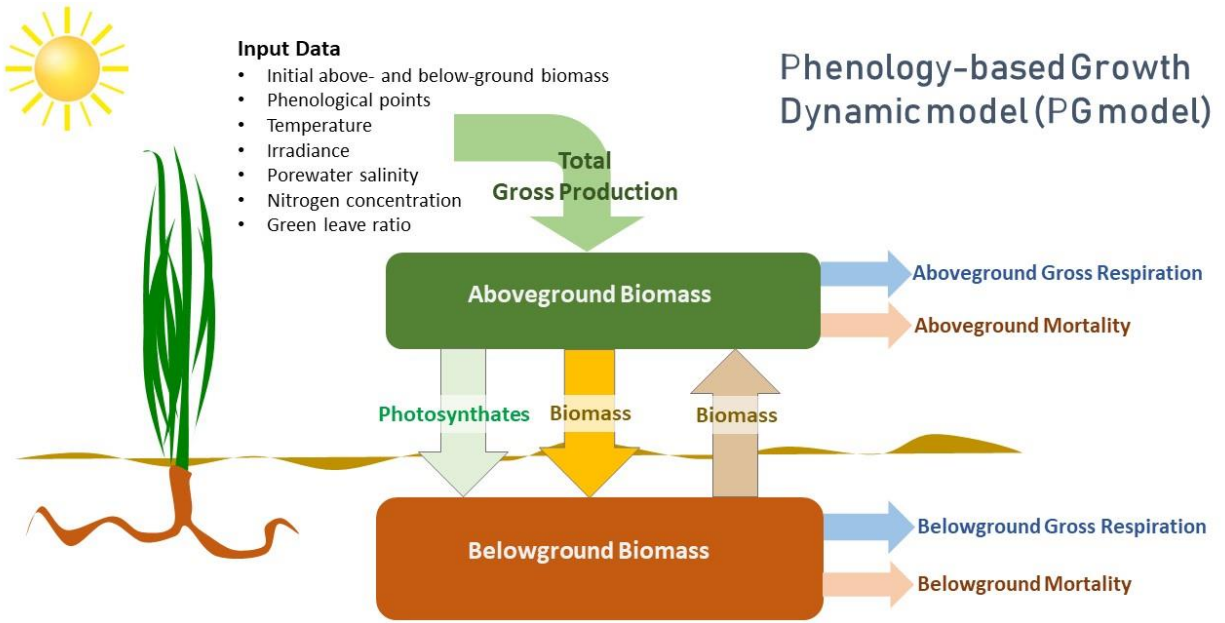
(AB_to_BG_START =60) <b>3/1 (This study)</b>	Variation (day)	AGB(%)	BGB(%)
	-20	-20.99	-21.49
	-10	-11.14	-11.44
	+10	25.57	26.54
	+20	55.90	58.55
<b>3/8 (O'Connell)</b>	<b>+ 7</b>	<b>14.17</b>	<b>14.65</b>

(AB_to_BG_END =275) <b>10/2 (This study)</b>	Variation (day)	AGB(%)	BGB(%)
	-20	21.96	15.57
	-10	-0.34	-0.81
	+10	6.03	1.39
	+20	12.53	4.52
<b>9/11 (O'Connell)</b>	<b>-21</b>	<b>26.40</b>	<b>18.68</b>



**Figure 3.1** Site map showing the location and boundary of the Georgia Coastal Ecosystem Long Term Ecological Research (GCE-LTER) site on Sapelo Island (Georgia, USA), the location of the flux tower, the Marsh Landing weather station, and the area of the 18 sampling plots where the destructive core samples were collected



**Figure 3.2** Structure of the *S. alterniflora* phenology-based growth dynamic model (PG model) adapted from Morris et al. (1984) and Zheng et al. (2016))

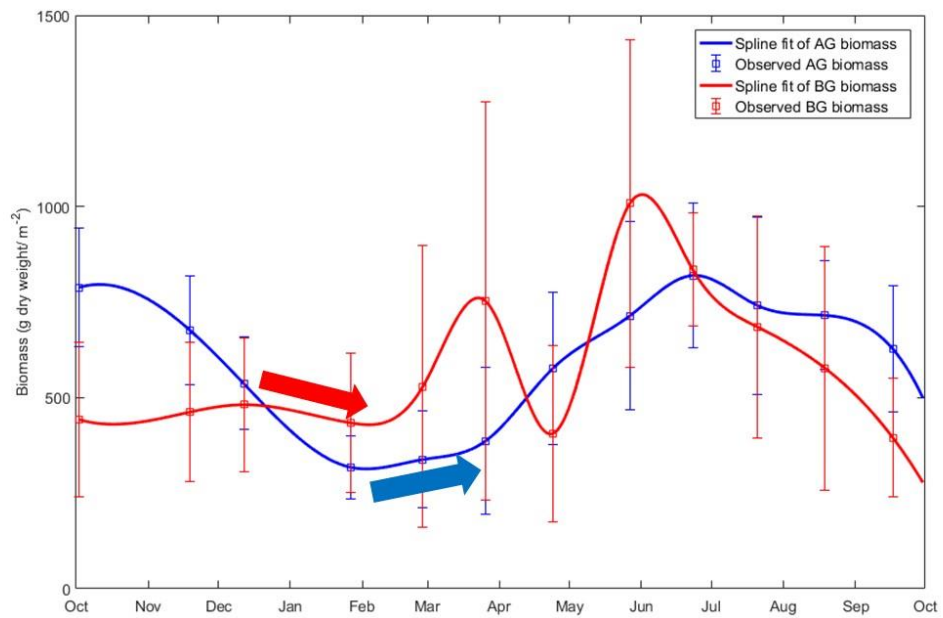


**Figure 3.3** Monthly above-ground (AG) and below-ground (BG) biomass from Oct. 2013 – Dec. 2015 in tall form *S. alterniflora* on Sapelo Island, Georgia, USA

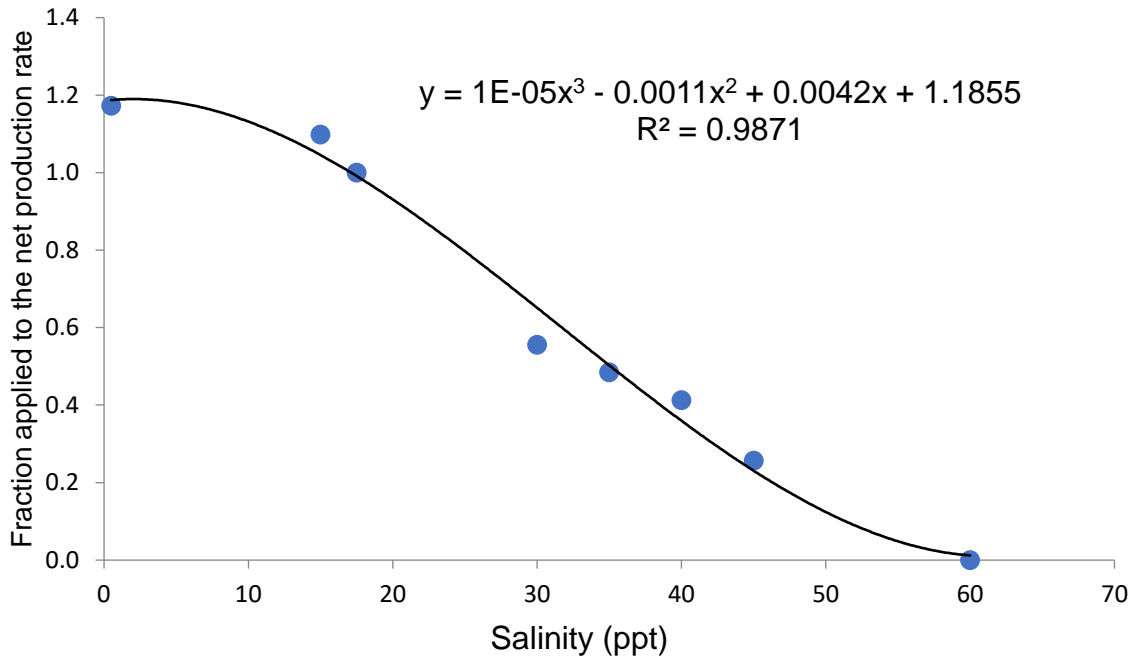


**Figure 3.4** The effect of salinity on the gross production rate in the PG model based on the data from Linthurst & Seneca (1981) and Ge et al. (2014).

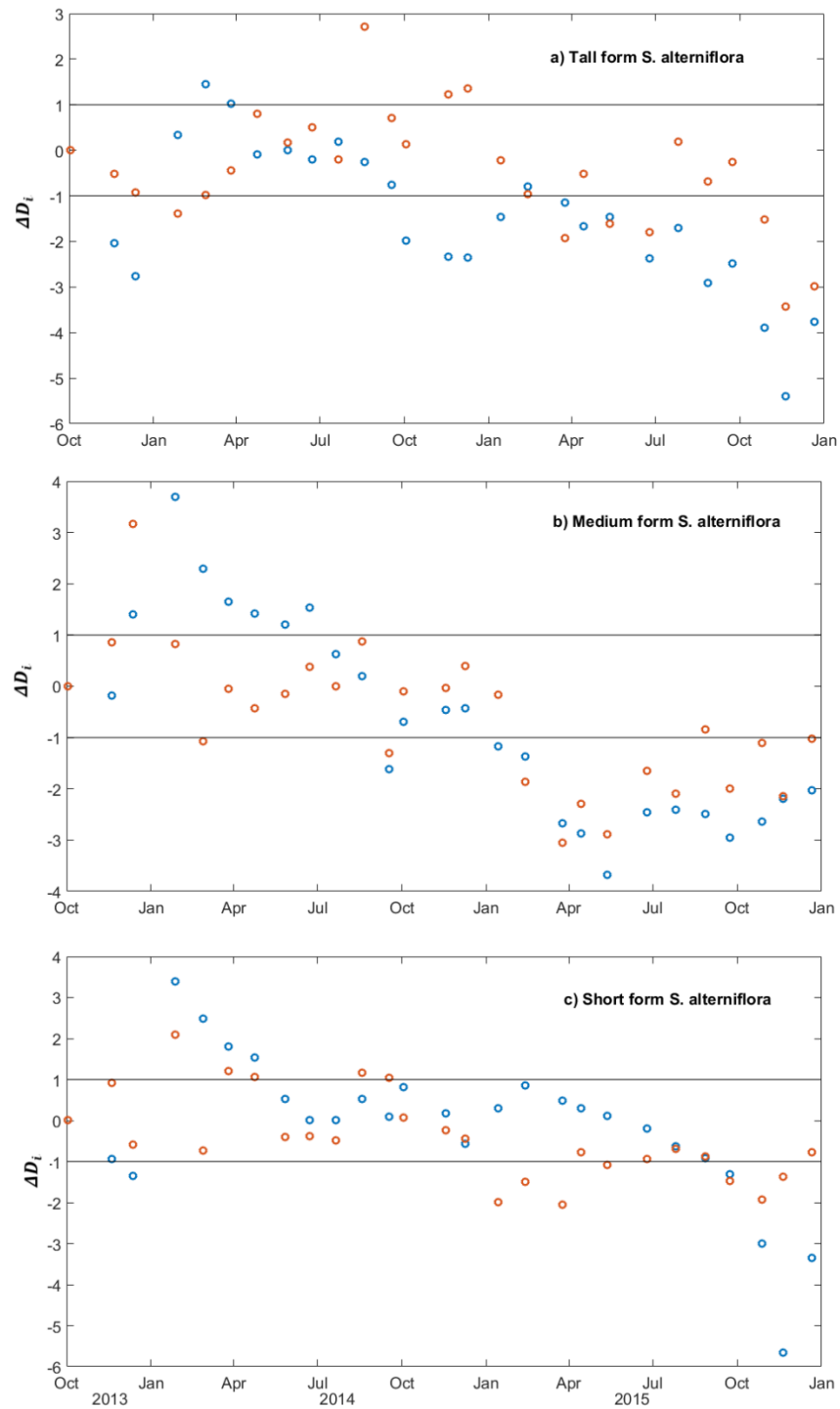


**Figure 3.5**  $\Delta D_i$  values quantifying the differences between observed and modeled biomass in above- (blue circles) and below-ground biomass (red circles) for three height forms of *S. alterniflora*

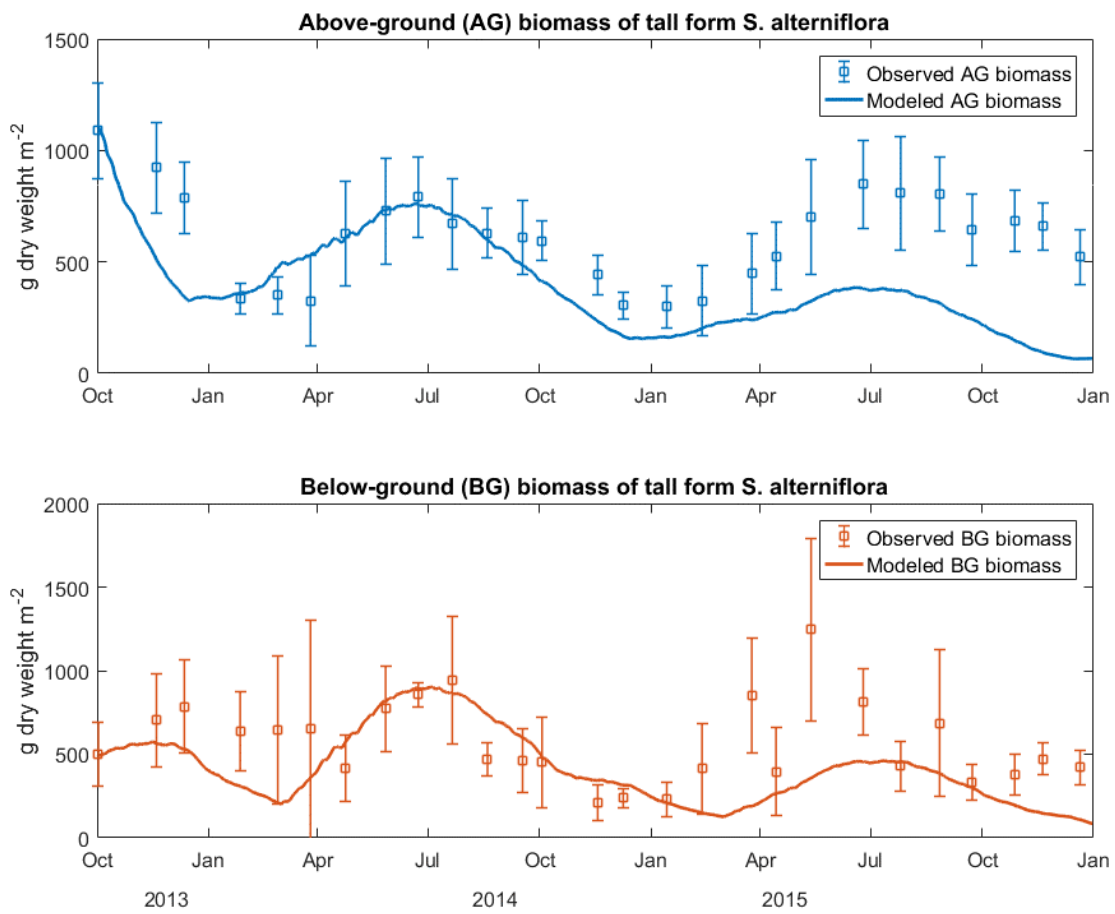


**Figure 3.6** The PG model result of tall form *S. alterniflora* on Sapelo Island, Georgia

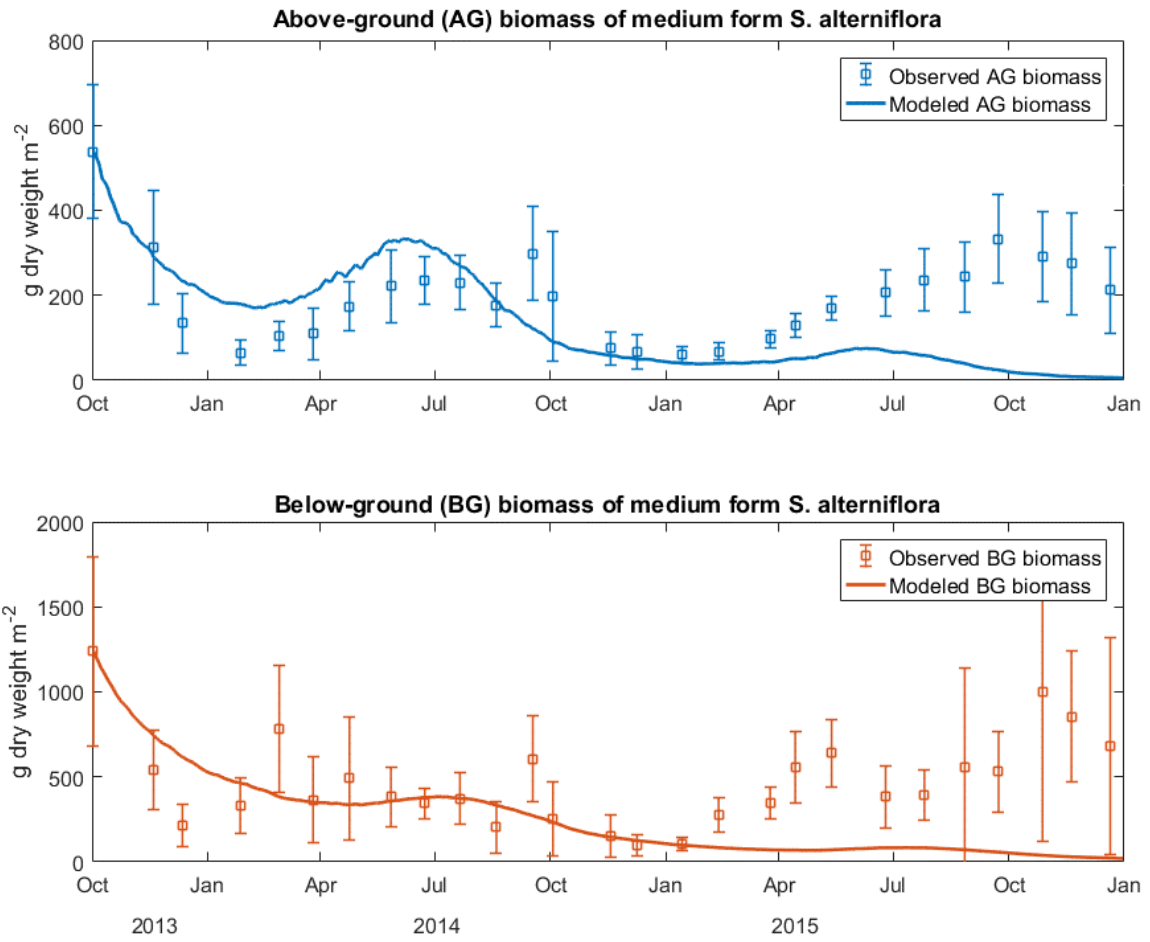


**Figure 3.7** The PG model result of medium form *S. alterniflora* on Sapelo Island, Georgia

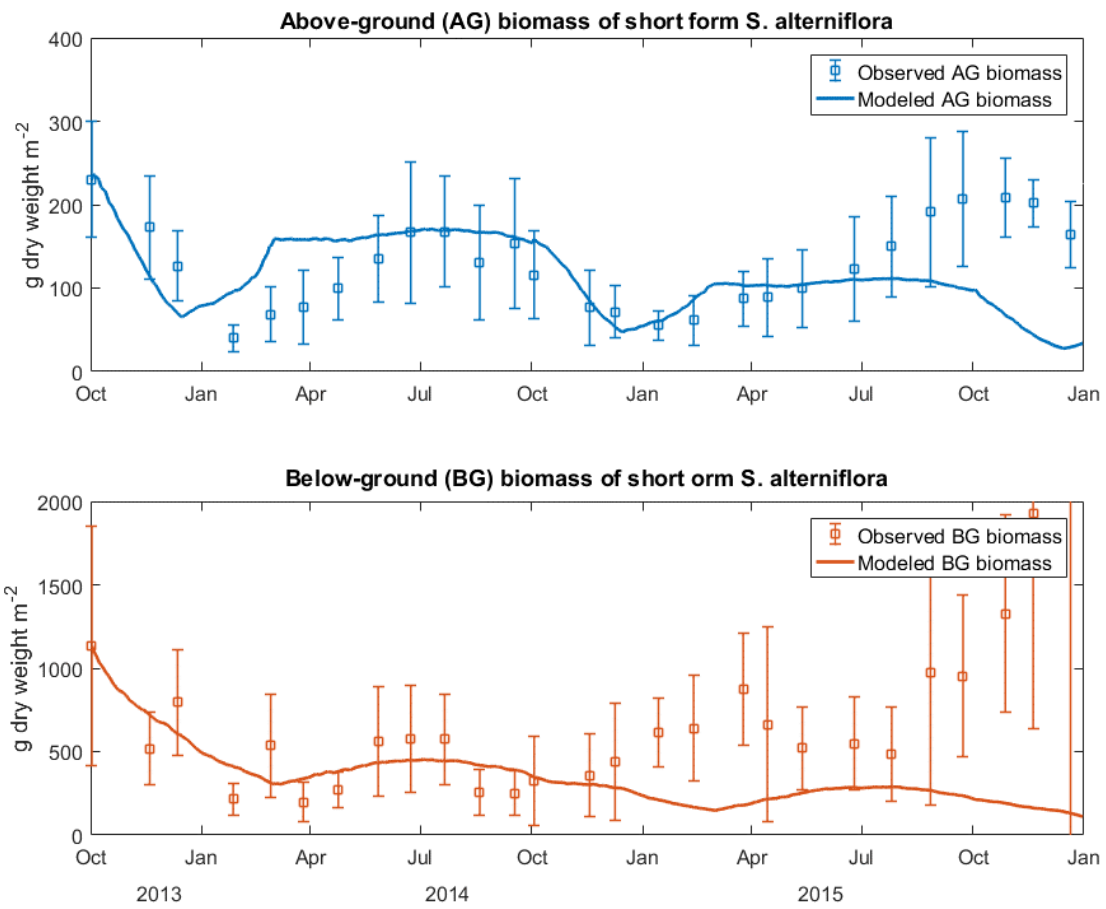


**Figure 3.8** The PG model result of short form *S. alterniflora* on Sapelo Island, Georgia

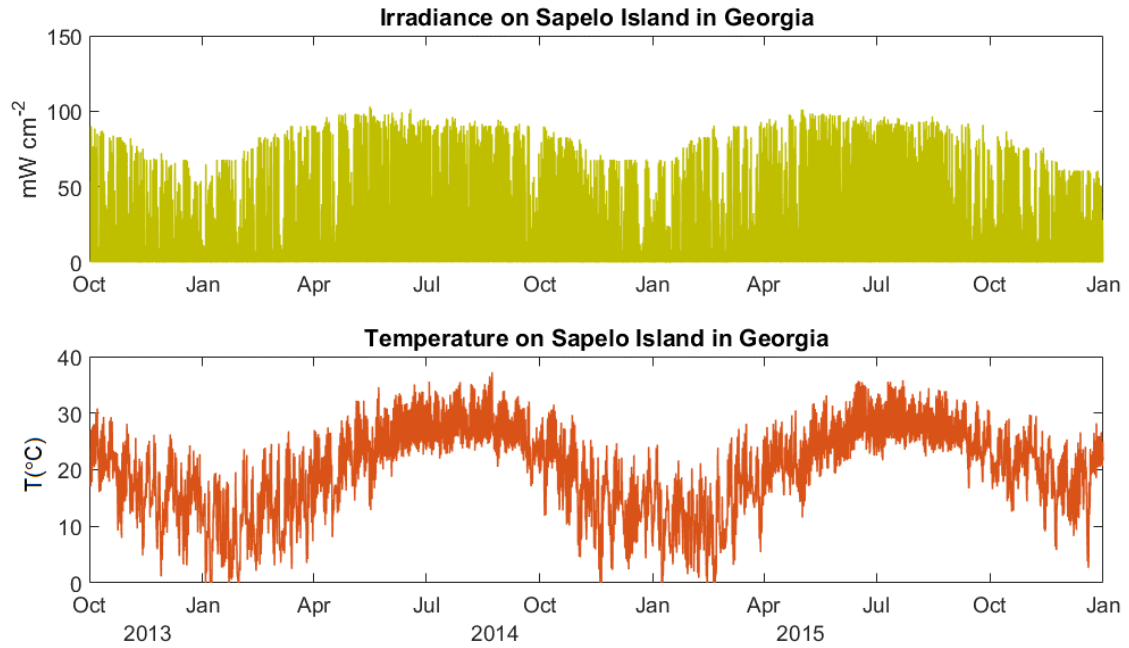


**Figure 3.9** Observed downwelling irradiance and temperature on Sapelo Island, Georgia USA

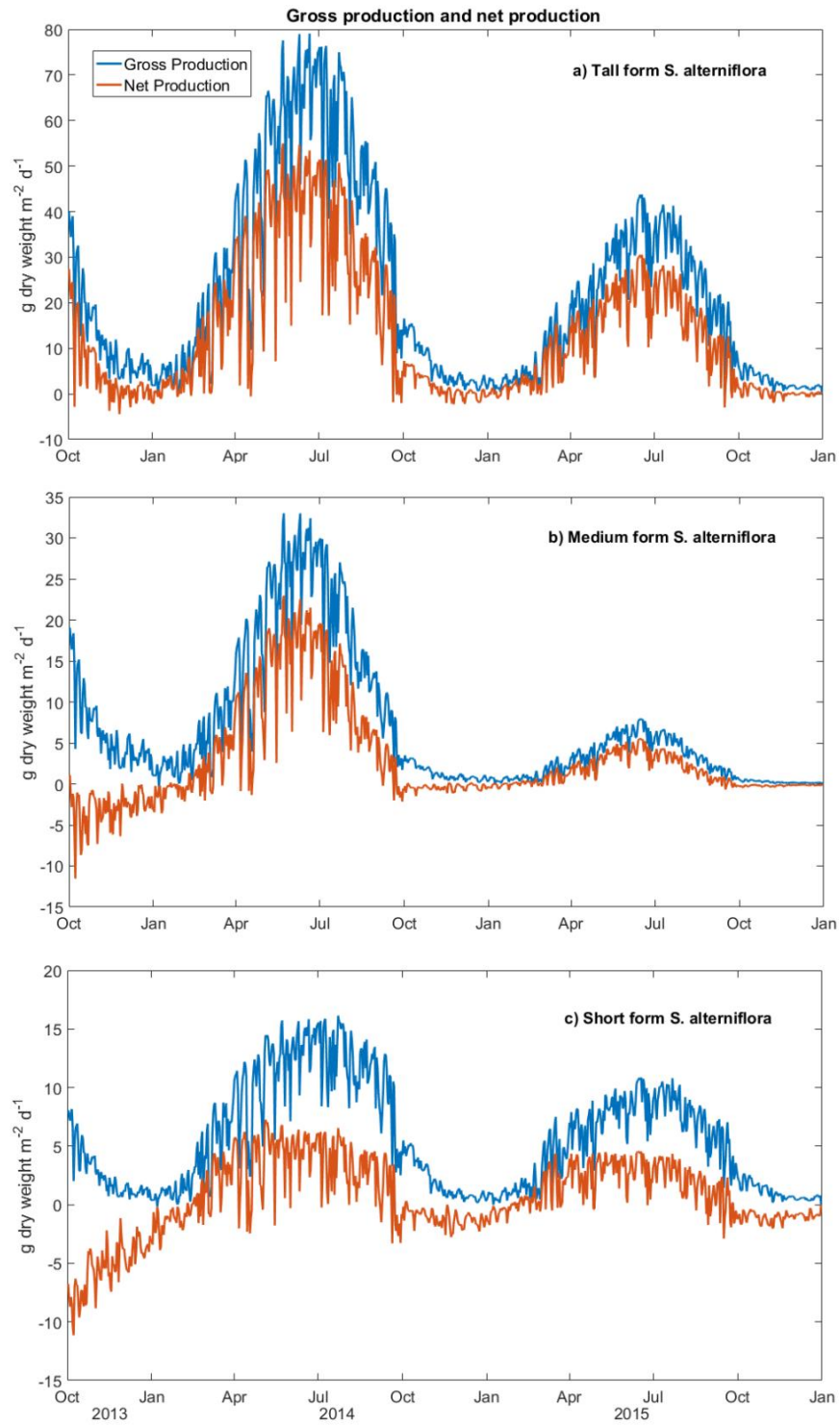


**Figure 3.10** Gross production and net production of the three types of *S. alterniflora* on Sapelo Island, Georgia

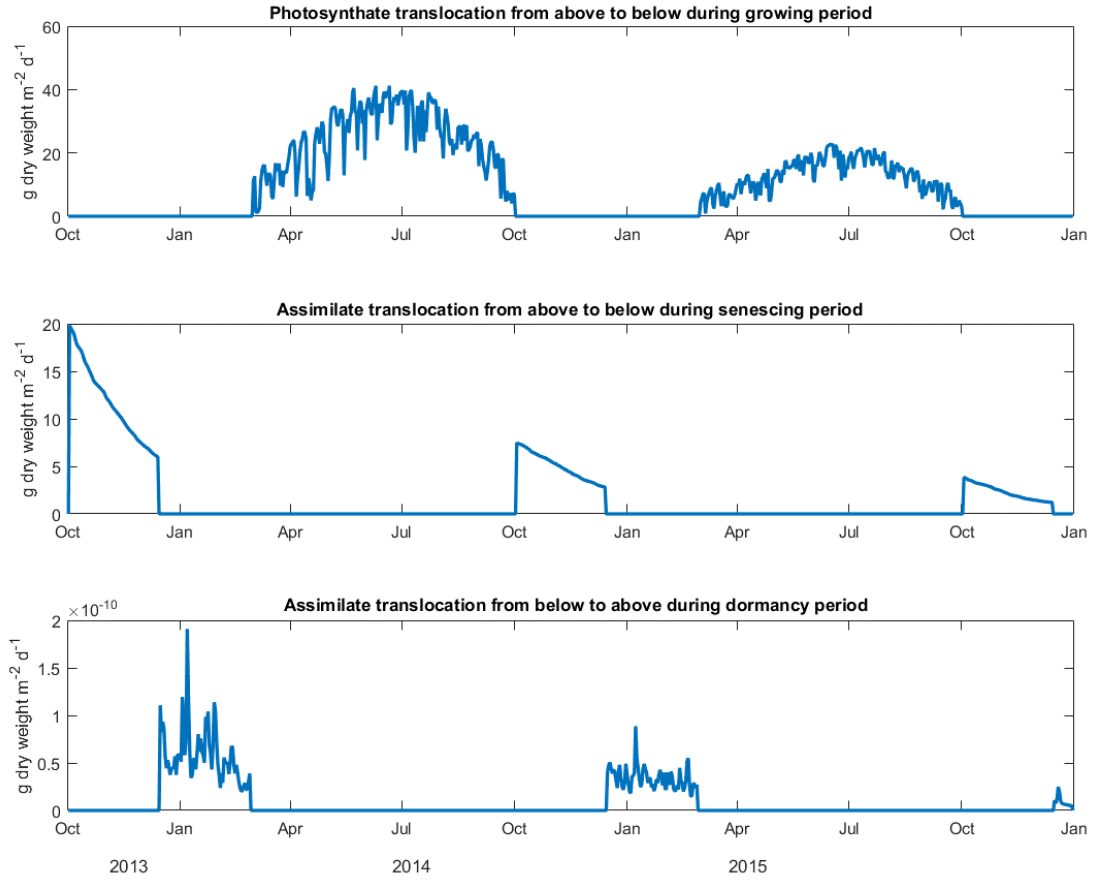


**Figure 3.11** Modeled daily carbon translocation rates for tall form *S. alterniflora* on Sapelo Island, Georgia

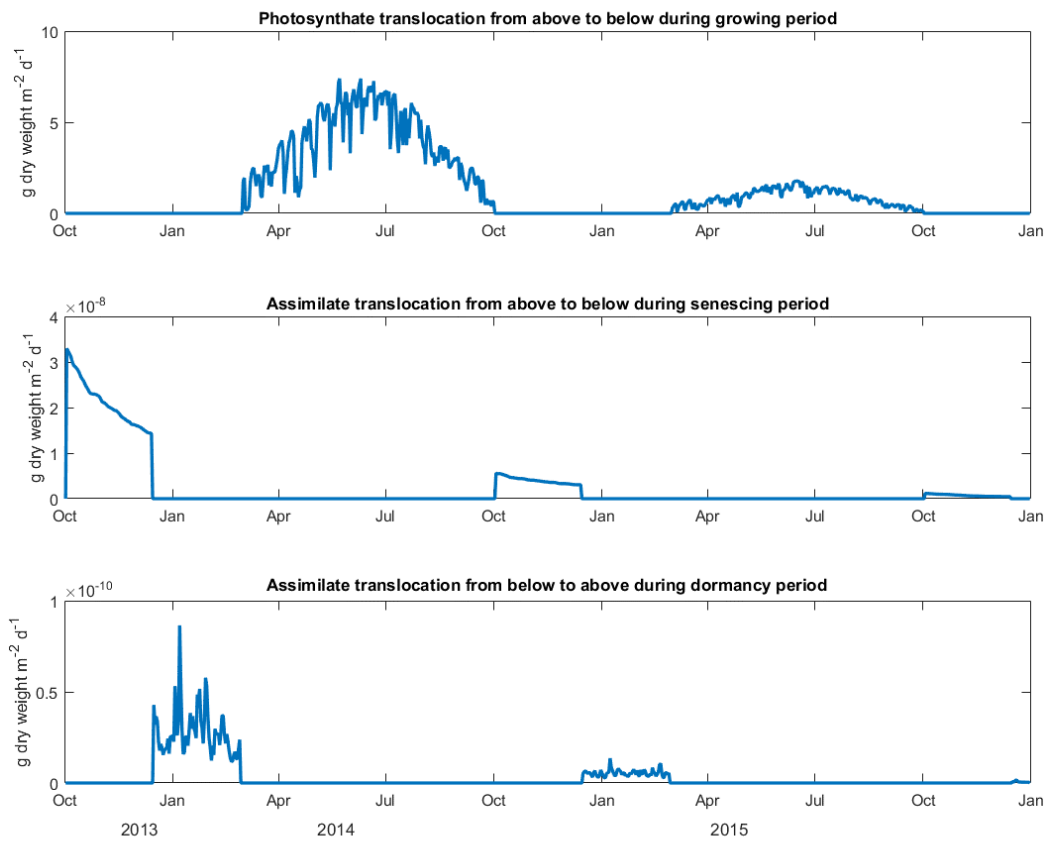


**Figure 3.12** Translocated photosynthate and assimilate of the medium form *S. alterniflora* on Sapelo Island, Georgia

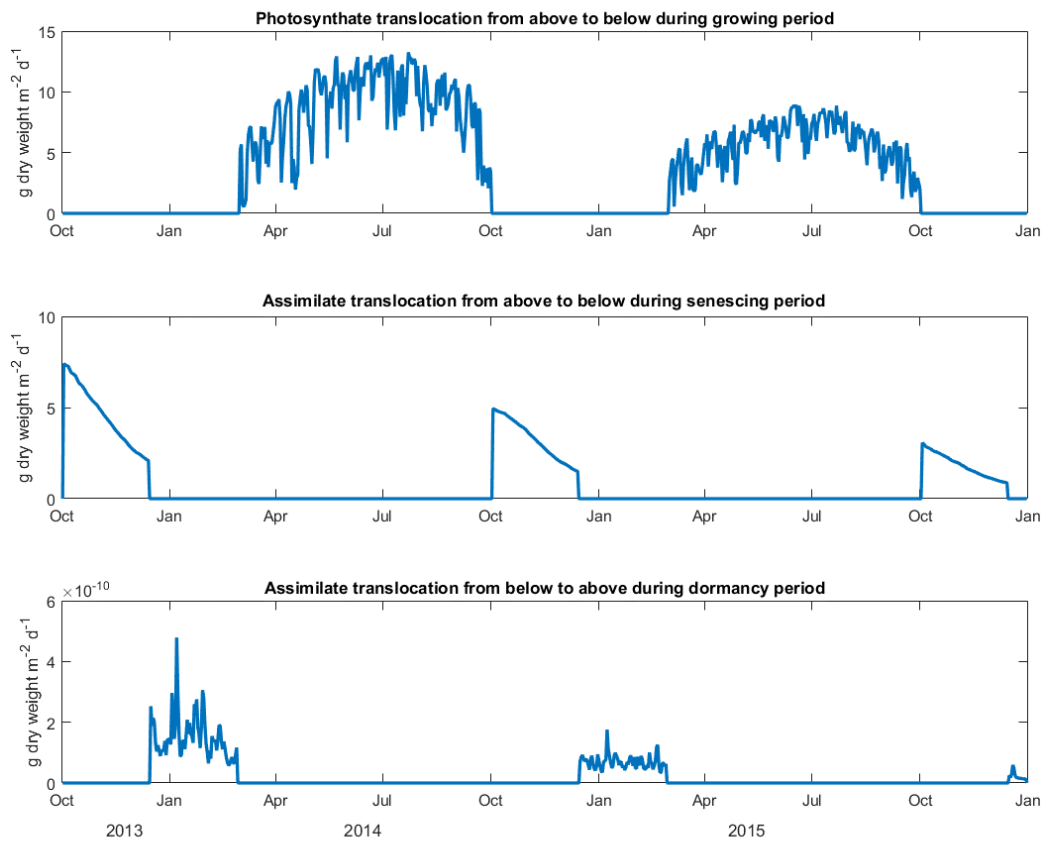


**Figure 3.13** Translocated photosynthate and assimilate of the short form *S. alterniflora* on Sapelo Island, Georgia

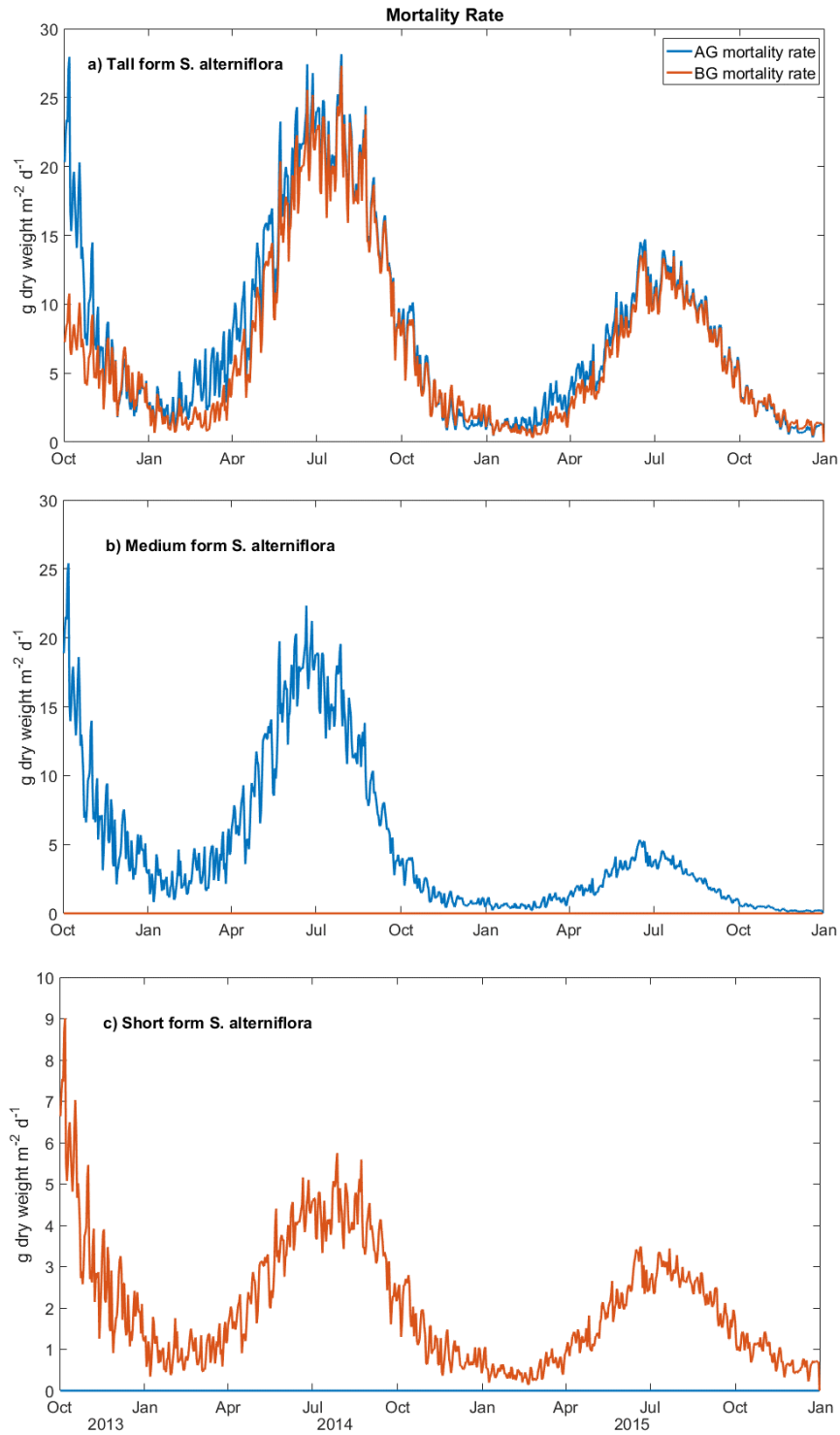


**Figure 3.14** Modeled mortality rates of the three types of *S. alterniflora* on Sapelo Island, Georgia

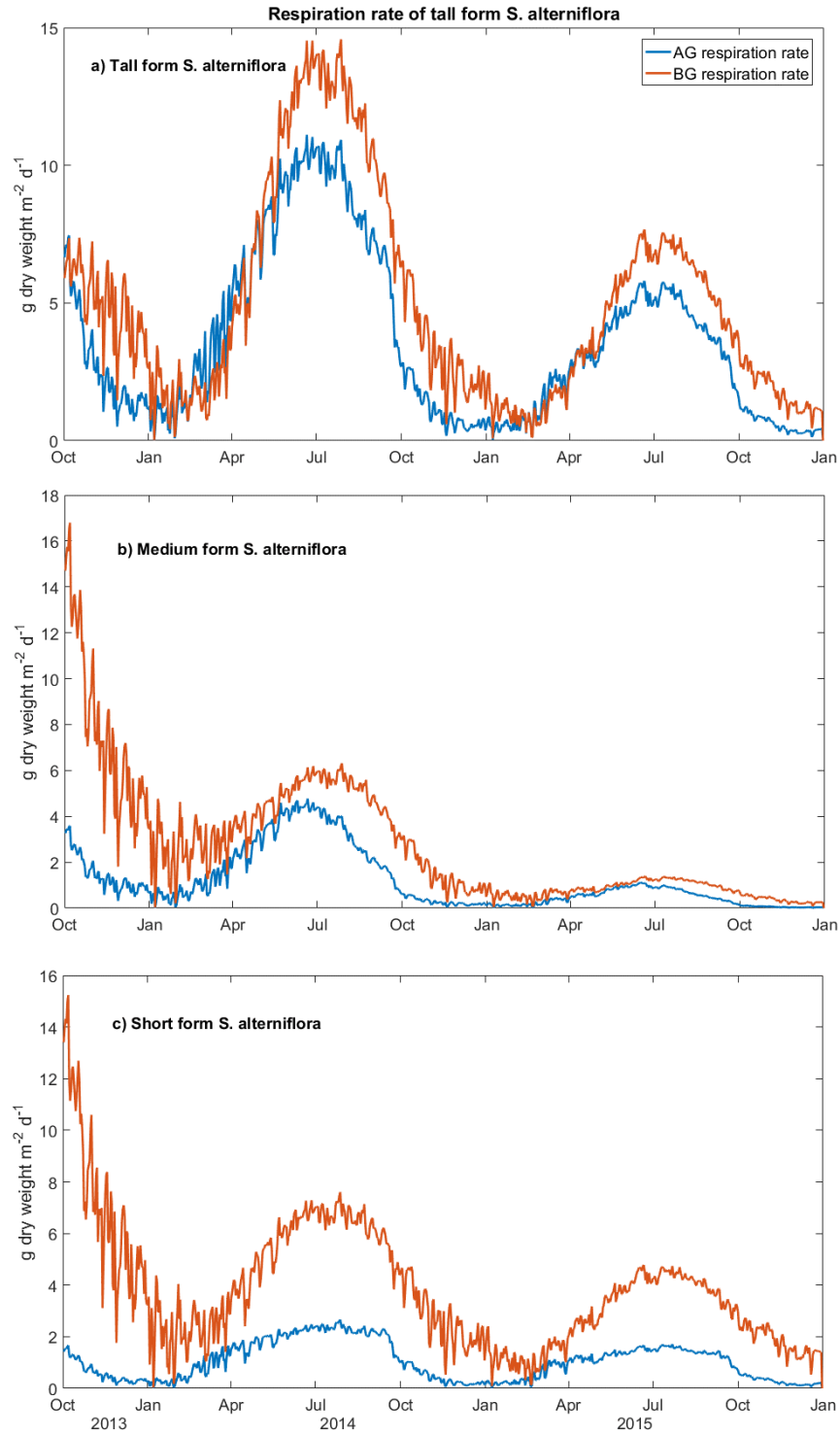


**Figure 3.15** Modeled respiration rates of the three types of *S. alterniflora* on Sapelo Island, Georgia

## CHAPTER 4

### MODELING THE VARIABILITY IN PHENOLOGY-BASED GROWTH DYNAMICS OF

### *SPARTINA ALTERNIFLORA* WITH LATITUDE<sup>1</sup>

---

<sup>1</sup>Jung, Y., & Burd, A. To be submitted to *Estuarine, Coastal and Shelf Science*

## **Abstract**

The variation in dynamics of translocation between above- and below-ground biomass of *Spartina alterniflora* with latitude was studied using a plant growth and production model. The study shows that the main sources of the carbon translocation to the below-ground tissues varies with latitude. The model analysis suggests that both photosynthates and the remobilization of assimilates during growing and senescing periods serve as the main sources of the carbon translocation from above- to below-ground tissues in a higher latitude. However, in the lower latitude regions with a warmer environment, the main source to build up the below-ground biomass was the immediate photosynthesis that occurred during growing seasons. The total photosynthates translocation from above- to below-ground tissues during growing seasons increase as the latitude decreases, whereas the assimilates translocation from the senescing shoots to below-ground during fall seasons increases as latitude increases. The translocation of assimilate from below- to above-ground tissues during the dormancy period increases with latitude. The model enables us to predict both above- and below-ground biomass and quantify the carbon translocation, which helps us understand the main sources of allocation to the below-ground tissues at different phenological events.

## **1. Introduction**

Phenology is the study of the timing of cycles of life history events in plant and animal life. Examples of such events for plants include bud-burst, leaf-expansion, flowering, and abscission. The timing of these events is affected by seasonal and inter-annual variations in climate, environment, and habitat factors (Fenner, 1998). Phenology of *S. alterniflora* varies throughout its geographic distribution. In Nova Scotia, green-up occurs in April and shoot biomass reaches

its maximum in October (Cranford et al., 1989), whereas the aerial growth starts in March and peak biomass occurs in September in South Carolina (Morris & Haskin, 1990). Flowering begins between September and November in Mississippi (Eleuterius & Caldwell, 1984), whereas *S. alterniflora* flowers in late July and seeds are produced in late September in South San Francisco Bay (Callaway & Josselyn, 1992). Although phenology is affected by abiotic factors such as temperature and precipitation on local scales (O'Donnell & Schalles, 2016), it is considered to be largely determined genetically. For example, Crosby et al. (2015) found from their greenhouse mesocosm experiment that northern marsh *S. alterniflora* from Massachusetts and Delaware flowered earlier (July - August) than plants from more southern marshes from North and South Carolina regions (October).

Phenology has been shown to be an effective indicator of the success of competition in community and growth dynamics of both above and below-ground biomass. In San Francisco bay, *S. alterniflora* begin spring growth approximately one month earlier than *Spartina foliosa* and are taller than *S. folis* with differences being greater than 60cm (Callaway, 1990) and thus contain more live above-ground biomass throughout the year (Callaway & Josselyn, 1992). Crosby et al. (2015) found that the onset of flower production leads to an increase in the below-ground allocation.

The quantity of the material that *S. alterniflora* contains in below-ground in forms of biomass or non-structural carbohydrates increases with latitude. Higher below-ground production of *S. alterniflora* was observed in Delaware, ranging from 4,400 – 7,700 g m<sup>-2</sup> y<sup>-1</sup> (Dame & Kenny, 1986) compared to South Carolina where it varied between 2,363 to 5,445 g m<sup>2</sup> y<sup>-1</sup> (Roman & Daiber, 1984). The total non-structural carbohydrates (NSC) stored in the below-ground tissues of *S. alterniflora* at higher latitude in Nova Scotia varied between 9 – 31% of total biomass

(Livingstone & Patriquin, 1981) whereas values between 1.4 and 17.3% were found in below-ground parts growing in further south in Georgia (Jung & Burd, 2017). This increasing pattern in below-ground biomass and NSC toward the higher latitude may have been because *S. alterniflora* in northern region flower earlier and that promotes earlier onset of allocation of biomass to below-ground tissues. This biomass stored during the winter is utilized for shoot growth in the following spring and rhizome growth in summer (Lytle & Hull, 1980). However, neither the source nor the amount of carbon translocated from above- to below-ground tissues during different phenological periods is known.

Understanding of phenology and its interaction with translocation dynamics in plants is therefore important to quantify plant growth and the carbon allocation between tissues. Species-specific phenology-based models allow us to examine the local to latitudinal shift in phenology (Kramer, 1994; Chuine et al., 2000; Cleland et al., 2007), to forecast shifts in species ranges (Chuine & Beaubien, 2001; Bertin, 2008; Ehrlén & Morris, 2015) and productivity (Heimann et al., 1998; Van Wijk & Williams, 2003; Euskirchen et al., 2014) in response to changing abiotic conditions.

In this study, we use the PG model to examine how translocation between above- and below-ground biomass compartments change with latitude and how this may be affected by environmental factors and in turn affect the timing of life-history events. Our goal is to use the model to understand the mechanistic links between phenological characteristics and the allocation dynamics of *S. alterniflora* at three different latitudes in the United States. We apply site-specific forcing data (e.g., irradiance, temperature, etc.) and estimate parameters using site-specific data (e.g. phenology timing, biomass) through the use of an inverse model. This theoretical study enhances our understanding of how phenology can vary with changing

environmental factors and how this influences plant below-ground allocation at different latitudes.

Our research questions are (1) Does the model predict differences in the importance of winter below-ground storage between *S. alterniflora* growing in colder vs. warmer climates? (2) How do the rates and amounts of translocated material during growth, senescence, and dormancy periods differ for *S. alterniflora* by latitude? (3) How do seasonal mortality and respiration rates of *S. alterniflora* change with latitude?

We hypothesize that, (1) *S. alterniflora* at lower latitudes translocates more biomass from above- to below-ground tissues during the growing period compared to *S. alterniflora* in higher latitudes. (2) The carbon translocation from senescing shoots increases as the latitude increases.

## **2. Methods and Applications**

### **2.1 Study sites**

We chose data from locations at three different latitudes, Delaware (38.79° N, -75.16° W), South Carolina (33.32° N, -79.17° W), and Louisiana (29.25° N, -90.66° W). These sites were selected for several reasons. First, we chose sites that used the same harvesting method (Smalley, 1958) because there are significant differences in production estimates using different methodologies (Roman & Daiber, 1984); the Smalley method considers changes in both live and dead above ground biomass and provides a better estimate of production than the peak live standing crop method. Second, we also chose studies that gave biomass of *S. alterniflora* with heights greater than 0.8 m growing in saline wetlands for investigating the near tall form *S. alterniflora* (Table 4.1).

## 2.2 Biotic variables

At each of the three locations, the ratio of live above-ground biomass to total above-ground biomass was used as an estimate of the green-leaf ratio required by the model. The sum of live and dead biomass was used for the observed above-ground biomass and only live below-ground biomass was used for the observed below-ground biomass. The sum of live and dead below-ground biomass was available in Delaware site (Roman & Daiber, 1984), so we calculated the live below-ground biomass using the tall *S. alterniflora* live:dead below-ground biomass ratio measured in Delaware by Gross et al. (1991). Leaf nitrogen data was either available as a yearly average value (Roman & Daiber, 1984) or less than 4% (Darby & Turner, 2008). Morris (1982) demonstrated that the growth rate of *S. alterniflora* was found to be insensitive to the leaf-nitrogen concentrations between 1% and 4%. Therefore, we used a similar time series of nitrogen data for the independent variable in the production function for all simulations.

## 2.3 Abiotic variables

The calculated temperature and irradiance data at each latitude were used as the main input data in the model. The hourly temperature normal data from 1981 to 2010 at three different latitudes were acquired from U.S. climate normal products database from NOAA national centers for environmental information website (<https://www.ncdc.noaa.gov/data-access/land-based-station-data/land-based-datasets/climate-normals/1981-2010-normals-data>). The temperature normal is calculated by taking the average of the 30 hourly values from year 1981 to 2010 at each hour. These climatological temperatures were utilized to determine parameter values of the temperature equation (1) in Morris et al.'s model (1984) by using the temperature model described below in inverse mode. The temperature was modeled as

$$T = a_1 \sin(0.017D + a_2) + a_3 \sin(0.26H + 4.45) + a_4 \quad (1)$$

where  $T$  is temperature ( $^{\circ}\text{C}$ ),  $D$  is the calendar day (1 to 365) and  $H$  is the hour (1 to 24).

The coefficient value,  $a_1$ , describes the degree of seasonal amplitude in temperature wave. For example, if  $a_1$  increases, the seasonal amplitude increases which in turn affects the annual maximum and minimum temperatures. The coefficient  $a_2$  represents a phase shift of the seasonal temperature period. The positive and negative phase shift  $a_2$  indicate a shift to the later or earlier, respectively. The coefficient value,  $a_3$ , determines the amplitude of daily temperature. As  $a_3$  increases, it gives the higher daily maximum temperature and the lower daily minimum temperature. Finally, the coefficient value,  $a_4$ , represents a yearly offset. The positive and negative offset  $a_4$  indicates a shift upward or downward, respectively. Values of the coefficients  $a_i$  enable us to quantify the amplitude and phase of seasonal and daily temperature variability at each latitude. The coefficients  $a_i$  (Table 4.2) were estimated by fitting equation (1) to the climatological temperatures using the cost function

$$Dt_i = \sum_i^n (NT_i - MT_i)^2 \quad (2)$$

where  $NT_i$  is climatological temperatures and  $MT_i$  is the modeled temperature at the  $i$ -th time point. The estimated parameters (Table 4.3) were used to generate temperature data in the PG model for each latitude.

Irradiance ( $\text{mW cm}^{-2}$ ) for each location was calculated using standard formulae (e.g. Iqbal, 1983). First, the ratio of Sun-Earth distance to mean Sun-Earth distance,  $E_0$  was estimated using the following equation.

$$E_0 = 1.000110 + 0.034221 \cos(\Psi_e) + 0.001280 \sin(\Psi_e) + 0.000719 \cos(2\Psi_e) + 0.00077 \sin(2\Psi_e) \quad (3)$$

where,

$$\Psi_e = \left(\frac{2\pi}{365}\right)(D - 1) \quad (4)$$

Finally, the irradiance ( $L$ ) was estimated by the following equation.

$$L = (A_f S_c E_0 \cos(\frac{Z\pi}{180})) \quad (5)$$

where  $A_f$  is a solar constant and  $S_c$  is an atmospheric absorption coefficient (Table 4.2).  $Z$  is the zenith angle (in degrees) calculated using standard equations (Kirk, 1994). The hourly irradiance was calculated only for times between sunrise and sunset.

#### **2.4 Effect of porewater salinity on the production of *S. alterniflora***

The effect of porewater salinity on gross primary production was incorporated into the model as described in Chapter 3. Howes et al. (1981) reported that creek bank sediments have porewater salinity that is similar to that in the creek during the flooding tide because of frequent drainage. For the latitudinal study, it was assumed that the average porewater salinity at each site was the same as the water column salinity reported at the study site since *S. alterniflora* collected at the three sites were located within 20 meters of the creek bank. The average porewater salinities for study sites in Delaware, South Carolina, and Louisiana were set as 27.5 ppt, 30.01 ppt, and 13.5 ppt by selecting the mid-point of the stated salinity range at the site (Roman & Daiber, 1984; Darby & Turner, 2008) or by calculating the average salinity when seasonal salinity values were available (Dame & Kenny 1986).

#### **2.5 Model formulation**

The PG model described in Chapter 3 was used to investigate the growth dynamics of *S. alterniflora* at the three locations. Five parameters,  $\alpha_{ab}$ ,  $\alpha_{ba}$ ,  $\gamma$ ,  $m_a$ , and  $m_b$  (Table 4.2) at the three latitudes were estimated using the PG in inverse mode as described in chapter 3. The gross production was estimated as a function of irradiance, temperature, green leaf ratio, and nitrogen concentration in green leaves. Net production was derived from the gross production by subtracting respiration rates. Differences between observed and modeled biomass,  $\Delta D_i$ , were

calculated using Equations (12) and (13) in chapter 3. The monthly below-ground biomasses were estimated from the bimonthly below-ground biomass data by interpolation using a cubic spline calculated using the Matlab functions, `pchip` and `spline`. The phenological dates for the start date of the senescence period of *S. alterniflora* at three sites were estimated using the timing of the first observation of a continuous increase in above-ground dead biomass. The start and end dates for translocation of photosynthates or assimilates between above-ground and below-ground tissues were estimated (Table 4.4) using the method introduced in chapter 3 which used the observation of the patterns in above- and below-ground biomass through the spline fitting method.

### 3. Results

#### 3.1 Parameter values from inverse model

The temperature inverse model estimated the coefficient values,  $a_i$ , for equation (1). Values of  $a_1$  were highest in Delaware indicating that the differences between the annual minimum and maximum temperatures was greater there than that in Louisiana or South Carolina. The  $a_3$  values, which indicate the extent of daily temperature fluctuations, were similar for all three latitudes (Table 4.3).

The PG model was used in inverse mode to calculate the model parameters that gave the best fit of modeled biomass to observed biomass for *S. alterniflora* taller than 0.8 meter in Delaware (DE), South Carolina (SC), and Louisiana(LA). The fraction of photosynthate translocated from above- to below-ground ( $\alpha_{ab}$ ) during the growing season was roughly similar ranging between 0.55 and 0.75 in all sites but the absolute amount of photosynthates translocation increases moving from higher to lower latitudes. The values of  $\alpha_{ab}$  (Table. 4.5)

indicate that *S. alterniflora* at the three latitudes translocates more than half of its production generated from photosynthesis to the below-ground tissues during the growing season.

In contrast, the fraction ( $\gamma$ ) of above-ground assimilates translocated to below-ground tissues during the senescence period was highest in Delaware (0.0024) whilst plants in South Carolina and Louisiana had a lower and similar value (0.0006). This suggests that plants at higher latitudes rely on the carbon translocation from above-ground senescing tissues to a greater extent than plants at lower latitudes (SC and LA) for building up the below-ground biomass during the senescence period.

The fraction of below-ground assimilates translocated from below- to above-ground tissues ( $\alpha_{ba}$ ) during the dormancy period was highest in Delaware ( $1.3 \times 10^{-5}$ ) compared to that in South Carolina ( $4.7 \times 10^{-13}$ ) and Louisiana ( $1.2 \times 10^{-14}$ ). The fraction,  $\alpha_{ba}$ , in Delaware seems reasonable value compared to the estimated value ( $8.2 \times 10^{-4}$ ) in Zheng et al.'s model (2016).

These model results indicate that *S. alterniflora* at higher latitudes translocates photosynthate to below-ground tissues during the growing season and assimilates from below-ground to above-ground tissues during the dormancy period. However, there is an apparent latitudinal difference in the relative amount of translocated material to the below-ground from different sources. The main source of carbon allocation to below-ground tissues at higher latitudes (DE) is a combination of photosynthate and senescing biomass, whereas it is mainly photosynthate in lower latitudes (LA).

The specific rate of both above- and below-ground mortality at 20 °C were very similar in all latitudes, ranging from 0.0006 – 0.0008  $\text{gg}^{-1} \text{d}^{-1}$ .

The coefficient value for dark respiration,  $\rho$ , that was additionally included in the model for the latitudinal study, showed different values throughout all regions (Table 4.5). The  $\rho$  value

was highest in Louisiana ( $5.4 \times 10^{-5}$ ) which is about two times than *S. alterniflora* in Delaware and four time higher than one in South Carolina. This  $\rho$  value in Louisiana was higher than the one on Sapelo Island, Georgia ( $2.3 \times 10^{-5}$ ). This is not surprising given the fact that the dark respiration rate increases with temperature and the highest air temperature were found in Louisiana.

The  $\Delta D_i$  values, which quantify the differences between modeled and observed biomass, were lowest (9.13) in South Carolina which indicates that the model prediction showed good match with field data compared to Delaware (96.60), Louisiana (79.04) and the three height forms of *S. alterniflora* on Sapelo Island in Georgia ranging 57.64 – 77.07 (Table. 4.5). Generally, the model matched well in below-ground biomass in all three regions but the larger deviations were observed in above-ground biomass in Delaware in most of months and in November in Louisiana (Figure 4.2 – 4.4).

### **3.2 PG Model above- and below-ground biomass results**

During the early spring season (Jan., Feb.) the observed below-ground biomass in Delaware was more than four times greater than the above-ground biomass and then decreased continuously until July (Figure 4.2). The observed above-ground biomass, which included both dead and live biomass, remained less than  $1,500 \text{ g m}^{-2}$ , and showed monthly variation throughout the late spring and fall but the annual variation was within  $545 \text{ g m}^{-2}$ . This relatively small variation compared to the one in below-ground was due to that the degree of the decreasing live above-ground biomass is similar to the increasing dead above-ground biomass throughout the year, so the sum of live and dead biomass stays consistent although the amount of the live above-ground tissues that can actively photosynthesize fluctuates seasonally. The average root:shoot ratio was highest (2.51) in Delaware (Table 4.6 and Figure 4.5). The model reproduced the

general behavior of the below-ground biomass but predicted larger than observed above-ground biomass in Delaware (Figure 4.2). Considering the fact that the model is an inverse model in this latitudinal study, the model results are expected to fit reasonably well to the observed data. but the model showed a great deviation in above-ground biomass throughout the year in Delaware.

The model fit gave best agreement with the both above- and below-ground biomass in South Carolina (Figure 4.3). The modeled below-ground biomass in South Carolina ranged between approximately 1,800 – 3,000 g m<sup>-2</sup>, which was about half of that seen in Delaware ranging from 2,000 to 5,000 g m<sup>-2</sup> throughout the year (Figure 4.2 & 4.3). The modeled below-ground biomass in South Carolina stayed above 2,500 g m<sup>-2</sup> between September and January and then dropped to below 2000 g m<sup>-2</sup> in May. The highest modeled above-ground biomass was observed in October in South Carolina, which agrees with the observed biomass (Figure 4.3).

Modeled Louisiana above-ground biomass successfully predicted the two peaks in fall (Sep.– Oct.) and in February. However, the model was not able to predict a winter minimum of above-ground biomass in November but instead predicted a minimum value in January. The modeled biomass showed the lowest average root:shoot ratio in Louisiana (0.92) (Table 4.6 & Figure 4.5).

### **3.3 Gross production and net production**

The modeled gross production was almost 0 from January to May in Delaware but increased rapidly from May onwards and reached over 55 g m<sup>-2</sup> d<sup>-1</sup> in September before decreasing in the following months (Figure 4.6). The total plant net production was always less than 0 in Delaware indicating that *S. alterniflora* consumed more carbon through respiration of both above- and below-ground tissues than the carbon produced from photosynthesis during the study period. The negative net production was reflected entirely in the decreasing below-ground

biomass (Fig. 4.2) though there was some decrease in above-ground biomass as well. Both gross production and net production in South Carolina were highest in late August and lowest between December and January (Figure 4.7). Gross production in Louisiana was highest from July through early October (Figure 4.8). Overall, the average daily gross production increased as the latitude of the site decreased (Table 4.7). The gross production patterns were similar with the climatological temperature cycle at all sites (Figure 4.6 – 4.8).

### **3.4 Translocated biomass at different phenological events**

The amount of photosynthate or assimilate translocated during three phenologically relevant periods at the three sites were estimated from the model. The largest amount ( $1,703 \text{ g m}^{-2}$ ) of material translocated from above- to below-ground tissue during senescence occurred in tall *S. alterniflora* at the northern site (Delaware). This was approximately three times greater than the assimilate translocated during senescence at the Louisiana site ( $458 \text{ g m}^{-2}$ ) (Table 4.8, Figure 4.9 & 4.11). A similar trend occurred for the assimilate translocated from below-ground to above-ground tissues during the dormancy period, where the largest assimilate translocation occurred at the Delaware site ( $261 \text{ g m}^{-2}$ ) and was close to zero at South Carolina and Louisiana sites. Plants at the Louisiana site translocated the largest amount ( $7,202 \text{ g m}^{-2}$ ) of photosynthate from above- to below-ground tissues during the growing season, approximately 2.5 times greater than the amount translocated at the Delaware site (Table 4.8).

This pattern suggests that at higher latitudes below-ground biomass is sustained by the remobilization of assimilate from the senescing above-ground tissues. The photosynthate translocated from above-ground to below-ground through photosynthesis increased as latitude decreased, which supports our first hypothesis. This suggests that the below-ground biomass in lower latitudes is supported mainly by photosynthate translocated from above-ground during the

growing season. The total assimilates allocated from below- to above-ground tissues during the dormancy period were highest in Delaware, compared to the almost zero value in South Carolina and Louisiana.

### **3.5 Mortality rates of above- and below-ground tissues**

The mortality rates in both above- and below-ground tissues peaked in September to October in all three latitudes (Figure 4.12). The highest and lowest mortality rates of below-ground tissues were observed in South Carolina and Louisiana, respectively. Overall, the mortality rates of below-ground biomass were more than two times greater than the above-ground mortality throughout the study periods except for the Louisiana site.

### **3.6 Respiration rates of above- and below-ground tissues**

The respiration rates were high during October and low during spring at all three sites (Figure 4.13). The daily mean above-ground respiration rate is highest in Louisiana but its below-ground rate was similar at all three sites ranging from 17 – 24 g m<sup>-2</sup> d<sup>-1</sup> (Table 4.9).

## **4. Discussion**

Our first hypothesis that *S. alterniflora* growing in lower latitudes would translocate more biomass from above- to below-ground tissues, especially during the growing season, was supported by the study results. Our results showed that tall *S. alterniflora* growing at a lower latitude in a warmer environment translocates a greater proportion of its photosynthate to the below-ground biomass during the growing season than plants grown at higher latitudes. The analysis of abiotic data shows that Louisiana provides the most favorable environment for plant growth. The highest average irradiance (14.77 mW cm<sup>-2</sup>) and the highest mean annual temperature (20.4 °C) was observed in Louisiana, compared to South Carolina (13.79 mW cm<sup>-2</sup>,

19.1°C) and Delaware (14.63 mW cm<sup>-2</sup>, 13.4 °C). Differences between the maximum and the minimum annual temperatures were smallest in Louisiana compared to South Carolina and Delaware. The longest growing seasons was also observed in Louisiana (Feb.– Nov.), followed by South Carolina (Feb.– Oct.) and Delaware (Mar.– Oct.). Kirwan et al. (2009) demonstrated that a significant latitudinal gradient in productivity is mainly determined by temperature and the length of growing season. Their simple linear regression showed an increase of 27 g m<sup>-2</sup> y<sup>-1</sup> in the end of season live *S. alterniflora* productivity with an increase of mean annual temperature by 1°C. Longstreth and Strain (1977) found that photosynthesis rates of *S. alterniflora* increase under high illumination. Thus, the high average irradiance and temperature with smaller annual temperature ranges could help plants photosynthesize, which result in more production in above-ground in Louisiana. This increased production may provide the capacity to translocate more carbon to below-ground tissues during the growing seasons.

The gross productions at all sites showed patterns similar to the regional temperature cycle, which support that the temperature is main driver in production. The highest gross production rates (40.19 g m<sup>-2</sup> d<sup>-1</sup>) were observed in Louisiana, followed by South Carolina (22.22 g m<sup>-2</sup> d<sup>-1</sup>) and Delaware (20.41 g m<sup>-2</sup> d<sup>-1</sup>). The greater negative net production in Delaware was shown in the steady decrease in below-ground biomass during the study period. The below-ground biomass decreased from approximately 5,000 g m<sup>-2</sup> in January to 1,100 g m<sup>-2</sup> in July whereas the above-ground biomass fluctuated within a range between 660 and 1,200 g m<sup>-2</sup> throughout the year in Delaware. The relatively higher below-ground biomass compared to the above-ground biomass may cause more respiration than the production through photosynthesis, which in turn result in the negative net production. This result indicates that the net production rates cannot be

explained simply by latitude but are site-specific although the gross production rates closely follow the environmental factor such as temperature and irradiance.

The model fitted well to the observed below-ground biomass in all three sites and both above- and below-ground biomass in South Carolina whereas it was not able to predict the pattern of the observed above-ground biomass in Delaware. This deviation may occur while the model fits to the greater below-ground biomass and could fail to fit to the relative smaller above-ground biomass in the situation where the above- and below-ground biomass is different with a great degree like in Delaware.

Interestingly, the carbon translocation from senescing above-ground tissues in the fall increases as the latitude increases, which support our second hypothesis. The highest amount and proportion ( $\gamma$ ) (1,703 g m<sup>-2</sup> and 0.0024, respectively) were observed at higher latitudes (Delaware) (Tables 4.5 and 4.8). This amount was more than three times that in Louisiana (458 g m<sup>-2</sup>) during senescence. The pattern of mortality rates (Figure 4.12) of both above- and below-ground peak during the late fall season, which in turn, may generate more senescence in the above-ground biomass. This may not only support the micro-organism food web in the soil but also enhance survival of *S. alterniflora*'s by storing carbon from senesced above-ground tissues in below-ground in preparation for the cold winter. This result suggests that photosynthates during growing season and the remobilization of assimilate from senescing shoots during fall seasons serve as the main two sources to grow the below-ground biomass in higher latitudes whereas the photosynthates generated in longer growing seasons are the main pathway to allocate carbon to the below-ground biomass in lower latitudes.

*Spartina alterniflora* grown in Delaware translocated more assimilate from the below-ground tissues to above-ground (261 g m<sup>-2</sup>) than the *S. alterniflora* in South Carolina (2.6 x10<sup>-6</sup> g m<sup>-2</sup>)

and Louisiana ( $6.1 \times 10^{-9} \text{ g m}^{-2}$ ) during the dormancy period (Table 4.8). During fall and winter, the shoots in higher latitudes almost die and are often removed by ice and the tide before mid-winter (Gallagher, 1983), whereas the above-ground tissues survive through the winter in lower latitudes (Gallagher & Seliskar, 1976). The live above-ground biomass observed data in the study sites also showed a similar pattern. The live above-ground biomass was very consistent in Louisiana from November to the following March ranging  $529 - 650 \text{ g m}^{-2}$  whereas it dropped dramatically from  $510 \text{ g m}^{-2}$  in December to  $84 \text{ g m}^{-2}$  in January in South Carolina. The decreased winter above-ground biomass in higher latitudes may result in a higher amount of the assimilate translocation from below- to above-ground to sustain the above-ground tissues during winter seasons and support the shoot emergence in early spring. In South Carolina, the assimilate translocation ( $\text{g m}^{-2}$ ) from below- to above-ground tissues during this period was almost zero and the similar pattern was observed in our Sapelo Island *S. alterniflora* study in chapter 3. Based on observations in the model, we can argue that these regions are where the photosynthates generated in above-ground tissues may be sufficient to support the metabolic needs of the above-ground biomass. In addition, all of the fractions of photosynthate ( $\alpha_{ab}$ ) and carbon translocation ( $\gamma, \alpha_{ba}$ ) between above- and below-ground tissues and the daily mean net production observed in South Carolina were very similar with one found in short form *S. alterniflora* on Sapelo Island in Georgia. However, the absolute amount of translocation between above- and below-ground biomass were most similar between tall form *S. alterniflora* in South Carolina and Sapelo Island. This result may be due to that its relatively close latitudinal sites provide comparable temperature and irradiance, which in turn cause similar translocation dynamics in *S. alterniflora*.

The mean below-ground respiration rates were similar, whereas the mean above-ground respiration rates were highest in Louisiana (Table 4.9). These high rates may have been because

of the higher temperature in Louisiana, since the respiration rates are positively correlated to the temperature in the model. The mean above-ground respiration rate in South Carolina ( $4.79 \text{ g m}^{-2} \text{ d}^{-1}$ ) was similar with that in the tall form *S. alterniflora* on Sapelo Island ( $3.60 \text{ g m}^{-2} \text{ d}^{-1}$ ) whereas the mean below-ground respiration rate in South Carolina was about 3 fold that for Sapelo Island. This higher below-ground respiration rates could be due to the greater below-ground biomass ranging from  $1600 - 3400 \text{ g m}^{-2}$  in South Carolina compared to that on Sapelo Island ranging from  $200 - 2000 \text{ g m}^{-2}$ .

Overall, *S. alterniflora* at higher latitudes (Delaware) appears to store relatively more below-ground biomass than plants grown at lower latitudes (South Carolina and Louisiana), based on its higher root:shoot ratio (Table 4.6). It appears that the maximum above-ground biomass is achieved earlier (Aug.) in the Delaware marshes than in the marshes of South Carolina and Louisiana (Oct.). Valiela et al. (1976) reported that the maximum aerial biomass was observed in early July in Massachusetts in 1971 and 1973. In the same years, Gallagher et al. (1980) discovered that the peak above-ground biomass occurred in August or September in the Duplin estuary marsh in Georgia. The below-ground biomass increases after the formation of flowers (Crosby et al., 2015) and as senescing tissues start to increase (Elsley-Quirk et al., 2011). Thus, the rapid growth early in the short growing season in Delaware may enable *S. alterniflora* to complete their flowering cycles before the onset of winter as was observed in alpine plants (Moony & Bilings, 1960), which in turn, advances the timing of translocating biomass to below-ground.

We further investigate what happens if we apply the native site-specific parameters to *S. alterniflora* from other regions. For example, in the model we “transplanted” Louisiana *S. alterniflora* in Delaware in the model by using the parameters of plants from Louisiana with the

environmental variables of Delaware (Figure 4.14). We assumed that the physiological parameters and phenology dates are determined genetically (Gross et al., 1991) and did not change during the first year of growth. The model results showed a different pattern between transplanted Louisiana *S. alterniflora* in Delaware and the native Louisiana above-ground biomass during the growing season. The modeled above-ground biomass declined to about one third during the following winter and spring seasons. The modeled decreasing biomass pattern could be due to the reduced air temperature in Delaware (Figure 4.14). However, the transplanted South Carolina *S. alterniflora* in Delaware showed very similar to the above-ground biomass pattern in South Carolina and even grew better in the above- and below-ground after the spring seasons (Figure 4.15). This result may be due to the decreased salinity environment from South Carolina with over 30 ppt to the 27.5 ppt in Delaware. The differences became greater when we transplanted the Delaware *S. alterniflora* in the Louisiana environment (Figure 4.16). In the previous case, the transplanted *S. alterniflora* thrive with increased above-ground biomass (Figure 4.16). The increased above-ground biomass in new habitats may be driven either by higher temperature than the native habitat, or the decreased salinity level from 27.5 ppt to 13.5 ppt. However, the below-ground biomass of the transplanted Delaware *S. alterniflora* in Louisiana continuously die off after September (Figure 4.16) as similarly shown in the transplanted Louisiana below-ground biomass with a continuous decreasing phase in Delaware (Figure 4.14). This result indicates that the below-ground tissues are more vulnerable to the different environment, especially during the winter season.

It is hard to generalize the latitudinal pattern of translocation between above- and below-ground biomass from our study results due to the limited number of sites we studied and the short duration of observational data. However, the model analysis suggests that the different

translocation pathways of *S. alterniflora* between above- and below-ground tissues need to be considered and that these differ according to the latitude. Additionally, this study enables us to observe how a mathematical model can aid in the analysis and interpretation of observations made in the field and lead to the derivation of physiological plant parameters and help to find gaps between models and observed data. The model also helps us quantify the photosynthates or assimilate translocation at each phenological cycle and understand the main sources of the below-ground biomass allocation by latitudes which are hard to grasp in field experiments.

Further studies may include the mechanism of phenology into the model. Soil temperature is known to be a main driver of the green-up phenology (Zhang et al., 2004). We would expect the more accurate prediction of biomass of *S. alterniflora* once the mechanism of phenology is fully investigated and applied in the model.

## **5. Conclusion**

The peak of above-ground biomass was observed earlier in a higher latitude (Delaware) in August than in the marshes of more southern latitude areas (South Carolina and Louisiana) in October. *Spartina alterniflora* in a higher latitude contains more below-ground biomass than *S. alterniflora* in a lower latitude area and receives the assimilate translocation from below- to the above-ground tissues most among the three latitudes during the dormancy period. The daily mean gross production rate increases as the latitude goes downward. The main sources of translocating carbon to below-ground tissues in *S. alterniflora* varied by latitude. *S. alterniflora* in a lower latitude with a warmer climate translocates mainly from the photosynthates produced in the above-ground tissues to the below-ground tissues during the longer growing seasons, whereas *S. alterniflora* in higher latitudes utilize the translocation both from photosynthates

during the growing season and assimilate from the senescing of tissues during the fall. The model results show good match with the below-ground field data in all latitudes and both above- and below-ground biomass for *S. alterniflora* in South Carolina. Generally, the below-ground respiration rates do not change by latitude, but the above-ground respiration rate was highest in a lower latitude (Louisiana). This could be due to the higher temperature in warmer regions. This study suggests that the different translocation dynamics need to be considered by latitude where the target *S. alterniflora* is growing in order to accurately assess the growth dynamics and the translocation pathways in *S. alterniflora* at each phenological cycle.

## References

- Bertin, R. I. (2008). Plant phenology and distribution in relation to recent climate change. *Journal of the Torrey Botanical Society*, 135(1), 126-146. doi: doi:10.3159/07-Rp-035r.1
- Bradley, P. M., & Morris, J. T. (1990). Influence of oxygen and sulfide concentration on nitrogen uptake kinetics in *Spartina alterniflora*. *Ecology*, 71(1), 282-287.
- Callaway, J. C. (1990). *The introduction of Spartina alterniflora in south San Francisco Bay* (Master thesis). San Francisco State University, San Francisco, CA.
- Callaway, J. C., & Josselyn, M. N. (1992). The introduction and spread of smooth cordgrass (*Spartina alterniflora*) in South San Francisco Bay. *Estuaries*, 15(2), 218-226. doi: 10.2307/1352695
- Chuine, I., & Beaubien, E. G. (2001). Phenology is a major determinant of tree species range. *Ecology Letters*, 4(5), 500-510.
- Chuine, I., Cambon, G., & Comtois, P. (2000). Scaling phenology from the local to the regional level: advances from species-specific phenological models. *Global Change Biology*, 6(8),

943-952.

- Cleland, E. E., Chuine, I., Menzel, A., Mooney, H. A., & Schwartz, M. D. (2007). Shifting plant phenology in response to global change. *Trends in ecology & evolution*, 22(7), 357-365.
- Cranford, P. J., Gordon, D. C., & Jarvis, C. M. (1989). Measurement of cordgrass, *Spartina alterniflora*, production in a macrotidal estuary, Bay of Fundy. *Estuaries*, 12(1), 27-34.
- Crosby, S. C., Ivens-Duran, M., Bertness, M. D., Davey, E., Deegan, L. A., & Leslie, H. M. (2015). Flowering and biomass allocation in U.S. Atlantic coast *Spartina alterniflora*. *American journal of botany*, 102(5), 669-676. doi:10.3732/ajb.1400534
- Dame, R. F., & Kenny, P. D. (1986). Variability of *Spartina alterniflora* primary production in the euhaline North Inlet estuary. *Marine Ecology Progress Series*, 32(1), 71-80.
- Darby, F. A., & Turner, R. E. (2008). Below-and aboveground biomass of *Spartina alterniflora*: response to nutrient addition in a Louisiana salt marsh. *Estuaries and Coasts*, 31(2), 326-334.
- Ehrlén, J., & Morris, W. F. (2015). Predicting changes in the distribution and abundance of species under environmental change. *Ecology Letters*, 18(3), 303-314. doi:10.1111/ele.12410
- Eleuterius, L. N., & Caldwell, J. D. (1984). Flowering phenology of tidal marsh plants in Mississippi. *Castanea*, 49(4), 172-179.
- Elsley-Quirk, T., Seliskar, D. M., & Gallagher, J. L. (2011). Differential population response of allocation, phenology, and tissue chemistry in *Spartina alterniflora*. *Plant Ecology*, 212(11), 1873-1885.
- Euskirchen, E. S., Carman, T. B., & McGuire, A. D. (2014). Changes in the structure and function of northern Alaskan ecosystems when considering variable leaf-out times across groupings of species in a dynamic vegetation model. *Global Change Biology*, 20(3), 963-978.

- Fenner, M. (1998). The phenology of growth and reproduction in plants. *Perspectives in Plant Ecology, Evolution and Systematics*, 1(1), 78-91.
- Gallagher, J. L. (1983). Seasonal patterns in recoverable underground reserves in *Spartina alterniflora* Loisel. *American Journal of Botany*, 70(2), 212-215.
- Gallagher, J. L., & Seliskar, D. M. (1976). The metabolism of senescing *Spartina alterniflora*. In *Annual Meeting Botany Society of America, New Orleans Abstract* (p. 34).
- Gallagher, J. L., Reimold, R. J., Linthurst, R. A., & Pfeiffer, W. J. (1980). Aerial production, mortality, and mineral accumulation-export dynamics in *Spartina alterniflora* and *Juncus roemerianus* plant stands in a Georgia salt marsh. *Ecology*, 61(2), 303-312. doi: 10.2307/1935189
- Gross, M. F., Hardisky, M. A., Wolf, P. L., & Klemas, V. (1991). Relationship between aboveground and belowground biomass of *Spartina alterniflora* (smooth cordgrass). *Estuaries*, 14(2), 180-191.
- Heimann, M., Esser, G., Haxeltine, A., Kaduk, J., Kicklighter, D. W., Knorr, W., ... & Otto, R. D. (1998). Evaluation of terrestrial carbon cycle models through simulations of the seasonal cycle of atmospheric CO<sub>2</sub>: First results of a model intercomparison study. *Global Biogeochemical Cycles*, 12(1), 1-24.
- Howes, B. L., Howarth, R. W., Teal, J. M., & Valiela, I. (1981). Oxidation-reduction potentials in a salt marsh: Spatial patterns and interactions with primary production<sup>1</sup>. *Limnology and Oceanography*, 26(2), 350-360. doi:10.4319/lo.1981.26.2.0350
- Jung, Y., & Burd, A. (2017). Seasonal changes in above- and below-ground non-structural carbohydrates (NSC) in *Spartina alterniflora* in a marsh in Georgia, USA. *Aquatic Botany*, 140, 13-22. doi:[10.1016/j.aquabot.2017.04.003](https://doi.org/10.1016/j.aquabot.2017.04.003)

- King, G. M., Klug, M. J., Wiegert, R. G., & Chalmers, A. G. (1982). Relation of soil water movement and sulfide concentration to *Spartina alterniflora* production in a Georgia salt marsh. *Science*, *218*(4567), 61-63.
- Kirk, J. T. O. (1994). *Light and photosynthesis in aquatic ecosystems*. Cambridge University Press
- Kirwan, M. L., Guntenspergen, G. R., & Morris, J. T. (2009). Latitudinal trends in *Spartina alterniflora* productivity and the response of coastal marshes to global change. *Global Change Biology*, *15*(8), 1982-1989.
- Koch, M. S., Mendelssohn, I. A., & McKee, K. L. (1990). Mechanism for the hydrogen sulfide-induced growth limitation in wetland macrophytes. *Limnology and Oceanography*, *35*(2), 399-408.
- Kramer, K. (1994). Selecting a model to predict the onset of growth of *Fagus sylvatica*. *Journal of Applied Ecology*, *31*(1), 172-181. doi: 10.2307/2404609
- Livingstone, D. C., & Patriquin, D. G. (1981). Belowground growth of *Spartina alterniflora* Loisel.: habit, functional biomass and non-structural carbohydrates. *Estuarine, Coastal and Shelf Science*, *12*(5), 579-587.
- Longstreth, D. J., & Strain, B. R. (1977). Effects of salinity and illumination on photosynthesis and water balance of *Spartina alterniflora* Loisel. *Oecologia*, *31*(2), 191-199.
- Lytle, R. W., & Hull, R. J. (1980). Photoassimilate distribution in *Spartina alterniflora* Loisel. II. autumn and winter storage and apring regrowth1. *Agronomy Journal*, *72*(6), 938-942.
- Mendelssohn, I. A., & Morris, J. T. (2002). Eco-physiological controls on the productivity of *Spartina alterniflora* Loisel. In M. P. Weinstein & D. A. Kreeger (Eds.), *Concepts and controversies in tidal marsh ecology* (pp. 59-80). Dordrecht, Netherlands: Springer.
- Mooney, H. A., & Billings, W. D. (1960). The annual carbohydrate cycle of alpine plants as related

- to growth. *American Journal of Botany*, 47(7), 594-598. doi:10.2307/2439439
- Morris, J. T. (1982). A model of growth responses by *Spartina alterniflora* to nitrogen limitation. *Journal of Ecology*, 70(1), 25-42. doi: 10.2307/2259862
- Morris, J. T., & Haskin, B. (1990). A 5-yr record of aerial primary production and stand characteristics of *Spartina alterniflora*. *Ecology*, 71(6), 2209-2217.
- Morris, J. T., Houghton, R. A., & Botkin, D. B. (1984). Theoretical limits of belowground production by *Spartina alterniflora*: An analysis through modelling. *Ecological Modelling*, 26(3), 155-175. doi:[10.1016/0304-3800\(84\)90068-1](https://doi.org/10.1016/0304-3800(84)90068-1)
- O'Donnell, J., & Schalles, J. (2016). Examination of abiotic drivers and their influence on *Spartina alterniflora* biomass over a twenty-eight year period using landsat 5 TM satellite imagery of the central Georgia coast. *Remote Sensing*, 8(6), 1-22.
- Roman, C. T., & Daiber, F. C. (1984). Aboveground and belowground primary production dynamics of two Delaware bay tidal marshes. *Bulletin of the Torrey Botanical Club*, 111(1), 34-41. doi:10.2307/2996208
- Smalley, A. E. 1958. *The role of two invertebrate populations, Littorina irrorata and Orchelimum fiducinum in the energy flow of a salt marsh eco- system* (Doctoral dissertaion). University of Georgia, Athens, GA.
- Valiela, I., Teal, J. M., & Persson, N. Y. (1976). Production and dynamics of experimentally enriched salt marsh vegetation: Belowground biomass1. *Limnology and Oceanography*, 21(2), 245-252. doi:10.4319/lo.1976.21.2.0245
- Van Wijk, M. T., & Williams, M. (2003). Interannual variability of plant phenology in tussock tundra: modelling interactions of plant productivity, plant phenology, snowmelt and soil thaw. *Global Change Biology*, 9(5), 743-758.

Zhang, X., Friedl, M. A., Schaaf, C. B., & Strahler, A. H. (2004). Climate controls on vegetation phenological patterns in northern mid-and high latitudes inferred from MODIS data. *Global change biology*, *10*(7), 1133-1145.

Zheng, S., Shao, D., Asaeda, T., Sun, T., Luo, S., & Cheng, M. (2016). Modeling the growth dynamics of *Spartina alterniflora* and the effects of its control measures. *Ecological Engineering*, *97*, 144-156. doi:[10.1016/j.ecoleng.2016.09.006](https://doi.org/10.1016/j.ecoleng.2016.09.006)

**Table 4.1** Characteristic of three regions (Delaware, South Carolina, and Louisiana) in latitudinal study using the PG model

	<b>Delaware (DE)</b> (lat: 38.79, long: -75.16)	<b>South Carolina (SC)</b> (lat: 33.32, long: -79.17)	<b>Louisiana (LA)</b> (lat: 29.25, long: -90.66)
<b>Data Reference</b>	Roman and Daiber, 1984	Dame and Kenny, 1986	Darby and Turner, 2008
<b>Study site</b>	The Blackbird Creek marsh, DE	High marsh site covered by short <i>S.</i> and located at the upper reaches of Bly Creek side in North Inlet, SC	Salt marsh located 0.5 km west of the Louisiana Universities Marine Consortium laboratory, in Cocodrie, LA
<b>Form of <i>Spartina alterniflora</i></b>	Tall form <i>Spartina</i>	Tall form <i>Spartina</i>	Inland form <i>Spartina</i> *
<b>Periods of observed biomass data</b>	Monthly data for both above- and below-ground data from Feb. 1975 to Oct. 1976	Monthly data for above-ground data and bimonthly data for below-ground data from Jun. 1983 to May 1984	Monthly data for both above- and below-ground data from Mar. 2004 to Mar. 2005
<b>Salinity ranges</b>	25~30 ppt (The average value, 27.5ppt was used in the model)	17~36 ppt (The average value, 30.01ppt was implied in the model)	7~20ppt (The average value 13.5ppt was applied in the model)

\* Inland form *S. alterniflora* in the microtidal environment such as the study site in Louisiana indicates the *S. alterniflora* that has a height ranging from 0.8 meter to 1.2 meter and grows 2 meters from the water's edge and represent 80~90 % of the total salt marsh landscape (Turner & Gosselink, 1975; Darby & Turner, 2008).

**Table 4.2** Definitions of symbols and parameter values

Symbol	Name	Units & Value
$E_0$	Ratio of Sun-Earth distance to mean distance	Dimensionless
$A_f$	Solar constant	1367 W m <sup>-2</sup>
$S_c$	Atmospheric absorption	0.4 Dimensionless
$Z$	Zenith angle	Degree
$P$	Total net production	gdwt m <sup>-2</sup> h <sup>-1</sup>
$B_{above}$	Above ground biomass	gdwt m <sup>-2</sup>
$B_{below}$	Below ground biomass	gdwt m <sup>-2</sup>
$T$	Air temperature	°C
$\vartheta$	Solar elevation	Radians
$L$	Solar irradiance at the top of the canopy	W m <sup>-2</sup>
$\lambda$	Half saturation constant for irradiance	300 ± 100 W m <sup>-2</sup>
$\alpha$	Irradiance extinction rate within the canopy	(3.4 ± 1.0) × 10 <sup>-4</sup> m <sup>2</sup> gdwt <sup>-1</sup>
$N$	Percent of nitrogen in the dry leaves	%
$F$	Ratio of green tissue to total canopy biomass	Dimensionless
$\psi$	Temperature coefficient for gross production	(7.1 ± 1.7) × 10 <sup>-4</sup> °C <sup>-1</sup> h <sup>-1</sup>
$\eta$	Half saturation constant for nitrogen	0.36 ± 0.29 % dwt
$F$	Green leave ratio	Percentage
$m_a$	Specific rate of above-ground mortality at 20°C	gg <sup>-1</sup> d <sup>-1</sup>
$m_b$	Specific rate of below-ground mortality at 20°C	gg <sup>-1</sup> d <sup>-1</sup>
$\theta$	Temperature constant	1.09

**Table 4.3** Least-square estimates of parameters used for temperature simulations in PG model

	<b>Delaware</b>	<b>South Carolina</b>	<b>Louisiana</b>
$a_1$	12.07	9.04	8.63
$a_2$	9.64	3.39	3.41
$a_3$	3.51	3.87	3.84
$a_4$	12.72	18.57	19.97

**Table 4.4** Site-specific phenological input data implied on the latitudinal study in the PG model

	<b>Delaware</b>	<b>South Carolina</b>	<b>Louisiana</b>
$SB_{\text{below\_to\_above}}$	305 (Nov. 1)	349 (Dec. 15)	365 (Dec. 31)
$EB_{\text{below\_to\_above}}$	60 (Mar. 1)	46 (Feb. 15)	31 (Jan. 1)
$SP_{\text{above\_to\_below}}$	60 (Mar. 1)	46 (Feb. 15)	31 (Jan. 1)
$EP_{\text{above\_to\_below}}$	274 (Oct. 1)	288 (Oct. 15)	334 (Nov. 30)

**Table 4.5** Parameter values from the inverse model run for the whole study period at each latitude and the sum of absolute values of  $\Delta Da_i$  and  $\Delta Db_i$  (Total  $\Delta D_i$ ) showing the level of differences between observed biomass and modeled biomass

	<i>S. alterniflora</i> in DE	<i>S. alterniflora</i> in SC	<i>S. alterniflora</i> in LA
$\alpha_{ab}$ (fraction)	0.56	0.75	0.55
$\alpha_{ba}$ (fraction)	$1.3 \times 10^{-5}$	$4.7 \times 10^{-13}$	$1.2 \times 10^{-14}$
$\gamma$ (fraction)	0.0024	0.0006	0.0006
$m_a$ ( $gg^{-1} d^{-1}$ )	0.0008	0.0006	0.0006
$m_b$ ( $gg^{-1} d^{-1}$ )	0.0008	0.0006	0.0006
$\rho$ ( $^{\circ}C^{-1} h^{-1}$ )	$3.0 \times 10^{-5}$	$1.5 \times 10^{-5}$	$5.4 \times 10^{-5}$
<b>Total <math>\Delta D_i</math></b>	96.60	9.13	79.04

**Table 4.6** The modeled mean root: shoot ratio at three latitudes

	Delaware	South Carolina	Louisiana
<b>Average root:shoot ratio</b>	2.51	1.88	0.92

**Table 4.7** Daily mean gross and net production ( $\text{g m}^{-2} \text{d}^{-1}$ ) of the whole plant of *S. alterniflora* calculated in the PG model

	<b>Delaware</b>	<b>South Carolina</b>	<b>Louisiana</b>
<b>Daily mean gross production (<math>\text{g m}^{-2} \text{d}^{-1}</math>)</b>	20.41	22.22	40.19
<b>Daily mean net production (<math>\text{g m}^{-2} \text{d}^{-1}</math>)</b>	-10.88	0.55	-0.61

**Table 4.8** Total carbon translocation at each phenological cycle at the three latitudes

	<b>Delaware</b>	<b>South Carolina</b>	<b>Louisiana</b>
<b>Total translocated photosynthate from above to below during growing season (<math>\text{g m}^{-2}</math>)</b>	2940	4363	7202
<b>Total translocated biomass from above to below during senescence (<math>\text{g m}^{-2}</math>)</b>	1703	1252	458
<b>Total translocated biomass from below to above during dormancy (<math>\text{g m}^{-2}</math>)</b>	261	$2.6 \times 10^{-6}$	$6.1 \times 10^{-9}$

**Table 4.9** Daily mean above- and below-ground respiration rates ( $\text{g m}^{-2} \text{d}^{-1}$ ) estimated in the PS model in the latitudinal study

	<b>Delaware</b>	<b>South Carolina</b>	<b>Louisiana</b>
<b>Daily mean above-ground respiration rate (<math>\text{g m}^{-2} \text{d}^{-1}</math>)</b>	7.69	4.79	16.91
<b>Daily mean below-ground respiration rate (<math>\text{g m}^{-2} \text{d}^{-1}</math>)</b>	23.60	16.87	23.89

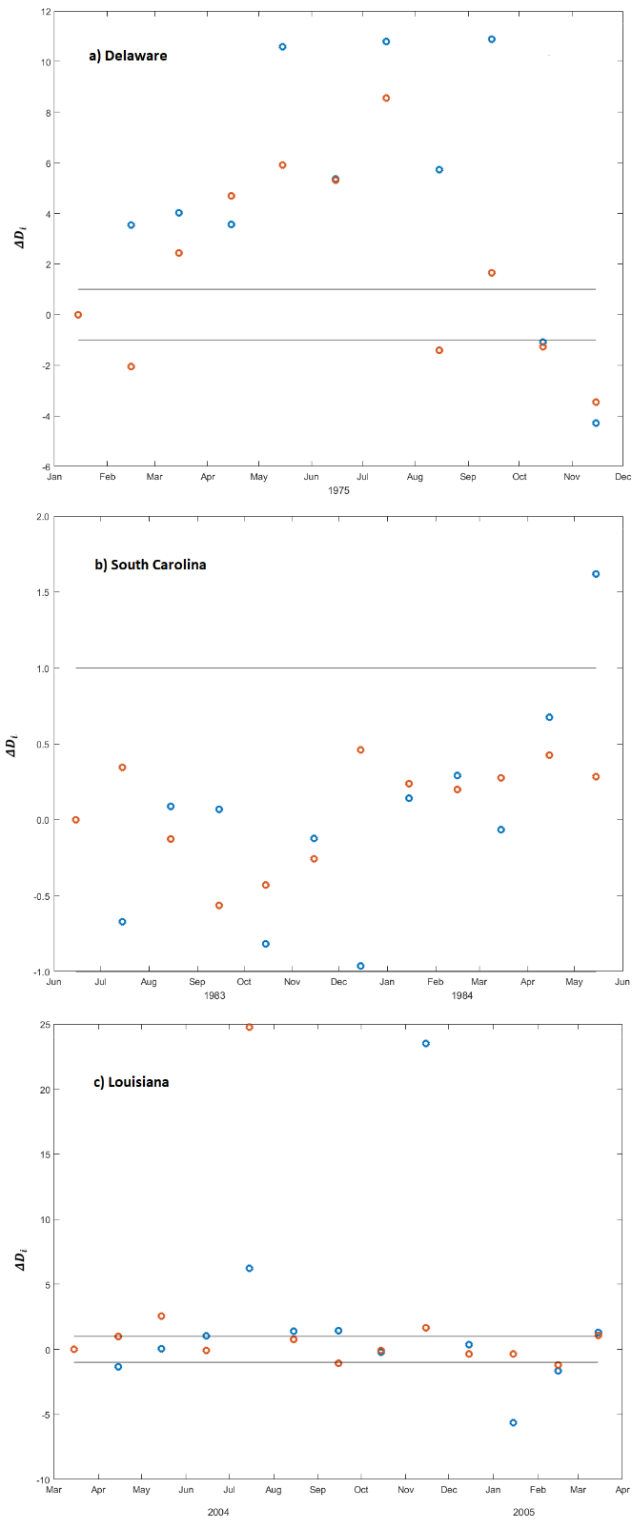


**Figure 4.1**  $\Delta D_i$  values quantifying the differences between observed and modeled biomass in above- (blue circles) and below-ground biomass (red circles) at three latitudinal regions

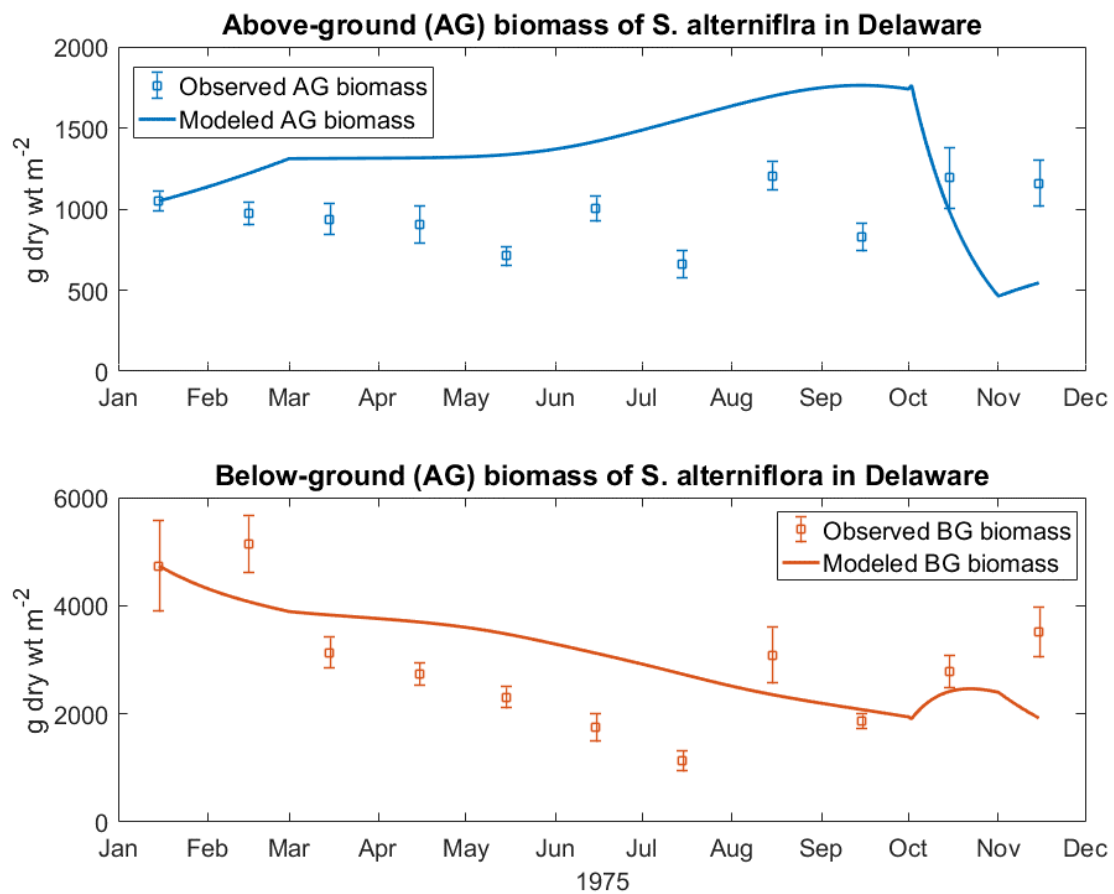


**Figure 4.2** Observed and modeled above- and below-ground biomass of *S. alterniflora* in Delaware

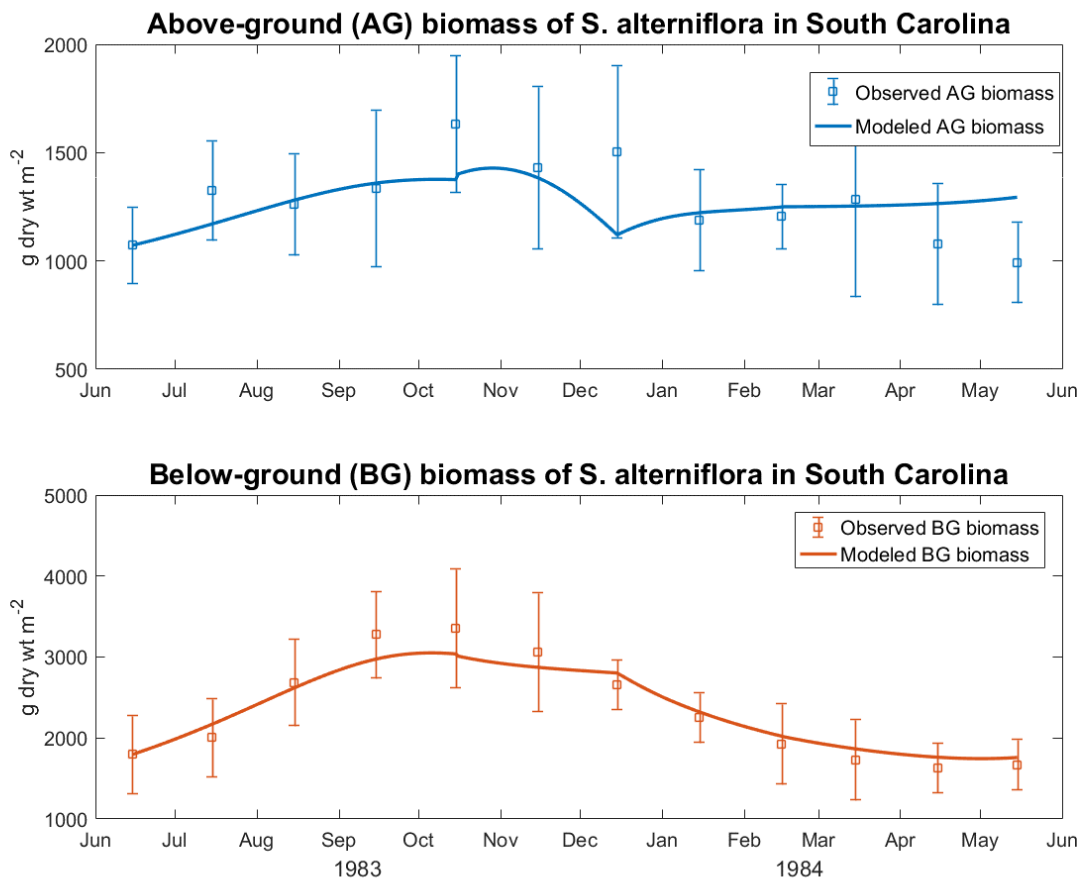


**Figure 4.3** Observed and modeled above- and below-ground biomass of *S. alterniflora* in South Carolina

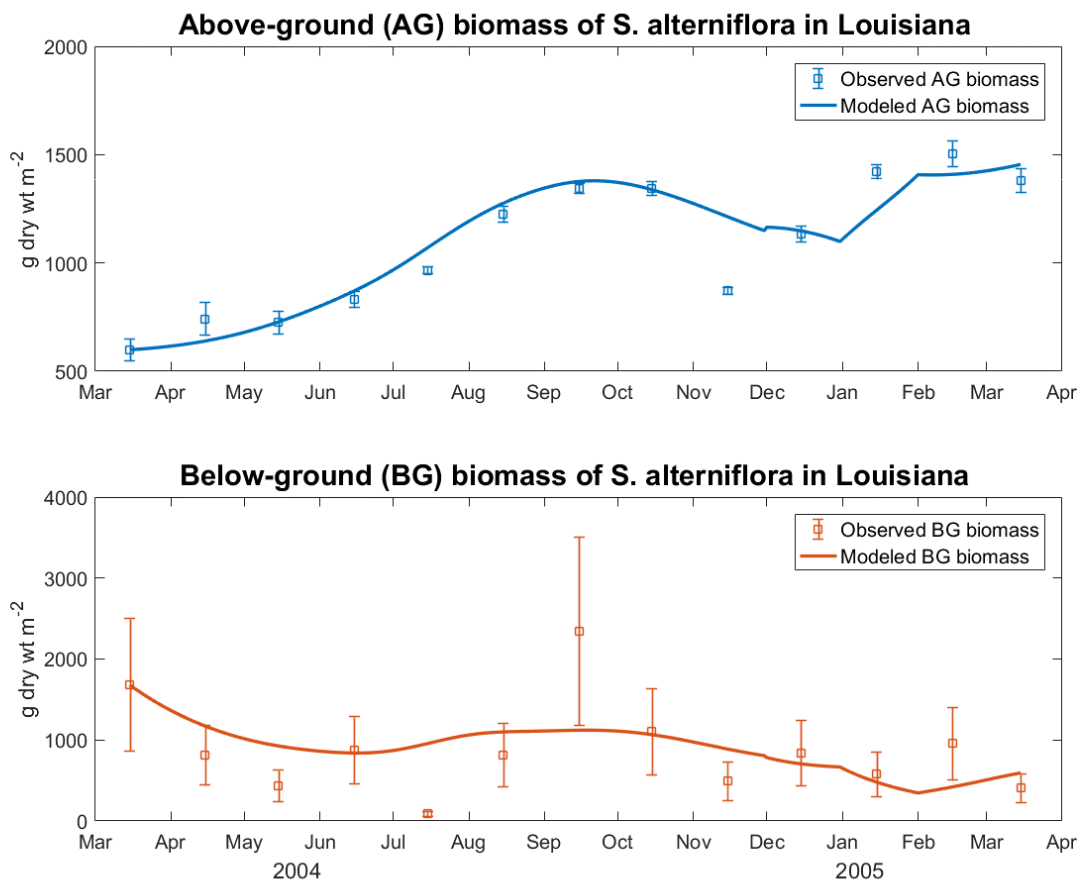


**Figure 4.4** Observed and modeled above- and below-ground biomass of *S. alterniflora* in Louisiana

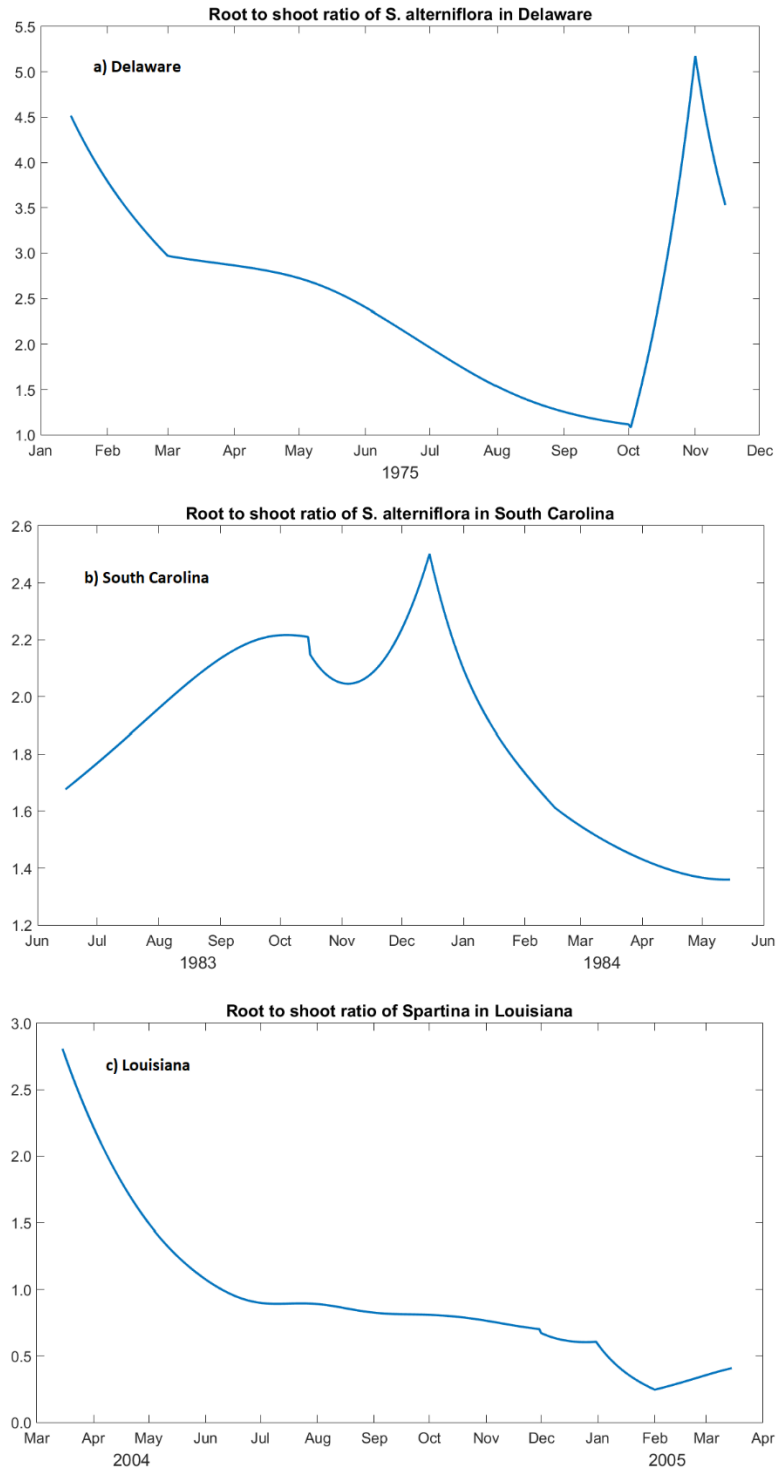


**Figure 4.5** Root to shoot ratio of modeled biomass of *S. alterniflora* at three different latitudes a) Delaware, b) South Carolina, c) Louisiana

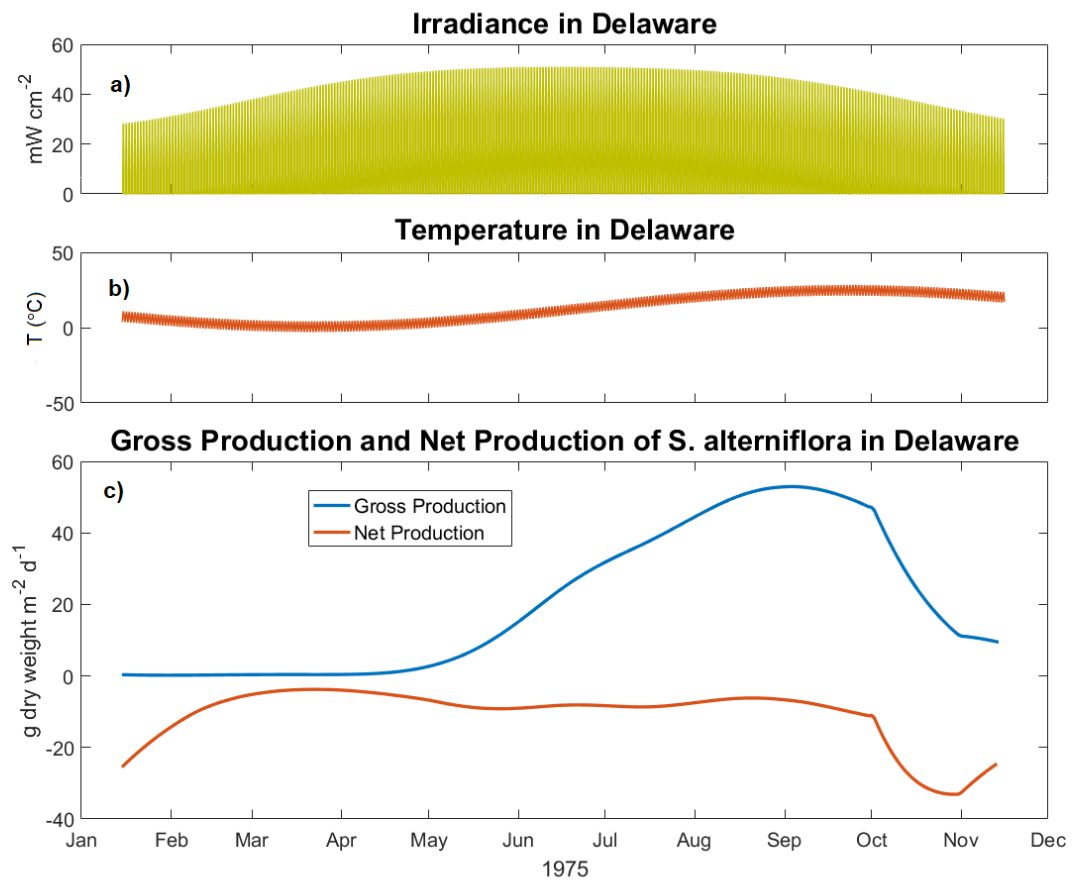


**Figure 4.6** Calculated a) irradiance and b) temperature and the estimated c) total plant gross production and net production of *S. alterniflora* in Delaware in the PG model

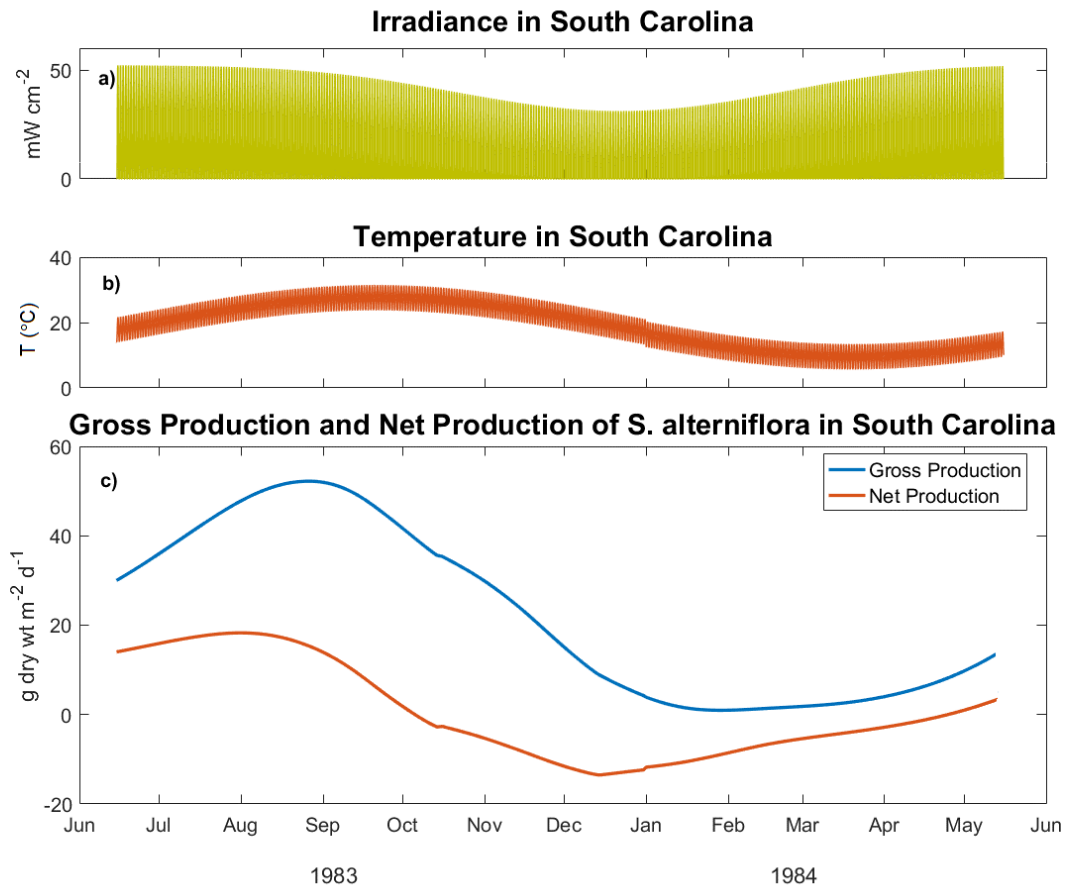


**Figure 4.7** Calculated a) irradiance and b) temperature and the estimated c) gross production and net production of *S. alterniflora* in South Carolina in the PG model

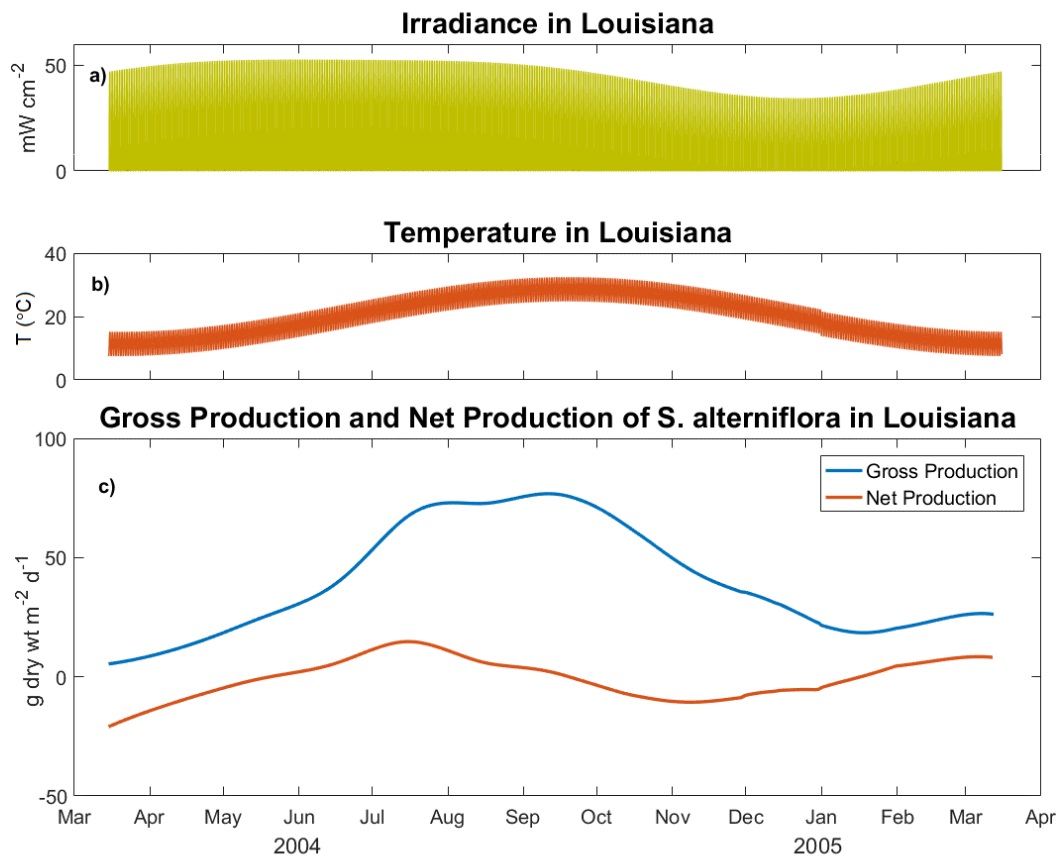


**Figure 4.8** Calculated a) irradiance and b) temperature and the estimated c) gross production and net production of the whole plant of *S. alterniflora* in Louisiana in the PG model

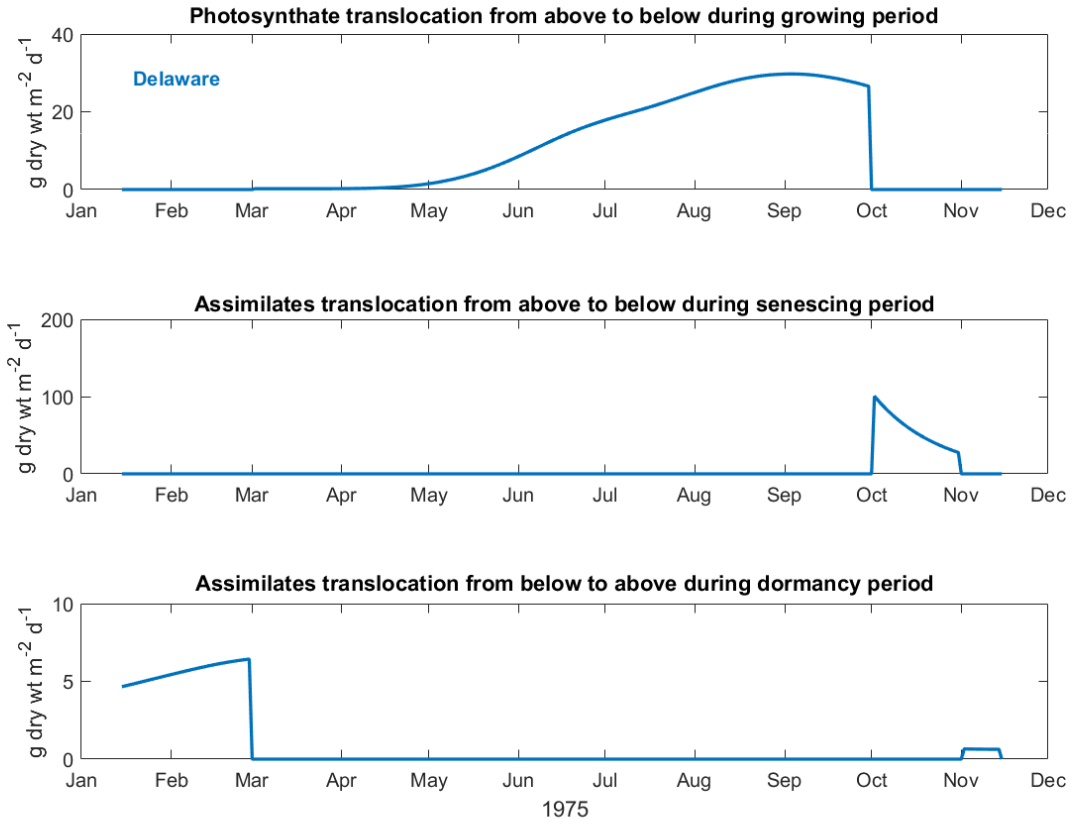


**Figure 4.9** Translocated photosynthates and assimilate of *S. alterniflora* in Delaware during three different phenological events

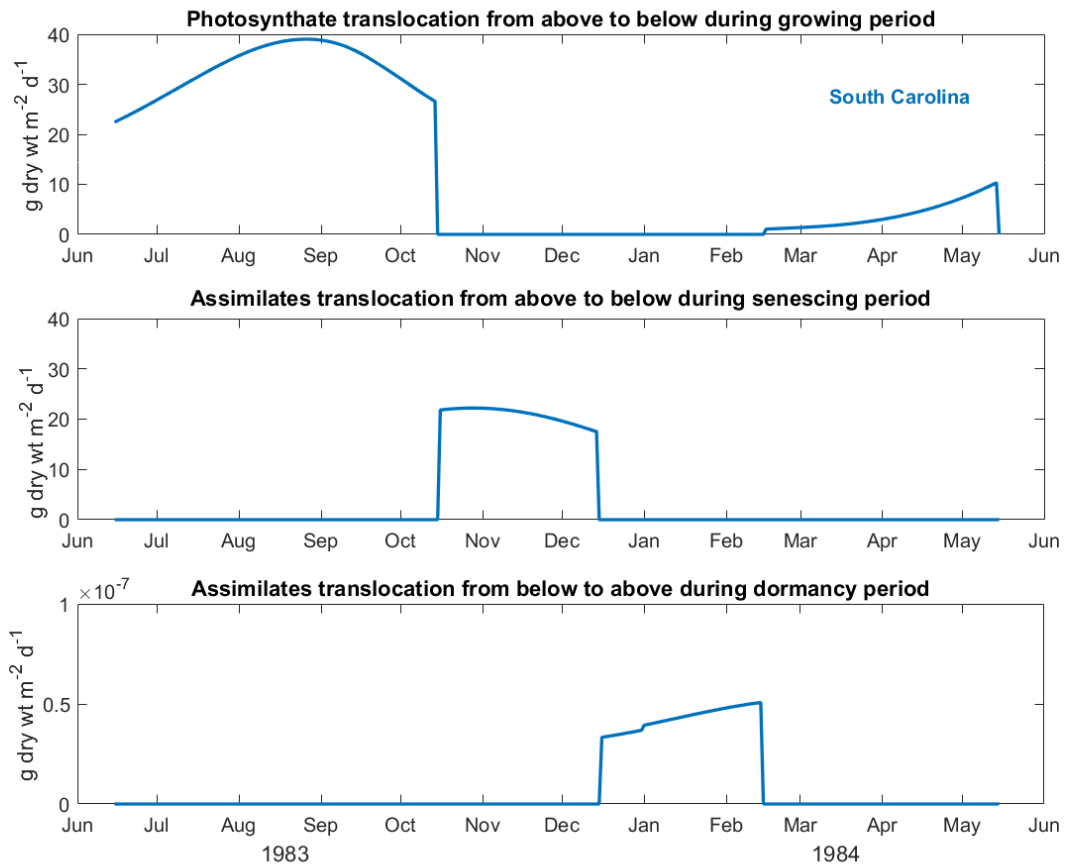


**Figure 4.10** Translocated photosynthates and assimilate of *S. alterniflora* in South Carolina during three different phenological events

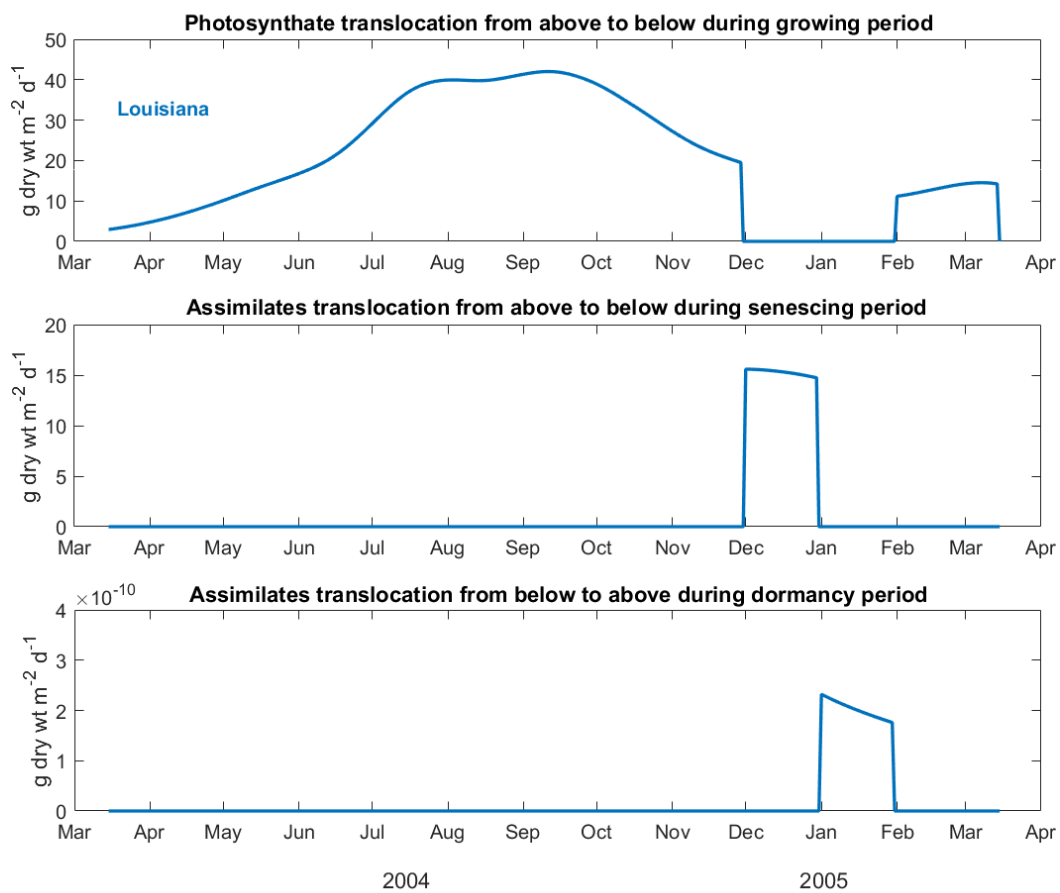


**Figure 4.11** Translocated photosynthates and carbon of *S. alterniflora* in Louisiana during three different phenological events

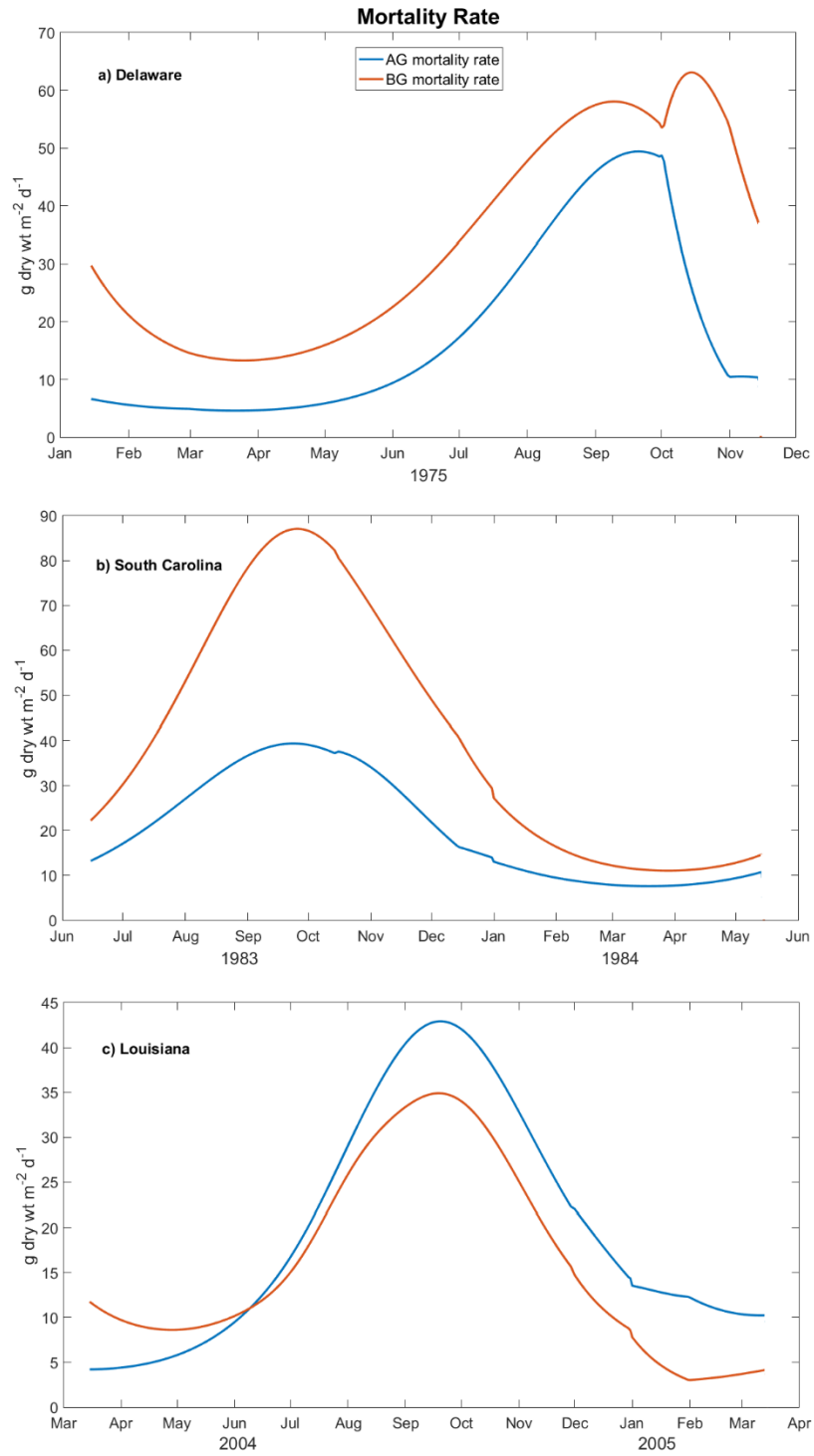


**Figure 4.12** Mortality rates of above- and below-ground biomass calculated in the PG model in the latitudinal study on a) Delaware, b) South Carolina, and c) Louisiana

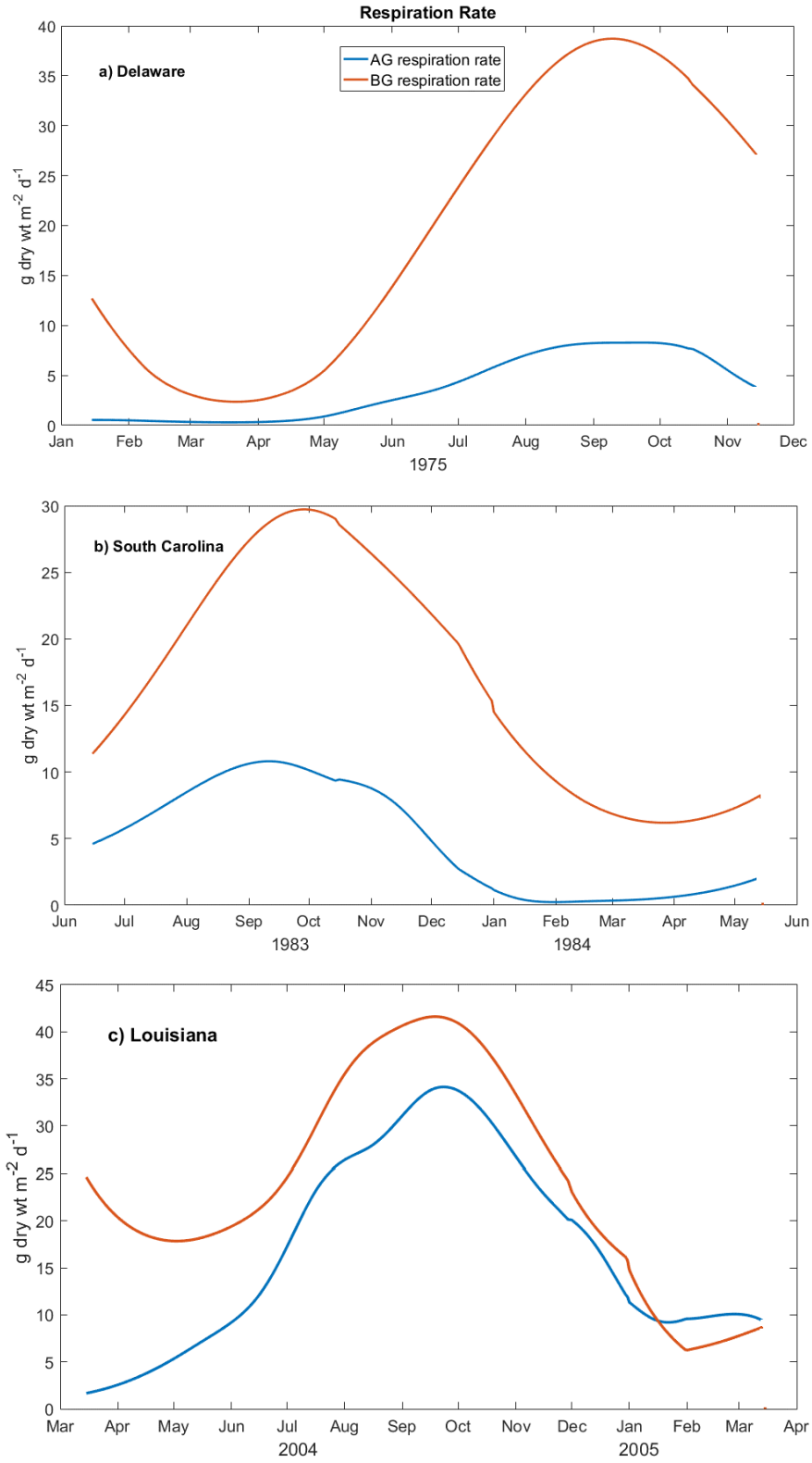


**Figure 4.13** Respiration rates of above- and below-ground biomass calculated by the PG model

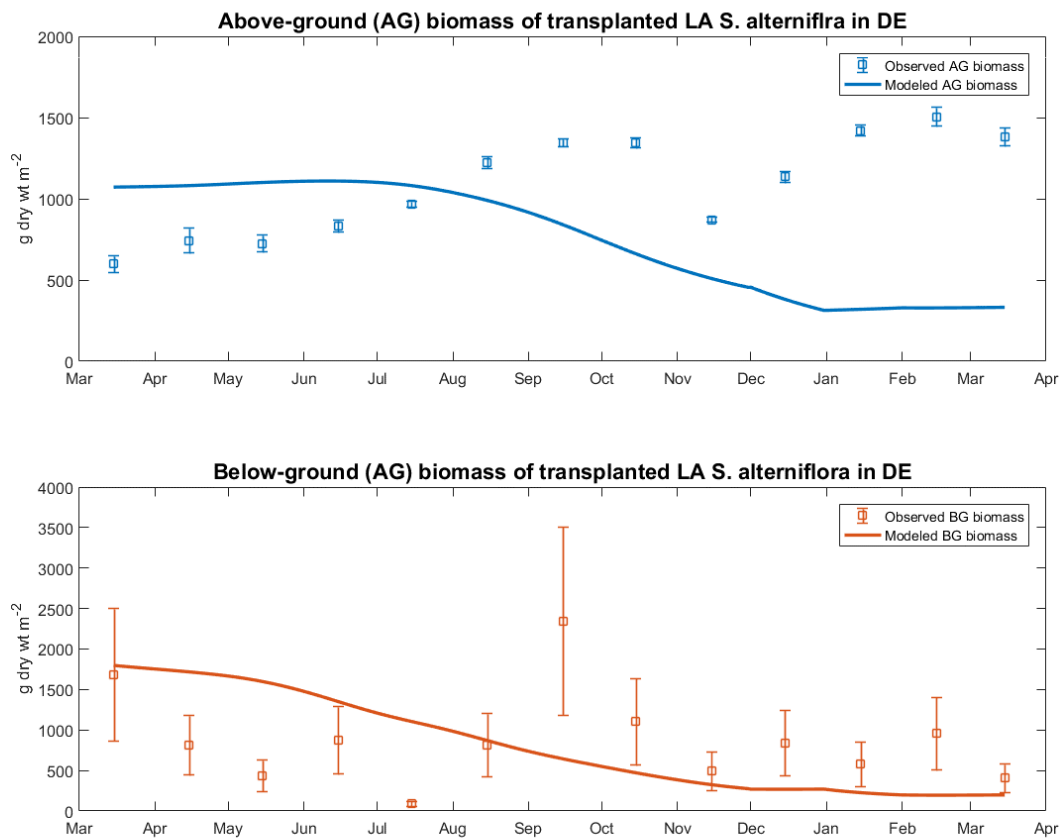


**Figure 4.14** Observed above- and below-ground biomass of Louisiana *S. alterniflora* in Louisiana and modeled above- and below-ground biomass of Louisiana *S. alterniflora* transplanted in Delaware

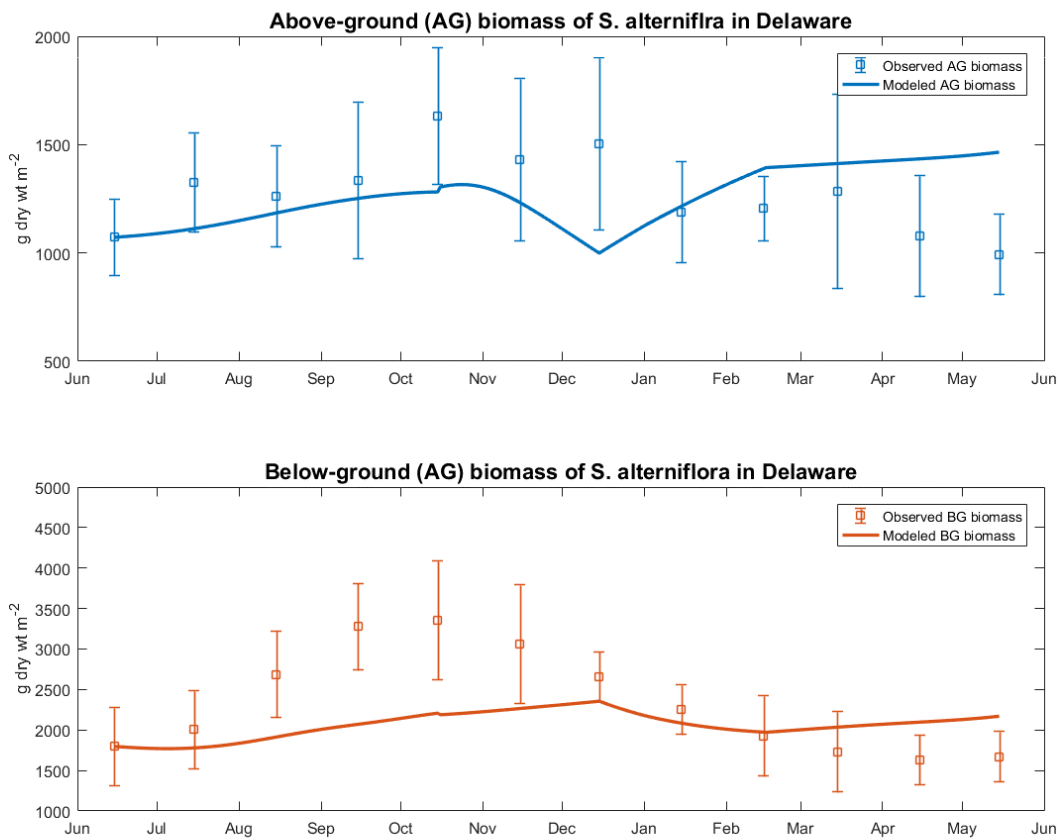


**Figure 4.15** Observed above- and below-ground biomass of South Carolina *S. alterniflora* in South Carolina and modeled above- and below-ground biomass of South Carolina *S. alterniflora* transplanted in Delaware

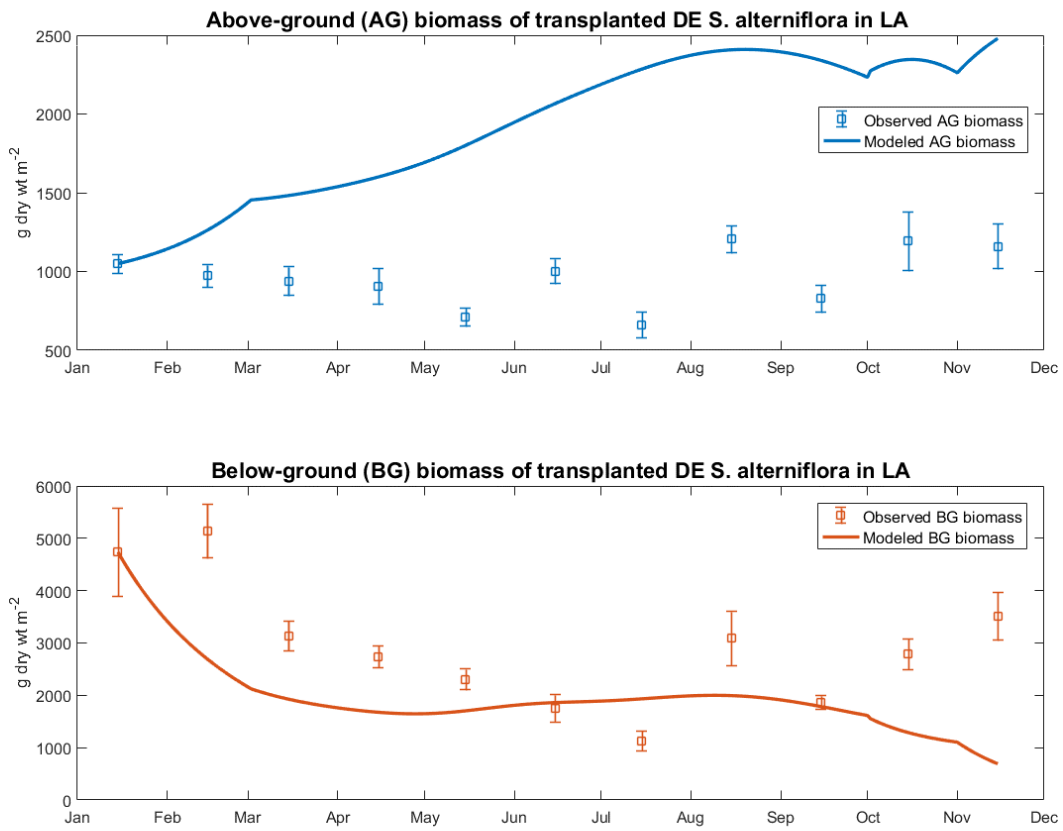


**Figure 4.16** Observed above- and below-ground biomass of Delaware *S. alterniflora* in Delaware and modeled above- and below-ground biomass of Delaware *S. alterniflora* transplanted in Louisiana

## CHAPTER 5

### SUMMARY

The objectives of this study were to: 1) document the seasonal variability of above- and below-ground non-structural carbohydrates (NSC) in *Spartina alterniflora* in Georgia salt marshes, 2) analyze how the growth and production dynamics and the translocated biomass differ with height form using phenology-based growth model (PG model), 3) compare Delaware, South Carolina, and Louisiana *S. alterniflora* to understand the variation of translocation dynamics with latitude using the PG model.

Chapter 1 includes a general introduction to the salt marsh halophyte *S. alterniflora*, the non-structural carbohydrates, and literature review of previous *S. alterniflora* growth and production models. *S. alterniflora* is the most dominant and productive plant in salt marshes along the eastern coast of the United States. The low salt marsh area sustains its platform held by the extensive below-ground components of *S. alterniflora*. Generally, the higher below-ground net production than the above-ground net production is observed in *S. alterniflora* throughout latitudes. This characteristic indicates that failure to include the below-ground growth dynamics can lead to considerable overestimate of total net production. Also, investigating both above- and below-ground growth and production dynamics of *S. alterniflora* is essential for acquiring the solid understanding of carbon flow pathways for sustainable management of coastal and wetland ecosystems.

The seasonal variability of non-structural carbohydrates in various tissues parts was documented for *S. alterniflora* in a Georgia marsh in Chapter 2. The results indicate that sucrose is the most dominant sugar stored in both above- and below-ground components of *S. alterniflora*. A greater seasonal variability in NSC than had been previously reported (McIntire & Dunstan, 1976) was observed, with concentration varying between 3.3% through 17.3% of the total biomass and between 0% and 19.5% of dry weight depending on the type of tissue. The three highest peaks of NSC with above 15 % of its total biomass were observed in October, December, and June. The total NSC was stored mostly in above-ground parts during the fall but its peak distribution moves to the below-ground in winter and return back to the above-ground in spring seasons. Through comparing the modeled net primary production and observed biomass data, we found that the need of including the additional respiration coming from dark respiration and senescing tissues.

The phenology-based growth model (PG model) combines Morris' production model (1984) with the phenological parts of the Zheng et al. model (2016) was developed to estimate physiological parameter values, investigate carbon translocation patterns and growth dynamics of the three height forms of *S. alterniflora* in a Georgia marsh, USA in Chapter 3. The model in inverse mode was used to estimate several physiological parameter values. The fractions of the photosynthate translocated from above- to below-ground tissues per hour ( $\alpha_{ab}$ ) during the growth period (the beginning of March to the beginning of October) was highest for short form *S. alterniflora* (0.82). This result shows that the short form *S. alterniflora* allocates the majority portion of its photosynthates produced from the photosynthesis to the below-ground tissues during the growing season. The fraction of above-ground biomass translocated from above-ground senescing tissues to below-ground biomass ( $\gamma$ ) during the senescence period (the

beginning of October - the middle of December) was also highest in short form *S. alterniflora*. This result indicates that the short form *S. alterniflora* actively remobilizes the carbon from its senescing above-ground tissues and translocates them to the below-ground tissues. However, the absolute carbon translocated from above- to below-ground tissues in the form of photosynthate or the remobilization of assimilates was highest in tall form *S. alterniflora* due to its greatest live and senescing above-ground biomass observed among three types of *S. alterniflora*. Model results indicate that translocation from below- to above-ground tissues may not be necessary for survival during the winter seasons on Sapelo Island, Georgia. Running the PG model for longer periods was limited by the great variability of observed below-ground biomass, which highlights the need for more accurate and precise field estimates of below-ground biomass.

The growth, production, and the carbon translocation of *S. alterniflora* in Delaware, South Carolina, and Louisiana were examined in Chapter 4. The similar gross production pattern with its regional temperature supported the previous studies demonstrating that temperature is a main driver causing latitudinal differences in the production of *S. alterniflora* (Kirwan 2009). The PG model show the daily mean gross production rates increased as the latitude decreases. The main source of translocated carbon to below-ground tissues varied with latitude. In a lower latitude, its main source is photosynthate generated in above-ground tissues during growth whereas *S. alterniflora* in higher latitudes builds up the below-ground biomass mainly from both photosynthates during growing seasons and the remobilization of assimilates from senescing above-ground tissues in the fall. The amount and the fraction of assimilates translocation from below- to above-ground tissues increases with latitude. The model results demonstrated reasonable agreement with the below-ground field data at all sites but showed less agreement with above-ground biomass in Delaware. The study results showed that the below-ground

respiration rates do not change by latitude, but the above-ground respiration rate was highest in a lower latitude. This study suggests that the different translocation dynamics need to be taken into account with latitude where the target *S. alterniflora* is growing in order to accurately assess the growth dynamics and the translocation pathways in *S. alterniflora* at each phenological cycle.

## References

- Kirwan, M. L., Guntenspergen, G. R., & Morris, J. T. (2009). Latitudinal trends in *Spartina alterniflora* productivity and the response of coastal marshes to global change. *Global Change Biology*, *15*(8), 1982-1989.
- McIntire, G. L., & Dunstan, W. M. (1976). Non-structural carbohydrates in *Spartina alterniflora* Loisel. *Botanica marina*, *19*(2), 93-96.
- Morris, J. T., Houghton, R. A., & Botkin, D. B. (1984). Theoretical limits of belowground production by *Spartina alterniflora*: An analysis through modelling. *Ecological Modelling*, *26*(3), 155-175. doi: [https://doi.org/10.1016/0304-3800\(84\)90068-1](https://doi.org/10.1016/0304-3800(84)90068-1)
- Zheng, S., Shao, D., Asaeda, T., Sun, T., Luo, S., & Cheng, M. (2016). Modeling the growth dynamics of *Spartina alterniflora* and the effects of its control measures. *Ecological Engineering*, *97*, 144-156. doi: <https://doi.org/10.1016/j.ecoleng.2016.09.006>